



Australian
National
University

Applications of
Resolutions of the Coulomb Operator
in Quantum Chemistry

Taweetham Limpanuparb

October 2011

A thesis submitted for the degree of
Doctor of Philosophy at the Australian National University

*For my parents who teach me the value of education
and do whatever it takes for me to be educated.*

*For Mahidol Wittayanusorn School and Junior Science Talent Project
which inspired and supported me to pursue a career in science.*

Declaration

The work in this thesis is my own except where otherwise stated.

Taweetham Limpanuparb
Canberra, October 2011

Acknowledgements

Though PhD candidates must complete their thesis by themselves, my three-year study in Canberra is not a journey alone. Many individuals and organizations have lent their helping hands to me. Without them, I would not be able to complete the journey towards my PhD.

First and foremost, I am indebted to Prof Peter M. W. Gill, chair of my supervisory panel, who accepted me to join his research group and whose advice is always helpful.

I also thank Dr Andrew T. B. Gilbert, Dr Ching-Yeh Lin, Dr Junming Ho and colleagues in Prof Gill's research group for their academic and moral support at the Research School of Chemistry. Likewise, I very much appreciate the friendship and understanding extended to me by ANU Thai community and Graduate House & University House community.

Last but not least, I acknowledge financial assistance from the Royal Thai Government (DPST program), ANU Residential Scholarship, Pinnacle Student Scholarship, ANU RSC & VC Travel Grant and ISTCP-VII Young Researcher Scholarship. I am also grateful for generous grant of supercomputing time from the NCI National Facility.

Taweetham Limpanuparb
Canberra, October 2011

Abstract

$$r_{ij}^{-1} \approx \sum_{k=1}^{\mathcal{K}} \phi_k(\mathbf{r}_i) \phi_k(\mathbf{r}_j)$$

$$\bar{\mathcal{H}}^{\mathcal{K}} = \sum_i^N \bar{h}(\mathbf{r}_i) + \sum_{k=1}^{\mathcal{K}} \sum_{i < j}^N \phi_k(\mathbf{r}_i) \phi_k(\mathbf{r}_j)$$

$$(\mu\nu | r_{12}^{-1} | \lambda\sigma) \approx \sum_{k=1}^{\mathcal{K}} (\mu\nu | \phi_k) (\phi_k | \lambda\sigma)$$

This dissertation shows that the Coulomb operator and the long-range Coulomb operators can be resolved as a sum of products of one-particle functions. These resolutions provide a potent new route to tackle quantum chemical problems. Replacing electron repulsion terms in Schrödinger equations by the truncated resolutions yields the reduced-rank Schrödinger equations (RRSE). RRSEs are simpler than the original equations but yield energies with chemical accuracy even for low-rank approximations. Resolutions of the Coulomb operator factorize Coulomb matrix elements to Cholesky-like sums of products of auxiliary integrals. This factorization is the key to the reduction of computational cost of quantum chemical methods.

Contents

Acknowledgements	vii
Abstract	ix
Publications and proceedings	xv
Notation and symbol	xvii
1 QM methods	1
1.1 Hartree-Fock wavefunction	3
1.1.1 Basis set	4
1.1.2 The self-consistent field procedure	5
1.2 Post-HF methods	8
1.2.1 Møller-Plesset perturbation theory	8
1.2.2 Configuration interaction	9
1.2.3 Coupled cluster	10
1.3 Alternative approaches	11
1.3.1 Composite methods	11
1.3.2 Multireference methods	12
1.3.3 Density functional theory	12
1.3.4 Other methods	14
2 Resolutions of the Coulomb operator	15
2.1 Basic theory	15
2.2 Extensions of resolution theory	20
2.2.1 Substitution	20
2.2.2 Diagonalization	22
2.2.3 Fourier orthonormalization	23
2.2.4 Real orthonormalization	25

2.3	Examples of $T(r_{12})$ resolutions	27
2.3.1	Decoupling of the angular and the radial parts	28
2.3.2	Resolution of the radial function T_l	28
2.4	Related techniques	35
2.4.1	Density fitting or resolution of the identity	36
2.4.2	Cholesky decomposition	36
2.4.3	Tensor product approximation	37
2.4.4	Linear scaling approaches	38
3	Reduced-Rank Schrödinger equations	39
3.1	Introduction	39
3.2	Reduced-rank Schrödinger equations	42
3.3	Reduced-rank quantum chemistry models	43
3.3.1	Hartree-Fock theory	43
3.3.2	Perturbation theory	44
3.3.3	Configuration interaction	44
3.4	Auxiliary integrals	45
3.5	Numerical results	46
3.5.1	Basis sets	46
3.5.2	He atom and H ₂ molecule	46
3.5.3	Cost and accuracy	49
3.6	Concluding remarks	50
4	Bessel resolution of the Coulomb operator	53
4.1	Introduction	53
4.2	Bessel quasi-resolution	55
4.3	Numerical results	58
4.4	Concluding remarks	61
5	Bessel resolution of the Ewald operator	63
5.1	Introduction	64
5.2	Resolutions of the Ewald operator	65
5.3	Computational considerations	67
5.4	Numerical results	69
5.5	Concluding remarks	70
5.6	Other resolutions of the Ewald operator	71

6	The evaluation of auxiliary integrals	73
6.1	Resolution of two-body operators	73
6.2	Auxiliary integrals	74
6.3	Bessel resolution and Gaussian function	75
6.4	Computational considerations	76
6.5	Numerical results	79
6.5.1	Accuracy test	80
6.5.2	Scaling test	80
6.6	Concluding remarks	83
7	A remarkable Bessel identity	85
7.1	Introduction	86
7.2	Preliminaries	88
7.3	Main results	90
7.4	Numerical results	95
7.5	Concluding remarks	96
8	Summary and future directions	97
8.1	Summary	97
8.2	Future directions	99
A	Computational notes	101
B	Molecular geometries	103
	Bibliography	112

Publications and proceedings

This thesis contains materials published in peer-reviewed journals, presented at international conferences and derived from work in collaboration with others. I present these here with contribution declarations. Resolutions of the Coulomb operator is a series of papers. Previous work [1, 2, 3] is reviewed in §2.1.

Publications:

- “Resolutions of the Coulomb operator:
III. Reduced-rank Schrödinger equations”
by Taweetham Limpanuparb and Peter M. W. Gill
published in *Phys. Chem. Chem. Phys.*, 2009, **11** (40), pp 9176–9181 [4]
This material is presented in Chapter 3. Taweetham Limpanuparb is the principal author and conducted the majority of the research under supervision of Peter M. W. Gill.
- “Resolutions of the Coulomb Operator:
IV. The Spherical Bessel Quasi-Resolution”
by Taweetham Limpanuparb, Andrew T. B. Gilbert and Peter M. W. Gill
published in *J. Chem. Theory Comput.*, 2011, **7** (4), pp 830–833 [5]
This material is presented in Chapter 4. Taweetham Limpanuparb is the principal author and conducted the majority of the research under supervision of Peter M. W. Gill and Andrew T. B. Gilbert.
- “Resolutions of the Coulomb Operator:
V. The Long-Range Ewald Operator”
by Taweetham Limpanuparb and Peter M. W. Gill
published in *J. Chem. Theory Comput.*, 2011, **7** (8), pp 2353–2357 [6]
This material is presented in Chapter 5. Taweetham Limpanuparb is the principal author and conducted the majority of the research under supervision of Peter M. W. Gill.

- “A Remarkable Identity Involving Bessel Functions”
by Diego E. Dominici, Peter M.W. Gill and Taweetham Limpanuparb
published online at arxiv.org (arXiv:1103.0058v1) [7]¹

This material is presented in Chapter 7. Taweetham Limpanuparb and Peter M. W. Gill discovered the identity. Introduction, numerical results and concluding remarks sections were written by Taweetham Limpanuparb under supervision of Peter M. W. Gill. Diego E. Dominici provided a proof and wrote preliminaries and main results sections.

Proceedings

- “Resolutions of $1/r_{12}$ and its application in quantum chemistry”
by Taweetham Limpanuparb and Peter M. W. Gill
A contributed talk in physical and theoretical chemistry session
Pure and Applied Chemistry International Conference, Bangkok, 2011

This material is presented in Chapter 3. Taweetham Limpanuparb conducted the research under supervision of Peter M. W. Gill.
- “Resolving the Coulomb operator:
A new approach towards faster QM Methods”
by Taweetham Limpanuparb and Peter M. W. Gill
A contributed talk in electron correlation theory session
The 7th Congress of the International Society for Theoretical Chemical
Physics, Tokyo, 2011

This material is presented in Chapter 3 to Chapter 5. Taweetham Limpanuparb conducted the the research under supervision of Peter M. W. Gill.

The structure of scientific manuscript is preserved in chapters mentioned above. However, for clarity and consistency, some parts of the materials were revised, removed or extended to fit the presentation of this thesis.

¹This was later expanded and submitted to *Proc. R. Soc. A* [10.1098/rspa.2011.0664].

Notation and symbol

In this thesis, we have used the following choice of notation and symbol. Atomic units and real orbitals are used throughout unless otherwise stated.

Notation

a	is a scalar.
a^*	is a complex conjugate of a .
$ a $	is an absolute value of a .
$(a)_n$	is the Pochhammer symbol or rising factorial
\mathbf{a}	is a vector.
$ \mathbf{a} $	is a norm of vector \mathbf{a} .
\mathbf{A}	is a matrix.
\mathbf{A}^\dagger	is a conjugate transpose of matrix \mathbf{A} .
\mathbf{I}	is the identity matrix.
$\text{Tr}[\mathbf{A}]$	is a trace of matrix \mathbf{A} .
i	is the imaginary unit, $i^2 = -1$.
$f(r)$	is a function of r .
$\hat{f}(x)$	is a Fourier transform of $f(r)$.
\overline{F}	is an operator.
$\Re(z)$	is the real part of z .
$\Im(z)$	is the imaginary part of z .

Mathematical symbol

$B_z(a, b)$	Incomplete beta function
$\binom{n}{k}$	binomial coefficient
$C_n^{(\lambda)}(z)$	Gegenbauer (or ultraspherical) polynomial
$C_{m,m',m+m'}^{l,l',k}$	Clebsch-Gordan coefficient
$\delta(x)$	Dirac delta function
$\delta_{i,j}$	Kronecker delta
${}_pF_q \left(\begin{matrix} a_1, \dots, a_p \\ b_1, \dots, b_q \end{matrix} ; z \right)$	hypergeometric function
${}_p\tilde{F}_q \left(\begin{matrix} a_1, \dots, a_p \\ b_1, \dots, b_q \end{matrix} ; z \right)$	regularized hypergeometric function
$\Gamma_n(z)$	Gamma function
$H(x)$	Heaviside step function
$H_n(z)$	Hermite polynomial (physicists' Hermite polynomial)
$I(z)$	modified Bessel function of the first kind
$i(z)$	modified spherical Bessel function of the first kind
$J(z)$	Bessel function of the first kind
$j(z)$	spherical Bessel function of the first kind
$L_n(z)$	Laguerre polynomial
$\mathbf{L}_\alpha(z)$	modified Struve function
P_l	Legendre polynomial
$U(x, y)$	parabolic cylinder function
$Y_l^m(\mathbf{r})$	complex spherical harmonic
$Y_{lm}(\mathbf{r})$	real spherical harmonic

For more comprehensive definition of these symbols, see [8, 9, 10].

Chemical symbol

B	number of basis functions
E	energy
L	angular momentum in basis set
N	number of electrons or normalization constant
ζ	Gaussian basis function's exponent
ω	range-separation parameter
$\rho(\mathbf{r})$	electron density
Ψ	wavefunction
φ_μ	atomic orbital
ψ_i	molecular orbital
ε_i	orbital energy
τ	spin variable
$\langle a b\rangle$	$\int a^*(\mathbf{r})b(\mathbf{r})d\mathbf{r}$
$\langle a \bar{T} b\rangle$	$\int \int a^*(\mathbf{r}_1)T(\mathbf{r}_1, \mathbf{r}_2)b(\mathbf{r}_2)d\mathbf{r}_1d\mathbf{r}_2$

For more comprehensive definition of these symbols, see [11].

Resolution symbol

ϕ_k	resolution function
$\mathcal{N}, \mathcal{L}, \mathcal{K}$	truncation points of infinite resolution
\mathcal{Z}	scaling factor
Δ	logarithm of absolute error of resolution calculation
ϵ	relative error of resolution calculation

For more comprehensive definition of these symbols, see §2.1, §3.3, §4.3 and §5.3.

Chapter 1

QM methods



Erwin Schrödinger (1887–1961) Paul Adrien Maurice Dirac (1902–1984)

The Nobel Prize in Physics 1933 was awarded jointly to Erwin Schrödinger and Paul Adrien Maurice Dirac “for the discovery of new productive forms of atomic theory” [12].

$$\overline{\mathcal{H}}\Psi = E\Psi$$

— Schrödinger, 1926 [13, 14]

“The underlying physical laws necessary for the mathematical theory of a large part of physics and the whole of chemistry are thus completely known, and the difficulty is only that the exact application of these laws leads to equations much too complicated to be soluble. It therefore becomes desirable that approximate **practical methods of applying quantum mechanics should be developed**, which can lead to an explanation of the main features of complex atomic systems without too much computation.”

— Dirac, 1929 [15]

The birth of quantum mechanics dates back to early 19th century. Classical or Newtonian mechanics failed to explain a number of experiments, for example, blackbody radiation, gas discharge tube and cathode ray. Attempts to explain these experiments led to the discovery of a new concept of physics whereby energy levels are not continuous but discrete.

During the 19th century and early 20th century, there were many renowned scientists including Boltzmann [16], Planck [17], Einstein [18], de Broglie [19] and Heisenberg [20] involved in the conception of this new field of physics. As the unique feature of this new theory is the discretization or quantization of energy levels, it later became known as “quantum mechanics”. The term was first used by Born in early 1920s [21].

The two most important theoretical developments to the field were the formulation of the Schrödinger equation in 1926 [13, 14] and its relativistic extension, the Dirac equation in 1928 [22]. In principle, we can predict any *observable* of a system of interest from the wavefunction Ψ obtained by solving one of the two equations. Therefore, the solutions are of great importance to scientists.

However, Dirac made the popular quote in his 1929 proceeding [15] that mathematical description of physics and chemistry is mostly known and the only major problem left is to obtain numerical solutions from the theory. Time has proven that Dirac’s comment is correct. The equations can be solved exactly for one-electron systems but have proven difficult in most other cases.

There have been numerous attempts to solve the Schrödinger and the Dirac equations. Even with the massive computing power available in the 21st century, *ab initio* methods, based on solving equations using the first principles of quantum mechanics, are still relatively expensive and are limited to moderately-sized molecules.

For molecular systems, the Hamiltonian operator $\overline{\mathcal{H}}$ and wavefunction Ψ depends on time and coordinates of all nuclei and electrons. In this thesis, we are only interested in time-independent non-relativistic electronic Schrödinger equation. The justification to remove the dependence on nuclear coordinates is the Born-Oppenheimer approximation [23] and the dependence on time is removed because we are interested in stationary states of a system. We will therefore deal with electronic Hamiltonian operator of the form:

$$\overline{\mathcal{H}}_e = -\frac{1}{2} \sum_i \nabla_i^2 - \sum_{i,A} \frac{Z_A}{r_{iA}} + \sum_{i>j} \frac{1}{r_{ij}} \quad (1.1)$$

where i and j represent electrons, A represents nuclei and ∇^2 is the Laplacian.

The electronic Schrödinger equation is a partial differential equation. The Hamiltonian operator $\bar{\mathcal{H}}$ is known from a description of the system – coordinates and charges of nuclei and total number of electrons. We want to solve the equation for wavefunction Ψ and energy E . The strategy mathematicians often use to solve this kind of equation is to start with a guess form of Ψ .

The most difficult terms in the equation are r_{ij}^{-1} which describe electron-electron interactions. Without these terms, the equation could be exactly solvable. However, we do not have a liberty to simply drop these terms from the Hamiltonian but rather have to deal with them wisely.

In this chapter, the standard quantum mechanics methods that will be referred to in later chapters are briefly summarized.

1.1 Hartree-Fock wavefunction

In 1928, Hartree [24] suggested that the wavefunction of an N -electron system is simply a product of one-electron wavefunctions.

$$\Psi(r_1, r_2, r_3, \dots, r_N) = \chi_1(r_1)\chi_2(r_2)\chi_3(r_3) \dots \chi_N(r_N) \quad (1.2)$$

This guess was inadequate because this form of wavefunction implies that electrons are distinguishable and does not comply with the well-known *Pauli exclusion principle* formulated in 1925 [25].

In 1930, Fock [26] improved this guess by using linear combination of all possible permutations of N individual wavefunctions. The general expression of Hartree-Fock Ψ can be described by a *Slater determinant*

$$\Psi(\mathbf{x}_1, \mathbf{x}_2, \dots, \mathbf{x}_N) = \frac{1}{\sqrt{N!}} \begin{vmatrix} \chi_1(\mathbf{x}_1) & \chi_2(\mathbf{x}_1) & \cdots & \chi_N(\mathbf{x}_1) \\ \chi_1(\mathbf{x}_2) & \chi_2(\mathbf{x}_2) & \cdots & \chi_N(\mathbf{x}_2) \\ \vdots & \vdots & & \vdots \\ \chi_1(\mathbf{x}_N) & \chi_2(\mathbf{x}_N) & \cdots & \chi_N(\mathbf{x}_N) \end{vmatrix} \quad (1.3)$$

where $\mathbf{x}=\{\mathbf{r}, \tau\}$. The one-electron spin orbital χ_i is a product of a spatial orbital $\psi(\mathbf{r})$ and a spin function $\alpha(\tau)$ or $\beta(\tau)$ which are orthonormal $\langle \chi_i | \chi_j \rangle = \delta_{ij}$, $\langle \alpha | \alpha \rangle = \langle \beta | \beta \rangle = 1$ and $\langle \alpha | \beta \rangle = 0$.

In an unrestricted Hartree-Fock (UHF) calculation, there are two sets of spatial orbitals $\psi^\alpha(\mathbf{r})$ and $\psi^\beta(\mathbf{r})$ for α and β electrons. This is the most general and expensive form of HF theory. However, it is not necessary to differentiate between the two spins in a closed-shell system (even number of electrons and all

electrons are paired), thus only one set of $\psi(\mathbf{r})$ is used in a restricted Hartree-Fock (RHF) calculation. A variant of RHF for open-shell system is “restricted open-shell Hartree-Fock” (ROHF) where doubly occupied molecular orbitals are used as far as possible and singly occupied orbitals are then used for unpaired electrons.

This *antisymmetric* HF wavefunction (1.3) leads to HF energy.

$$E_{\text{HF}} = \sum_i H_i + \sum_{i < j} (J_{ij} - K_{ij}) \quad (1.4)$$

where H_{ii} are one-electron integrals and Coulomb integral J_{ij} and exchange integral K_{ij} are two-electron integrals.

$$H_i = \int \chi_i^*(\mathbf{x}_1) \left(\frac{1}{2} \nabla_1^2 - \sum_A \frac{Z_A}{r_{1A}} \right) \chi_i(\mathbf{x}_1) d\mathbf{x}_1 \quad (1.5)$$

$$J_{ij} = \int \int \chi_i^*(\mathbf{x}_1) \chi_i(\mathbf{x}_1) \frac{1}{r_{12}} \chi_j^*(\mathbf{x}_2) \chi_j(\mathbf{x}_2) d\mathbf{x}_1 d\mathbf{x}_2 \quad (1.6)$$

$$K_{ij} = \int \int \chi_i^*(\mathbf{x}_1) \chi_j(\mathbf{x}_1) \frac{1}{r_{12}} \chi_j^*(\mathbf{x}_2) \chi_i(\mathbf{x}_2) d\mathbf{x}_1 d\mathbf{x}_2 \quad (1.7)$$

The Coulomb term can be classically interpreted as the repulsion energy between two spatial orbitals which have electron densities $|\psi_i|^2$ and $|\psi_j|^2$. In contrast, the exchange interaction is a result of the exclusion principle and is a purely quantum mechanical effect with no classical analog.

The above formulae describe the heart of HF theory but in practice one still need further information about molecular orbitals ψ_i to calculate the energy. The two subsections below explain how we obtain the HF orbitals.

1.1.1 Basis set

In 1929, Lennard–Jones [27] proposed the Linear Combination of Atomic Orbitals (LCAO) approximations. The means spatial molecular orbitals (MO) $\psi(\mathbf{r})$ are expanded in the basis of atomic orbitals (AO) $\varphi(\mathbf{r})$.

$$\psi_i(\mathbf{r}) = \sum_{\nu} c_{\nu i} \varphi_{\nu}(\mathbf{r}) \quad (1.8)$$

The AOs can be modelled by a set of basis functions.

In theory, there is a myriad of basis functions that one can use for AOs. In 1930, Slater proposed Slater-type orbitals (STO) which decay exponentially with distance [28].

$$\varphi^{\text{STO}}(x, y, z) = N_{\alpha, a_x, a_y, a_z}^{\text{STO}} (x - A_x)^{a_x} (y - A_y)^{a_y} (z - A_z)^{a_z} \exp(-\alpha |\mathbf{r} - \mathbf{A}|) \quad (1.9)$$

The rationale behind STOs is that they resemble the exact solution of the Schrödinger equation for hydrogenic ions. However, the STO basis has led to difficulties in the two-electron integral calculations that are at the heart of quantum chemical methods.

In 1950, Boys suggested Gaussian-type orbitals (GTO) [29].

$$\varphi^{\text{GTO}}(x, y, z) = N_{\alpha, a_x, a_y, a_z}^{\text{GTO}} (x - A_x)^{a_x} (y - A_y)^{a_y} (z - A_z)^{a_z} \exp(-\alpha |\mathbf{r} - \mathbf{A}|^2) \quad (1.10)$$

They do not have a cusp nor correct long-range decay behavior for wavefunctions but are much easier to manipulate. This was an important breakthrough and calculations today are mostly performed using GTOs. There are numerous GTO basis sets available for quantum chemical calculations. Most of basis sets often used in quantum chemistry fall into three categories.

- Minimal basis sets, for example, STO-nG, are relatively small basis sets. They often yield rough results but are computationally cheap.
- Split-valence basis sets, for example, Pople's X-YZG and X-YZWG are basis sets that represent valence orbitals by more than one basis function.
- Correlation-consistent basis sets, for example, Dunning's cc-pVNZ are basis sets that are designed to converge systematically to the complete-basis-set (CBS) limit.

1.1.2 The self-consistent field procedure

From the time-independent electronic Schrödinger equation and HF theory with LCAO approximation one can derive Pople-Nesbet-Berthier equations [30].

$$\begin{aligned} \mathbf{F}^\alpha \mathbf{C}^\alpha &= \mathbf{S} \mathbf{C}^\alpha \epsilon^\alpha \\ \mathbf{F}^\beta \mathbf{C}^\beta &= \mathbf{S} \mathbf{C}^\beta \epsilon^\beta \end{aligned} \quad (1.11)$$

In the RHF version, the two matrix equations above are reduced to one because we just need one spatial orbital per pair of electrons. In this case, the

equations are called Roothaan-Hall equations [31, 32].

$$\mathbf{FC} = \mathbf{SC}\varepsilon \quad (1.12)$$

$$F_{\mu\nu} = H_{\mu\nu}^{\text{core}} + \sum_{\lambda\sigma} P_{\lambda\sigma} \left[(\mu\nu|\lambda\sigma) - \frac{1}{2}(\mu\sigma|\lambda\nu) \right] \quad (1.13)$$

$$H_{\mu\nu}^{\text{core}} = \int \varphi_{\mu}^*(\mathbf{r}_1) \left(\frac{1}{2}\nabla_1^2 - \sum_A \frac{Z_A}{r_{1A}} \right) \varphi_{\nu}(\mathbf{r}_1) d\mathbf{r}_1 \quad (1.14)$$

$$P_{\mu\nu} = 2 \sum_i^N c_{\mu i} c_{\nu i} \quad (1.15)$$

$$(\mu\nu|\lambda\sigma) = \int \int \varphi_{\mu}^*(\mathbf{r}_1) \varphi_{\nu}(\mathbf{r}_1) \frac{1}{r_{12}} \varphi_{\lambda}^*(\mathbf{r}_2) \varphi_{\sigma}(\mathbf{r}_2) d\mathbf{r}_1 d\mathbf{r}_2 \quad (1.16)$$

$$S_{\mu\nu} = \int \varphi_{\mu}^*(\mathbf{r}_1) \varphi_{\nu}(\mathbf{r}_1) d\mathbf{r}_1 \quad (1.17)$$

The MO coefficients \mathbf{C} and the orbital energies ε are unknown and need to be determined. The overlap matrix \mathbf{S} can be calculated independently. However, \mathbf{F} depends on \mathbf{C} and this suggests that the equations must be solved iteratively.

The equations can be further simplified to an eigenvalue problem. First, we need to find a matrix \mathbf{X} which orthonormalizes the AO basis.

$$\mathbf{X}^{\dagger} \mathbf{S} \mathbf{X} = \mathbf{I} \quad (1.18)$$

An obvious choice of \mathbf{X} is $\mathbf{S}^{-1/2}$. This matrix is multiplied to the left of Roothaan-Hall equations and yields

$$\mathbf{F}' \mathbf{C}' = \mathbf{C}' \varepsilon \quad (1.19)$$

$$\mathbf{F}' = \mathbf{X}^{\dagger} \mathbf{F} \mathbf{X} \quad (1.20)$$

$$\mathbf{C} = \mathbf{X} \mathbf{C}' \quad (1.21)$$

We solve these equations by the self-consistent field (SCF) procedure:

1. Obtain an initial guess for the density matrix \mathbf{P} .
2. Build the Fock matrix \mathbf{F} .
3. Construct \mathbf{F}' and diagonalize it to get \mathbf{C}' .
4. Construct the MO coefficient \mathbf{C} .
5. Calculate the new density matrix \mathbf{P} and energy $E = \frac{1}{2} \text{Tr}[\mathbf{P}(H^{\text{core}} + \mathbf{F})]$.
6. If E and/or \mathbf{P} are not converged go to step 2. Otherwise, stop.

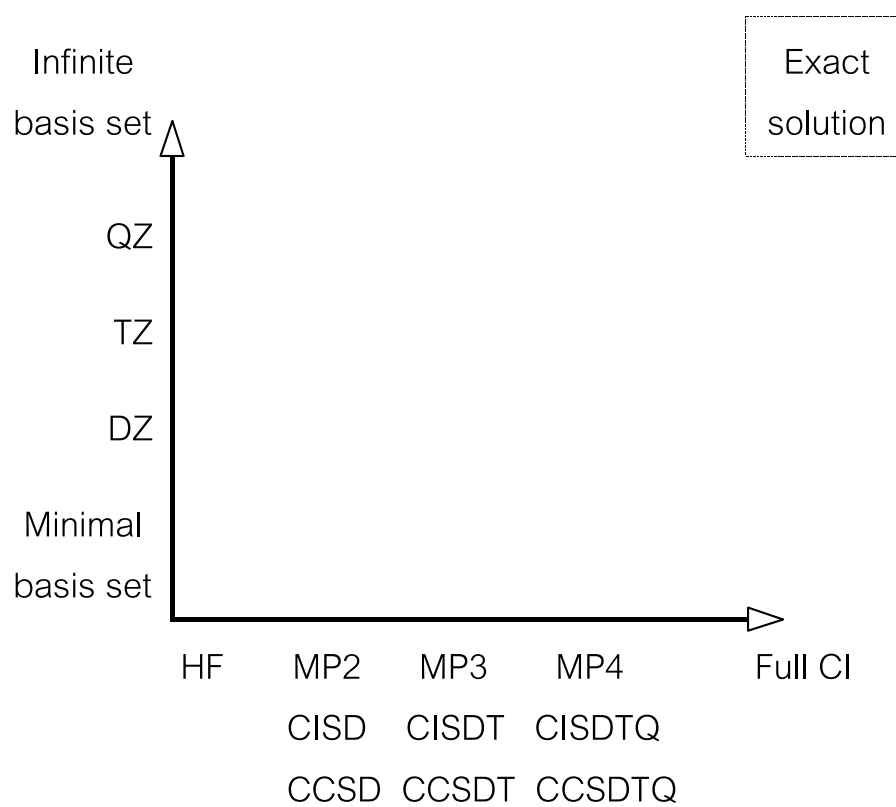


Figure 1.1: Pople diagram [33]

1.2 Post-HF methods

Hartree-Fock theory is arguably the simplest approach to obtain approximate ground-state wavefunctions and energies, that is to obtain solutions to the Schrödinger equation. However, there are a number of factors that make HF solutions differ from the correct answers.

- External electromagnetic field and relativistic effect are usually neglected. This is only noticeable for calculation involving heavy atoms or strong external field.
- We solely deal with electronic wavefunction because nuclear masses are much greater than electronic masses (Born-Oppenheimer approximation). This can lead to an incorrect description of tunneling for light atoms.
- Theoretically, we need an infinite number of basis functions to completely and accurately model molecular wavefunctions. However, in reality, we have a finite computing resource and are forced to use sensible and affordable basis sets. It is usually not practical to perform calculations at CBS limit.
- Mean-field approximation is a fundamental flaw in HF theory. Replacing the electron-electron interactions by an average interaction neglects electron correlation. (Some electron correlation, between like-spin electrons, is already treated in the exchange term.)

The last two factors are often most pronounced and need to be systematically addressed together. This can be summarized in a Pople diagram which shows a combination of method and basis set chosen for a calculation.

We discuss below three methods that provide remedy to HF fundamental failure to capture electron correlation. They are classified as post-HF methods because HF solutions form a basis for the construction of more a flexible wavefunction whose exact form is determined by the nature of each post-HF method.

1.2.1 Møller-Plesset perturbation theory

Rayleigh-Schrödinger perturbation theory (RSPT) was introduced to quantum mechanics in Schrödinger's 1926 paper [34] that made a reference to the work of Lord Rayleigh [35]. Møller-Plesset perturbation theory (MPPT) is a special application of RSPT proposed by Møller and Plesset [36].

Perturbation theory is based on the assumption that $\overline{\mathcal{H}}_0$ differs only slightly from the exact $\overline{\mathcal{H}}$ and the contribution from perturbation term \overline{V} is small. Under this condition, one can expand the eigenvalues and eigenfunctions as Taylor series in λ , a parameter which will be set to unity later.

$$\overline{\mathcal{H}} = \overline{\mathcal{H}}_0 + \lambda \overline{V} \quad (1.22)$$

$$E = \lambda^0 E^{(0)} + \lambda^1 E^{(1)} + \lambda^2 E^{(2)} + \dots \quad (1.23)$$

$$\Psi = \lambda^0 \Psi^{(0)} + \lambda^1 \Psi^{(1)} + \lambda^2 \Psi^{(2)} + \dots \quad (1.24)$$

$$E_{\text{MP}n} \equiv E^{(n)} \quad (1.25)$$

There exists two formulations of perturbation theory. The original one gives $E_{\text{MP}0} = E_{\text{HF}}$ and $E_{\text{MP}1} = 0$ while the chemistry formulation gives $E_{\text{MP}0} + E_{\text{MP}1} = E_{\text{HF}}$. The higher-order corrections are the same in both formulations and we first obtain a correction to HF energy at MP2 level. The MP2 energy is given by

$$E_{\text{MP}2} = \sum_{ijab} (ia|jb) \times \frac{2(ia|jb) - (ja|ib)}{\varepsilon_i + \varepsilon_j - \varepsilon_a - \varepsilon_b} \quad (1.26)$$

$$(ia|jb) = \int \int \psi_i^*(\mathbf{r}_1) \psi_a(\mathbf{r}_1) \frac{1}{r_{12}} \psi_j^*(\mathbf{r}_2) \psi_b(\mathbf{r}_2) d\mathbf{r}_1 d\mathbf{r}_2 \quad (1.27)$$

where i, j are labels of occupied orbitals and a, b are labels of virtual orbitals.

Though the MP n calculation can be done up to an arbitrary order in theory, the cost of the calculation will skyrocket. Perturbation theory is not variational but size consistent at any order. MP2 is considered as one of the computationally cheapest methods to obtain a correlation correction to HF energy. However, the MP n convergence behavior was described as “slow, rapid, oscillatory, regular, highly erratic or simply non-existent, depending on the precise chemical system or basis set” in Leininger *et. al.*’s 2000 paper. [37]

MP2, MP3, MP4 and sometimes MP5 are used in quantum chemistry calculations. Typically a large fraction of the correlation energy is recovered at MP2 level whose formal computational cost is quintic with respect to the size of basis set. Higher-order MP theory are expensive and may be less competitive compared to other post-HF methods.

1.2.2 Configuration interaction

Configuration interaction (CI), the conceptually simplest method for post-HF correlation energy was developed by Boys in 1950s [38]. In this method, the exact

electronic wavefunction is obtained by mixing (interaction) all the different electronic states (configurations).

$$\Psi_{\text{FCI}} = c_0\Psi_0 + \sum_{ar} c_a^r\Psi_a^r + \sum_{abrs} c_{ab}^{rs}\Psi_{ab}^{rs} + \sum_{abcrst} c_{abc}^{rst}\Psi_{abc}^{rst} + \dots \quad (1.28)$$

$$|\Psi_0\rangle = |\chi_1\chi_2\dots\chi_a\chi_b\dots\chi_N\rangle \quad (1.29)$$

$$|\Psi_a^r\rangle = |\chi_1\chi_2\dots\chi_r\chi_b\dots\chi_N\rangle \quad (1.30)$$

$$|\Psi_{ab}^{rs}\rangle = |\chi_1\chi_2\dots\chi_r\chi_s\dots\chi_N\rangle \quad (1.31)$$

where a, b, c, \dots represents occupied orbitals and r, s, t, \dots represent virtual orbitals. $|\Psi_0\rangle, |\Psi_a^r\rangle, |\Psi_{ab}^{rs}\rangle$ are ground state, singly-excited and doubly-excited determinants respectively. (See the definition of Slater determinant in HF section.)

If the basis set is complete and all configurations are used, the CI method gives the exact solution to Schrödinger equation. This is the most accurate, the most expensive, size-consistent and variational procedure in quantum chemistry. Unfortunately, because the computational cost grows exponentially with respect to the size of basis set, CI methods are still only applicable to small atoms and molecules.

However, there are other cheaper variants of CI methods. To avoid confusion, we refer to the method that use all configurations as full CI (FCI). One can obtain less expensive and computationally feasible methods by truncating the FCI wavefunction. CID, CISD and CISDT are examples of these variants. The S, D or T mean that the method incorporates single, double or triple electronic excitations into the wavefunction. Unlike MP theory, truncated CI methods are not size-consistent but variational.

1.2.3 Coupled cluster

Coupled cluster (CC) method was developed in 1950s by Coester and Kümmel for nuclear physics problems. It was later introduced into quantum chemistry by Čížek [39] and Paldus [40]. The derivation starts from the excitation operator $\bar{\mathcal{T}}$ which is related to the FCI wavefunction.

$$\bar{\mathcal{T}} = \bar{\mathcal{T}}_1 + \bar{\mathcal{T}}_2 + \bar{\mathcal{T}}_3 + \dots \quad (1.32)$$

$$\bar{\mathcal{T}}_1|\Psi_0\rangle = \sum_{ar} c_a^r|\Psi_a^r\rangle \quad (1.33)$$

$$\bar{\mathcal{T}}_2|\Psi_0\rangle = \sum_{abrs} c_{ab}^{rs}|\Psi_{ab}^{rs}\rangle \quad (1.34)$$

$$|\Psi_{\text{FCI}}\rangle = (1 + \bar{\mathcal{T}})|\Psi_0\rangle \quad (1.35)$$

The CC wavefunction is defined by

$$|\Psi_{\text{CC}}\rangle = e^{\bar{\mathcal{T}}}\Psi_0 \quad (1.36)$$

$$e^{\bar{\mathcal{T}}} = \frac{\bar{\mathcal{T}}^0}{0!} + \frac{\bar{\mathcal{T}}^1}{1!} + \frac{\bar{\mathcal{T}}^2}{2!} + \dots \quad (1.37)$$

As in CI methods, in practice, $\bar{\mathcal{T}}$ is truncated so that only the few first terms are included. The same name conventions are used for CC, for example, CCSD means single excitation operator $\bar{\mathcal{T}}_1$ and double excitation operator $\bar{\mathcal{T}}_2$ are used in the method. CCSD are size-consistent and capture more correlation energy than CISD. However, it should be noted that CC methods are not variational.

CCSD(T) [41] is often called a gold standard in quantum chemistry for its excellent compromise between the accuracy and computational cost. CCSDT and CCSDTQ are expensive and only used for small molecules.

1.3 Alternative approaches

In the previous two sections, the HF and post-HF methods, traditional ways of solving electronic Schrödinger equation are presented. In this section, we turn to a number of recent promising alternatives.

1.3.1 Composite methods

Quantum chemistry composite methods (or thermochemical recipes [42]) combine results of several calculations at different theory/basis set levels to get high accuracy results (often within 1 kcal/mol of the experimental value or chemical accuracy). The approach carefully mixes high level of theory/small basis set and low level of theory/large basis set to mimic the result of high level of theory/large basis set. Composite methods often start with geometry optimization, follow by several electronic calculations and end with a frequency calculation to obtain the zero-point vibrational energy (ZPVE).

In 1989, Pople introduced his first composite method for broad chemistry application, Gaussian-1 (G1) [43]. It was quickly replaced by its successor G2 [44]. Composite methods used today include CBS [45, 46], G_n [45, 47], W_n [48], T1 [42], ccCA [49], HEAT [50] and their variants.

1.3.2 Multireference methods

Instead of using a single Slater determinant obtained from HF, multireference methods start with several chemically relevant determinants.

$$\Psi_{\text{MCSCF}} = \sum_i^{N_{\text{CONFIG}}} C_i \Psi_i \quad (1.38)$$

The SCF process in this context is called multi-configurational self-consistent field (MCSCF) [51]. MCSCF can be classified into

- Complete active space SCF (CASSCF)
- Restricted active space SCF (RASSCF)

MCSCF can also be regarded to as a generalization of CI with restricted excitation space and concurrent orbital optimization. In analogous to HF and post-HF methods, there are a number of methods that build upon MCSCF, for example,

- Multireference configuration interaction (MRCI)
- Complete active space perturbation theory (CASPT2)
- Multireference coupled-cluster (MRCC)

1.3.3 Density functional theory

The QM methods described in the previous sections are based on the electronic wavefunction that is a function of the coordinates of all electrons. This makes these theories computationally expensive. Density functional theory (DFT) is instead concerned with the electron density.

$$\rho(\mathbf{r}) = N \int \int \dots \int |\Psi(\mathbf{r}, \mathbf{r}_2, \mathbf{r}_3, \dots, \mathbf{r}_N)|^2 d\mathbf{r}_2 d\mathbf{r}_3 \dots d\mathbf{r}_N \quad (1.39)$$

The root of DFT concept is in the Thomas-Fermi model of electron gas [52, 53] but is rigorously proven by two Hohenberg-Kohn theorems [54].

- The first theorem states that the electronic ground state of a system can be uniquely determined by the electron density that depends on only three spatial coordinates.
- The second theorem states that DFT is variational *i.e.* the correct density with a hypothetical “exact functional” will give the lowest energy.

Kohn and Sham [55] developed the theory further by partitioning the energy into terms and introducing orbitals that provide a practical implementation of the theory. The Kohn-Sham equation is analogous to HF equation and can be solved by a similar SCF procedure.

$$E[\rho(\mathbf{r})] = E_V[\rho(\mathbf{r})] + E_T[\rho(\mathbf{r})] + E_J[\rho(\mathbf{r})] + E_{XC}[\rho(\mathbf{r})] \quad (1.40)$$

The first three terms on the right are the nuclear potential, kinetic and Coulomb energies that can be calculated in the same way as in HF calculation. However, the last term, the exchange-correlation energy, is not trivial and is the most important issue in DFT.

The first Hohenberg-Kohn theorem only states the existence of relationship between electron density and energy but does not give any further information on how to extract energy from the density.

There have been countless attempts to obtain the best functional that works for all chemical systems. It was not until 1990s that reasonably accurate DFT functionals were developed and became popular among computational chemists.

B3LYP (Becke, three-parameter, Lee-Yang-Parr) [56, 57, 58] is arguably the most popular DFT functional at present.

$$E_{xc}^{\text{B3LYP}} = E_{xc}^{\text{LDA}} + a_0(E_x^{\text{HF}} - E_x^{\text{LDA}}) + a_x(E_x^{\text{GGA}} - E_x^{\text{LDA}}) + a_c(E_c^{\text{GGA}} - E_c^{\text{LDA}}) \quad (1.41)$$

The B3LYP parameters $a_0 = 0.20$, $a_x = 0.72$ and $a_c = 0.81$ were empirically determined by fitting the DFT energy to reproduce experimental results. LDA stands for local-density approximation and GGA stands for generalized gradient approximations.

B3LYP is a *hybrid functional* because it incorporates exchange energy from the Hartree-Fock theory with exchange and correlation from other sources. The hybrid approach was introduced by Becke in 1993 [56] and was found to improve many molecular properties.

Because of the parameterization and theoretical inadequacy of functionals, DFT may give erroneous results when used beyond their fitting data sets or assumptions of the functionals [59, 60].

DFT is also known to be incompetent for the description of intermolecular interactions, especially dispersion or van der Waals forces. One simple modification to solve this problem is to incorporate energy from long-range Coulomb operator $\text{erf}(\omega r_{12})/r_{12}$ into DFT functionals [61, 62, 63, 64, 65] but there exists a number of other attempts [66, 67, 68].

1.3.4 Other methods

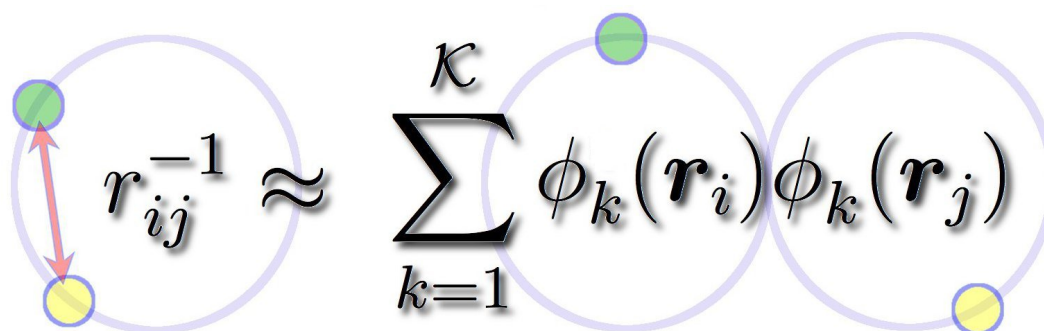
Apart of the mainstream methods briefly described above, there are also other theoretically promising QM methods being developed that are worth mentioning.

- Explicit r_{12} methods explicitly includes interelectronic distance into trial wavefunctions. The idea was first suggested by Hylleraas in 1927 [69] and later revisited by Kutzelnigg and explored by many others [70]. R12 approach speeds up the basis set convergence because they have correct description of the Coulomb cusp.
- Intracule functional theory (IFT) [71] is the two-electron analogue of DFT. It aims to remedy DFT well-known systematic failure by using two-electron “Fertile Crescent”, a largely unexplored land of quantum chemistry.
- Scaled Schrödinger equation developed by Nakatsuji [72] provides extremely accurate results beyond chemical accuracy for very small atoms and molecules.
- Reduced density matrix (RDM) idea was proposed by Coulson in 1959 [73]. The calculation was done using a reduced density matrix instead of a wavefunction.
- Quantum Monte Carlo (QMC) calculations use Monte Carlo method to simulate quantum systems [74].

For a comprehensive recent review, see “Solving the Schrödinger Equation: Has Everything Been Tried?” a 2011 book edited by Popelier [75].

Chapter 2

Resolutions of the Coulomb operator


$$r_{ij}^{-1} \approx \sum_{k=1}^{\mathcal{K}} \phi_k(\mathbf{r}_i) \phi_k(\mathbf{r}_j)$$

The idea of resolutions of the Coulomb operator was first conceived in Gilbert's 1996 Honours thesis supervised by Gill [1]. It was expanded and published in a series of papers [2, 3, 4, 5, 6, 7]. We summarize some basic concepts of resolutions of the Coulomb operator (RO) [1, 2, 3] in §2.1, derive an extension to symmetric kernel functions in §2.2 and discuss related techniques in §2.3.

2.1 Basic theory

In Chapter 1, we have described the non-relativistic electronic Schrödinger equation for an N -electron system. The Hamiltonian consists of two major parts, the trivial one-electron terms and the troublesome two-electron terms.

$$\left[\sum_i^N \bar{h}(\mathbf{r}_i) + \sum_{i<j}^N r_{ij}^{-1} \right] \Psi = E\Psi \quad (2.1)$$

Why are these r_{ij}^{-1} terms so difficult? A theoretical answer is that the terms are responsible for the coupling of electron motion and create many body effects. A practical answer, on the other hand, is simply the difficulty in dealing with four-center two-electron integrals. The integrals resulting from r_{ij}^{-1} are at the heart of virtually all QM methods. Though efficient algorithms for integral evaluation *e.g.* PRISM [76] exists, the bottlenecks of QM calculations are still manipulation of these integrals.

A simple way to eliminate the coupling effect that makes the terms difficult is to write r_{ij}^{-1} as a sum of products of one-particle functions, in other words, resolving them. Historically, there have been a number of interests in resolving a two-particle symmetric function into one-particle functions.

In 1782, the Legendre expansion [77] partially resolves the radial part of r_{12}^{-1} into $r_>$ and $r_<$ (shorthand for $\min(r_1, r_2)$ and $\max(r_1, r_2)$ respectively). The Legendre polynomial P_l which represents the angular part can also be resolved into a sum of products of real spherical harmonics Y_{lm} .

$$\begin{aligned} r_{12}^{-1} &= \sum_{l=0}^{\infty} \frac{r_<^l}{r_>^{l+1}} P_l(\cos \gamma) \\ &= \sum_{l=0}^{\infty} \frac{4\pi}{2l+1} \frac{r_<^l}{r_>^{l+1}} \sum_{m=-l}^l Y_{lm}(\mathbf{r}_1) Y_{lm}(\mathbf{r}_2) \end{aligned} \quad (2.2)$$

In the early 20th century, the resolution problem was considered by Hilbert [78], Schmidt [79] and Mercer [80, 81]. In these works, only the convergence rate of resolutions was discussed for functions on compact domains.

Though Mercer's theorem or "kernel trick" does not apply to functions on an unbounded domain, it has been widely used in many computer science applications particularly machine learning since 1964 [82].

The first chemical interest in resolving two-particle functions was the work by Gilbert in 1996 [1]. The aim was to achieve linear-scaling Coulomb energy calculation by resolving the long-range Ewald operator based on the Coulomb orthonormal polynomials f_{lmn} . The original resolution was in the Cartesian form.

$$\frac{\text{erf}(\omega r_{12})}{r_{12}} \equiv \sum_{lmn} \phi_{lmn}(\mathbf{r}_1) \phi_{lmn}(\mathbf{r}_2) \quad (2.3)$$

$$\phi_{lmn}(\mathbf{r}) = \int f_{lmn}(\mathbf{r}') \frac{\text{erf}(\omega |\mathbf{r} - \mathbf{r}'|)}{|\mathbf{r} - \mathbf{r}'|} d\mathbf{r}' \quad (2.4)$$

$$f_{lmn}(\mathbf{r}) = \sum_{ijk} ijk C_{lmn} r_x^i r_y^j r_z^k \quad (2.5)$$

$${}_{ijk}M_{lmn} = \int \int r_x^i r_y^j r_z^k \exp \left[-2 \frac{|\mathbf{r}|^2 + |\mathbf{u}|^2}{\beta^2} \right] \frac{\text{erf}(|\mathbf{r} - \mathbf{u}|)}{|\mathbf{r} - \mathbf{u}|} u_x^l u_y^m u_z^n d\mathbf{r} d\mathbf{u} \quad (2.6)$$

Coefficients ${}_{ijk}C_{lmn}$ of the Coulomb orthogonal polynomials are obtained by inversion of the Cholesky decomposition of the monomials ${}_{ijk}M_{lmn}$ [1, 83].

Another related work was by Gill in 1997 [84]. The Ewald operator was expanded in a Taylor series.

$$\frac{\text{erf}(\omega r_{12})}{r_{12}} = \frac{2\omega}{\sqrt{\pi}} \sum_{n=0}^{\infty} \frac{(-\omega^2)^n}{n!(2n+1)} (r_1^2 + r_2^2 - 2\mathbf{r}_1 \cdot \mathbf{r}_2)^n \quad (2.7)$$

This was not satisfactory because it includes off-diagonal terms $r_1^2 + r_2^2$ [3]. Later in this chapter we discuss how they can be diagonalized.

It was not until 2008 that a rigorous foundation of resolutions of the Coulomb operator was published [2]. This first paper in the series discusses the resolution of a two-particle operator $T(r_{12})$ and provides an example for the Coulomb operator.

The derivation in [2] begins with $\{f_i\}$ which is a complete set of functions that are orthonormal with respect to an operator \bar{T} , *i.e.* \bar{T} -orthonormal.

$$\langle f_i | \bar{T} | f_j \rangle = \delta_{ij} \quad (2.8)$$

\bar{T} is a symmetric two-body operator that yields ϕ_k when it operates on f_k .

$$\bar{T}[f_k(\mathbf{r})] = \int f_k(\mathbf{r}') T(|\mathbf{r} - \mathbf{r}'|) d\mathbf{r}' \equiv \phi_k(\mathbf{r}) \quad (2.9)$$

From these definitions, one can expand arbitrary functions $a(\mathbf{r})$ and $b(\mathbf{r})$ as

$$\langle a | = \sum_i c_i \langle f_i | = \sum_i \langle a | \bar{T} | f_i \rangle \langle f_i | = \sum_i \langle a | \phi_i \rangle \langle f_i |, \quad (2.10)$$

$$|b\rangle = \sum_j |f_j\rangle c_j = \sum_j |f_j\rangle \langle f_j | \bar{T} | b \rangle = \sum_j |f_j\rangle \langle \phi_j | b \rangle. \quad (2.11)$$

The two-particle integral between the two functions can be factorized into a sum of one-particle overlap integrals or *auxiliary integrals*.

$$\begin{aligned} \langle a | \bar{T} | b \rangle &= \sum_{ij} \langle a | \phi_i \rangle \langle f_i | \bar{T} | f_j \rangle \langle \phi_j | b \rangle \\ &= \sum_{ij} \langle a | \phi_i \rangle \delta_{ij} \langle \phi_j | b \rangle = \sum_k \langle a | \phi_k \rangle \langle \phi_k | b \rangle \end{aligned} \quad (2.12)$$

This also shows that the operator \bar{T} and the kernel function $T(r_{12})$ may be resolved as a sum of products of ϕ_k .

$$\bar{T} = |\phi_k\rangle \langle \phi_k| \quad (2.13)$$

$$T(r_{12}) = \sum_k^{\infty} \phi_k^*(\mathbf{r}_1) \phi_k(\mathbf{r}_2) \quad (2.14)$$

As one specific practical example, the paper [2] describes a resolution of the Coulomb operator based on Hermite polynomials, H_n , which results in ϕ_k in a spherical form.

$$r_{12}^{-1} = \sum_{n=0}^{\infty} \sum_{l=0}^{\infty} \sum_{l=-m}^m \phi_{nlm}(\mathbf{r}_1) \phi_{nlm}(\mathbf{r}_2) \quad (2.15)$$

$$\phi_{nlm}(\mathbf{r}) = 2\sqrt{2}Y_{lm}(\mathbf{r}) \int \frac{(2/\pi)^{1/4}}{2^n \sqrt{(2n)!}} H_{2n}\left(\frac{x}{\sqrt{2}}\right) \exp\left(-\frac{x^2}{4}\right) j_l(xr) dx \quad (2.16)$$

where j_l are spherical Bessel functions.

This resolution was truncated and used to compute the Coulomb self-interaction energy of point charges. It was shown that the resolution technique provides linear scaling Coulomb energy calculations while classical particle-particle algorithm scales quadratically with the number of particles. For a large system, this is a considerable computational saving with a tunable accuracy.

The second paper in the series [3] described a different resolution of r_{12}^{-1} based on Laguerre polynomials, L_n , where the resolution is easier to manipulate.

$$\phi_{nlm}(\mathbf{r}) = 4Y_{lm}(\mathbf{r}) \int L_n(2x) \exp(-x) j_l(xr) dx \quad (2.17)$$

This resolution was used to calculate Coulomb and exchange energies of Slater orbitals of hydrogenic ions, the hydrogen molecule and the beryllium atom.

The three works [1, 2, 3] have laid a foundation for RO theory in quantum chemistry. The Cartesian choice of ϕ_k was proven to be numerically unfavorable [1] and abandoned. Thus, two choices of spherical ϕ_k , based on Hermite and Laguerre polynomials were considered in the two papers [2, 3]. Recurrence relations are given to construct ϕ_k in both cases, but the Laguerre generator one is simpler and more stable. Thus it is a subject of further investigation in Chapter 3.

We note that our resolutions are also used by other research groups to study Slater-type orbitals [85, 86, 87]. The cumbersome orbital translation problem can be circumvented by using RO theory.

Apart from the choice of ϕ_k , there are generally three parameters \mathcal{N} , \mathcal{L} and \mathcal{Z} involved in an RO calculation. The first two are from rectangular truncation of the resolution of the function $T(r_{12})$.

$$\begin{aligned} T(r_{12}) &= \sum_{n=0}^{\infty} \sum_{l=0}^{\infty} \sum_{m=-l}^l \phi_{nlm}^*(\mathbf{r}_1) \phi_{nlm}(\mathbf{r}_2) \\ &\approx \sum_{n=0}^{\mathcal{N}} \sum_{l=0}^{\mathcal{L}} \sum_{m=-l}^l \phi_{nlm}^*(\mathbf{r}_1) \phi_{nlm}(\mathbf{r}_2) \equiv \sum_{k=1}^{\mathcal{K}} \phi_k^*(\mathbf{r}_1) \phi_k(\mathbf{r}_2) \end{aligned} \quad (2.18)$$

$$\begin{aligned}
\langle a|\bar{T}|b\rangle &= \sum_{n=0}^{\infty} \sum_{l=0}^{\infty} \sum_{m=-l}^l \langle a|\phi_{nlm}\rangle \langle \phi_{nlm}|b\rangle \\
&\approx \sum_{n=0}^{\mathcal{N}} \sum_{l=0}^{\mathcal{L}} \sum_{m=-l}^l \langle a|\phi_{nlm}\rangle \langle \phi_{nlm}|b\rangle \equiv \sum_{k=1}^{\mathcal{K}} \langle a|\phi_k\rangle \langle \phi_k|b\rangle
\end{aligned} \tag{2.19}$$

We note that $\mathcal{K} \equiv (\mathcal{N} + 1)(\mathcal{L} + 1)^2$ and we choose to relate the index k to the indices n , l and m through $k = n(\mathcal{L} + 1)^2 + l(l + 1) + m + 1$.

The compression factor \mathcal{Z} also plays a role in RO calculations. The system can be scaled down by \mathcal{Z} before invoking the resolution calculation. The scaling can change how close the truncated sum is to the integral in (2.19). Of course, if \mathcal{N} , \mathcal{L} are infinite, the resolution is exact for all \mathcal{Z} . Nonetheless, some resolutions are insensitive to \mathcal{Z} *i.e.* scaling does not change the convergence rate of the sum to the integral. (See an example in Chapter 5.) This scaling idea was inspired by atomic number of hydrogenic ions studied in [3].

The scaling is first introduced in Chapter 3 and also used in Chapter 4. All relevant input parameters *i.e.* nuclear coordinates \mathbf{R}_A , basis set exponents ζ_i and the range-separation parameter ω are scaled accordingly before running the calculation and output variables are scaled back by the same factor before reporting.

The following formulae describe the relationship between the scaled system denoted by primed variables and the original system.

$$\mathbf{R}'_A = \mathcal{Z}^{-1} \mathbf{R}_A \tag{2.20}$$

$$\zeta'_i = \mathcal{Z}^2 \zeta_i \tag{2.21}$$

$$\omega' = \mathcal{Z} \omega \tag{2.22}$$

$$E'_J = \mathcal{Z} E_J \tag{2.23}$$

$$E'_T = \mathcal{Z}^2 E_T \tag{2.24}$$

$$\psi'(\mathbf{r}') = \mathcal{Z}^{3/2} \psi(\mathbf{r}) \tag{2.25}$$

$$\rho'(\mathbf{r}') = \mathcal{Z}^3 \rho(\mathbf{r}) \tag{2.26}$$

Equation (2.23) applies to all Columbic energies including nuclear-nuclear, nuclear-electron and electron-electron interactions while Equation (2.24) applies to kinetic energy only.

Alternatively, of course, one could scale the $\phi_k(\mathbf{r})$ to match the density but we prefer, for aesthetic reasons, not to introduce a \mathcal{Z} -dependence into the potentials.

2.2 Extensions of resolution theory

In this section, we consider some extensions of resolution theory to functions of the form $T(r_1, r_2, \theta_{12})$ that is symmetric with respect to the interchange of \mathbf{r}_1 and \mathbf{r}_2 . The three parameters of the function are defined by the dot product $\mathbf{r}_1 \cdot \mathbf{r}_2 = r_1 r_2 \cos \theta_{12}$.

We derive four approaches: substitution, diagonalization, Fourier orthonormalization and real orthonormalization. Figure 2.1 summarizes the use of these methods in various circumstances.

2.2.1 Substitution

If T can be written in terms of sums, differences and/or products of resolved functions, it is trivial and straightforward to substitute known resolutions into T and rearrange them to obtain a resolution.

Substitution is the simplest technique but it is not applicable to many cases. A more general and systematic approach to resolve T involves decoupling and resolving the angular part of T .

Decoupling and resolving the angular part

We recall a radial-angular decoupling of the Newtonian potential in terms of Legendre polynomial [77].

$$r_{12}^{-1} = \sum_{l=0}^{\infty} \left[\frac{2l+1}{2} \int_{-1}^1 P_l(x) (r_1^2 + r_2^2 - 2r_1 r_2 x)^{-1/2} dx \right] P_l(\cos \theta_{12}) \quad (2.27)$$

The Legendre polynomial $P_l(\cos \theta_{12})$ can then be resolved into a sum products of real spherical harmonics Y_{lm} .

We generalize this approach to $T(r_1, r_2, \theta_{12})$.

$$\begin{aligned} T(r_1, r_2, \theta_{12}) &= \sum_{l=0}^{\infty} \left[\frac{2l+1}{2} \int_{-1}^1 P_l(x) T(r_1, r_2, \cos^{-1} x) dx \right] P_l(\cos \theta_{12}) \\ &= \sum_{l=0}^{\infty} \sum_{m=-l}^m \left[2\pi \int_{-1}^1 P_l(x) T(r_1, r_2, \cos^{-1} x) dx \right] Y_{lm}(\mathbf{r}_1) Y_{lm}(\mathbf{r}_2) \\ &= \sum_{l=0}^{\infty} \sum_{m=-l}^m T_l(r_1, r_2) Y_{lm}(\mathbf{r}_1) Y_{lm}(\mathbf{r}_2) \end{aligned} \quad (2.28)$$

The angular part is now decoupled from T and resolved by Y_{lm} . The expansion is also valid for other \mathcal{D} -dimensional spaces provided that P_l and Y_{lm} are replaced

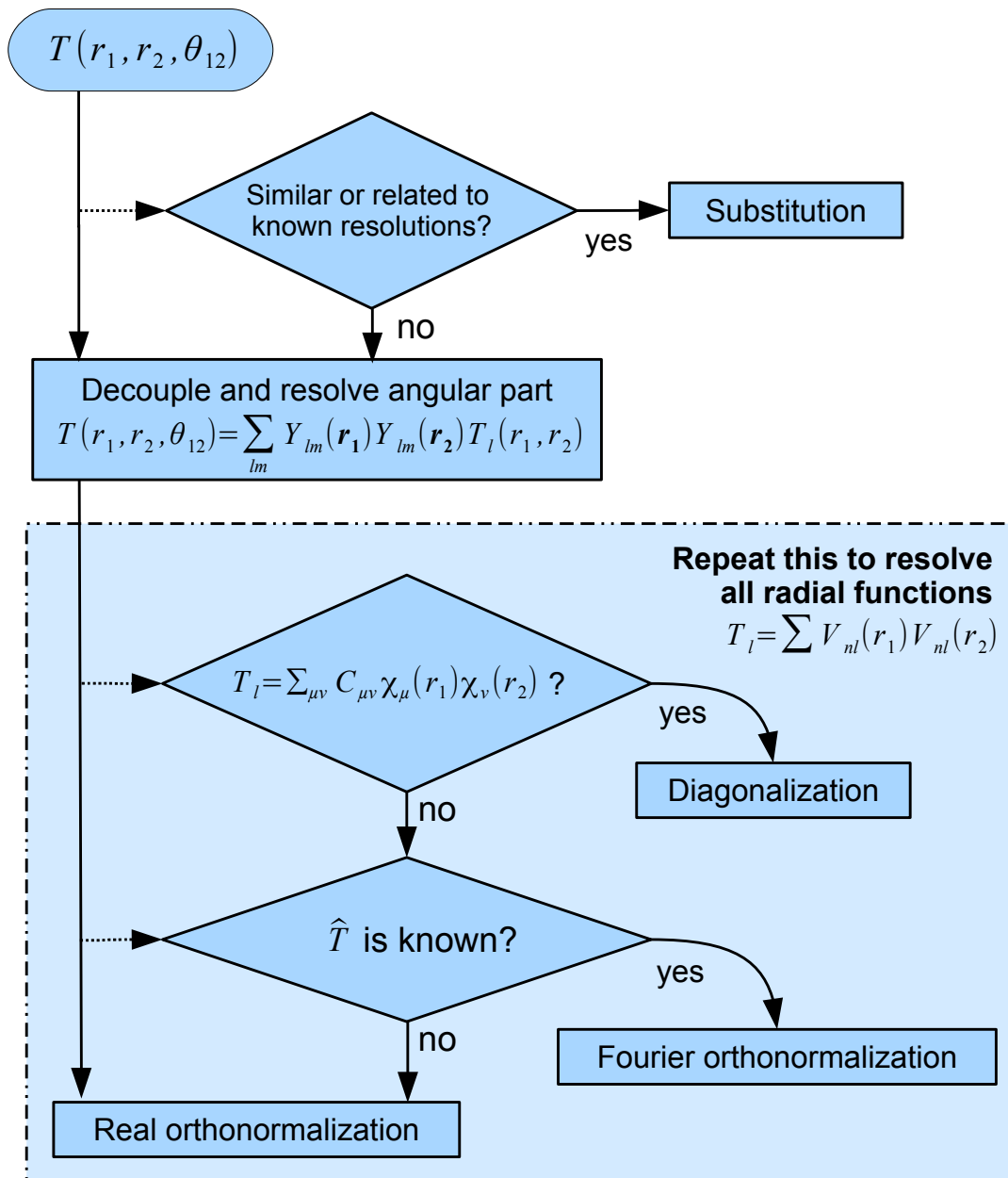


Figure 2.1: Four resolution techniques and their specific uses

with the appropriate orthogonal polynomials and harmonic functions [88]. The next step is to resolve the radial function T_l into a sum of products of V_{nl} .

$$T_l(r_1, r_2) = 2\pi \int_{-1}^1 P_l(x) T(r_1, r_2, \cos^{-1} x) dx \quad (2.29)$$

$$= \sum_n V_{nl}(r_1) V_{nl}(r_2) \quad (2.30)$$

We obtain the resolution of the function T by combining the angular resolution and the radial resolution.

$$T(r_1, r_2, \theta_{12}) = \phi_{nlm}(\mathbf{r}_1) \phi_{nlm}(\mathbf{r}_2) \quad (2.31)$$

$$\phi_{nlm}(\mathbf{r}) = V_{nl}(r) Y_{lm}(\mathbf{r}) \quad (2.32)$$

As opposed to the resolutions in the previous section, Y_{lm} must be a real spherical harmonic but V_{nl} may be complex. This choice of $T_l = \sum V_{nl}(r_1) V_{nl}(r_2)$ is better than $T_l = \sum V_{nl}^*(r_1) V_{nl}(r_2)$ used in [2] because if $T_l(r, r) < 0$ we can achieve a resolution by the former but not by the later. The Heaviside and the optimum operator in §2.3 are examples of $T_l < 0$ that can only be resolved if $T_l = \sum V_{nl}(r_1) V_{nl}(r_2)$.

We now present three methods below to obtain V_{nl} which are the key to the resolution problem.

2.2.2 Diagonalization

If the radial functions T_l can be written as a finite sum of products of function of r_1 and function of r_2 ,

$$T_l(r_1, r_2) = \sum_{\mu\nu} C_{\mu\nu} \chi_\mu(r_1) \chi_\nu(r_2) \quad (2.33)$$

we can write it in a matrix form,

$$\begin{aligned} T_l(r_1, r_2) &= \boldsymbol{\chi}_1 \mathbf{C} \boldsymbol{\chi}_2 \\ &= \boldsymbol{\chi}_1 \mathbf{U} \mathbf{D} \mathbf{U}^\dagger \boldsymbol{\chi}_2 \\ &= \mathbf{V}_1 \mathbf{I} \mathbf{V}_2 \end{aligned} \quad (2.34)$$

where \mathbf{C} is a symmetric matrix of coefficients $C_{\mu\nu}$, \mathbf{I} is the identity matrix and $\boldsymbol{\chi}_1$, $\boldsymbol{\chi}_2$ are vectors containing linearly independent functions of r_1 and r_2 respectively. It follows from diagonalization of \mathbf{C} that we can obtain a row vector \mathbf{V}_1 and a column vector \mathbf{V}_2 which have elements V_{nl} . The number of non-zero eigenvalues in \mathbf{D} is the number of terms in the resolution of T_l .

Basis functions f_{nlm}

If T_l cannot be rearranged into the form (2.33), we need to introduce basis functions to resolve it and this usually results in infinite terms in the resolution.

For simple T_l , the most straightforward attempt is to find a series expansion of T_l in terms of r_1 which may be truncated and diagonalized if required. This naive approach is, however, not applicable to Coulomb operator.

In general, one can resolve T_l by considering a set of complete and \bar{T} -orthonormal functions $\{f_{nlm}\}$ [2] as discussed in §2.1. We have a slightly different definition here since there is no complex conjugate in the orthonormality condition.

$$\int \int f_{nlm}(\mathbf{r}_1) T(r_1, r_2, \theta_{12}) f_{n'l'm'}(\mathbf{r}_2) d\mathbf{r}_1 d\mathbf{r}_2 = \delta_{nn'} \delta_{ll'} \delta_{mm'} \quad (2.35)$$

We shall derive orthonormalization methods on Fourier and real space that help us find f_{nlm} . They are applicable to a wide range of functions. The resolution function can be derived from f_{nlm} .

$$\phi_{nlm}(\mathbf{r}) = \int T(r_1, r_2, \theta_{12}) f_{nlm}(\mathbf{r}) d\mathbf{r} \quad (2.36)$$

2.2.3 Fourier orthonormalization

If T is a function of r_{12} only, we may start with $\hat{f}_{nlm} \equiv Y_{lm}(\mathbf{x})(-i)^l \eta_n(x)$ where \hat{f} and \hat{T} are Fourier transform of f and T respectively.

$$\begin{aligned} \langle f_{nlm}^* | \bar{T} | f_{n'l'm'} \rangle &\equiv \delta_{nn'} \delta_{ll'} \delta_{mm'} \equiv \int \int f_{nlm}(\mathbf{r}_1) T(r_{12}) f_{n'l'm'}(\mathbf{r}_2) d\mathbf{r}_1 d\mathbf{r}_2 \\ &= \frac{1}{(2\pi)^3} \int \hat{T}(x) \int \int f_{nlm}(\mathbf{r}_1) f_{n'l'm'}(\mathbf{r}_2) e^{i\mathbf{x} \cdot (\mathbf{r}_1 - \mathbf{r}_2)} d\mathbf{r}_1 d\mathbf{r}_2 dx \\ &= (2\pi)^{-3} \int \hat{f}_{nlm}(-\mathbf{x}) \hat{f}_{n'l'm'}(\mathbf{x}) \hat{T}(x) d\mathbf{x} \\ &= (2\pi)^{-3} \int Y_{lm}(-\mathbf{x})(-i)^l \eta_n(x) Y_{l'm'}(\mathbf{x})(-i)^{l'} \eta_{n'}(x) \hat{T}(x) d\mathbf{x} \\ &= (2\pi)^{-3} \delta_{ll'} \delta_{mm'} \int_0^\infty \eta_n(x) \eta_{n'}(x) \hat{T}(x) x^2 dx \end{aligned} \quad (2.37)$$

It follows from the orthonormality condition and the choice of f_{nlm} that η_n must be orthonormal with respect to $\hat{T}(x)x^2/(2\pi)^3$.

$$\int_0^\infty \eta_n(x) \eta_{n'}(x) \frac{\hat{T}(x)x^2}{(2\pi)^3} dx = \delta_{nn'} \quad (2.38)$$

We find η_n that satisfies the above condition by using a set of complete and orthonormal polynomials p_n .

$$\int_0^\infty p_n(x) p_{n'}(x) w(x) dx = \delta_{nn'} \quad (2.39)$$

$$\widehat{T}(x) \equiv \int T(r_{12}) \exp[-i\mathbf{x} \cdot \mathbf{r}_{12}] d\mathbf{r}_{12} \quad (2.40)$$

$$\eta_n(x) = p_n(x) \sqrt{\frac{(2\pi)^3 w(x)}{\widehat{T}(x) x^2}} \quad (2.41)$$

Once η_n is determined, we obtain a resolution of T by the following formulae.

$$f_{nlm}(\mathbf{r}) = \frac{Y_{lm}(\mathbf{r})}{2\pi^2} \int_0^\infty \eta_n(x) j_l(rx) x^2 dx \quad (2.42)$$

$$\begin{aligned} \phi_{nlm}(\mathbf{r}) &= \overline{T} [f_{nlm}(\mathbf{r})] = \int T(\mathbf{r}, \mathbf{r}') f_{nlm}(\mathbf{r}') d\mathbf{r}' \\ &= \frac{Y_{lm}(\mathbf{r})}{2\pi^2} \int_0^\infty \eta_n(x) j_l(rx) \widehat{T}(x) x^2 dx \\ &= Y_{lm}(\mathbf{r}) \int_0^\infty p_n(x) j_l(rx) \sqrt{\frac{2}{\pi} \widehat{T}(x) x^2 w(x)} dx \end{aligned} \quad (2.43)$$

$$V_{nl} = \int_0^\infty p_n(x) j_l(rx) \sqrt{\frac{2}{\pi} \widehat{T}(x) x^2 w(x)} dx \quad (2.44)$$

Bessel resolutions

From Rayleigh expansion (plane wave expansion) [89]

$$\begin{aligned} e^{\pm i\mathbf{x} \cdot \mathbf{r}} &= 4\pi \sum_{l=0}^\infty \sum_{m=-l}^l (\pm i)^l j_l(xr) Y_l^{m*}(\mathbf{x}) Y_l^m(\mathbf{r}) \\ &= 4\pi \sum_{l=0}^\infty \sum_{m=-l}^l (\pm i)^l j_l(xr) Y_{lm}(\mathbf{x}) Y_{lm}(\mathbf{r}) \end{aligned} \quad (2.45)$$

and Fourier representation of function T

$$\begin{aligned} T(r_{12}) &= \frac{1}{(2\pi)^3} \int \widehat{T}(x) e^{i\mathbf{x} \cdot (\mathbf{r}_1 - \mathbf{r}_2)} d\mathbf{x} \\ &= \frac{2}{\pi} \int \widehat{T}(x) \sum_{lm} \sum_{l'm'} i^l (-i)^{l'} j_l(xr_1) j_{l'}(xr_2) Y_{lm}(\mathbf{x}) Y_{lm}(\mathbf{r}_1) Y_{l'm'}(\mathbf{x}) Y_{l'm'}(\mathbf{r}_2) d\mathbf{x} \\ &= \frac{2}{\pi} \int \widehat{T}(x) \sum_{lm} \sum_{l'm'} i^l (-i)^{l'} j_l(xr_1) j_{l'}(xr_2) \delta_{ll'} \delta_{mm'} Y_{lm}(\mathbf{r}_1) Y_{l'm'}(\mathbf{r}_2) x^2 dx \\ &= \frac{2}{\pi} \sum_{lm} Y_{lm}(\mathbf{r}_1) Y_{lm}(\mathbf{r}_2) \int_0^\infty j_l(xr_1) j_l(xr_2) \widehat{T}(x) x^2 dx, \end{aligned} \quad (2.46)$$

one can derive another expression of T_l .

$$T_l(r_1, r_2) = \frac{2}{\pi} \int_0^\infty j_l(xr_1)j_l(xr_2)\widehat{T}(x)x^2 dx \quad (2.47)$$

The V_{nl} formulae in (2.43) can also be derived from the above formulae by expanding $j_l(xr_1)\sqrt{\frac{2}{\pi}\widehat{T}(x)x^2}$ and $j_l(xr_2)\sqrt{\frac{2}{\pi}\widehat{T}(x)x^2}$ in terms of $p_n(x)$ and integrating over x .

We have investigated the possibility of evaluating (2.47) by a numerical quadrature. After a number of quadrature abscissas and weights were obtained for $T(r_{12}) = 1/r_{12}$, we realized that we had obtained an identity rather than a quadrature. (See Chapter 4 and Chapter 7.)

We also started with this line of thought when we derived a Bessel resolution for the long-range Ewald operator $T(r_{12}) = \text{erf}(\omega r_{12})/r_{12}$. Initially, we obtained abscissas and weights and found that they are related to Hermite polynomials. Thus, the function must have the integral representation (5.6). (See Chapter 5.)

2.2.4 Real orthonormalization

Alternatively, we can begin with $f_{nlm} \equiv Y_{lm}(\mathbf{r})h_{nl}(r)$. Substituting this into (2.35), we get orthonormalization condition on real space,

$$\int_0^\infty \int_0^\infty h_{nl}(r_1)h_{n'l}(r_2)T_l(r_1, r_2)r_1^2r_2^2dr_1dr_2 = \delta_{nn'} \quad (2.48)$$

We can choose a form for the basis functions and find the h_{nl} that satisfy the above equation by the the Gram-Schmidt procedure [90]. After the h_{nl} are determined, one can obtain the V_{nl} from (2.36) which are simplified to the following one-dimensional integral.

$$\begin{aligned} \phi_{nlm}(\mathbf{r}_1) &= \int T(r_1, r_2, \theta_{12})f_{nlm}(\mathbf{r}_2)d\mathbf{r}_2 \\ &= \int Y_{lm}(\mathbf{r}_2)h_n(r_2) \sum_{l'm'} T_{l'}(r)Y_{l'm'}(\mathbf{r}_1)Y_{l'm'}(\mathbf{r}_2)d\mathbf{r}_2 \\ &= Y_{lm}(\mathbf{r}_1) \int_0^\infty T_l(r_1, r_2)h_n(r_2)r_2^2dr_2 \end{aligned} \quad (2.49)$$

Table 2.1: Examples of r_{12}^{2n} resolutions by Substitution and Diagonalization

T	Method	Resolution	\mathcal{K}
r_{12}^2	Diagonalization	In spherical form, $\phi_{0,0,0} = Y_{0,0}(\mathbf{r})\sqrt{2\pi}(1+r^2)$ $\phi_{1,0,0} = Y_{0,0}(\mathbf{r})\sqrt{2\pi}(1-r^2)\iota$ $\phi_{0,1,m} = Y_{1,m}(\mathbf{r})\sqrt{\frac{8}{3}\pi}r\iota$ [3 functions] In the Cartesian form, $\phi_{0,0,0} = \frac{1}{\sqrt{2}}(1+x^2+y^2+z^2)$ $\phi_{1,0,0} = \frac{1}{\sqrt{2}}(1-x^2-y^2-z^2)\iota$ $\phi_{0,1,-1} = \sqrt{2}x\iota$ $\phi_{0,1,0} = \sqrt{2}z\iota$ $\phi_{0,1,1} = \sqrt{2}y\iota$	5
r_{12}^4	Substitution	Given resolution functions of r_{12}^2 as χ_k , $\phi_1 = \chi_1\chi_1, \phi_2 = \chi_2\chi_2, \dots, \phi_5 = \chi_5\chi_5$, $\phi_6 = \sqrt{2}\chi_1\chi_2, \phi_7 = \sqrt{2}\chi_1\chi_3, \dots, \phi_{15} = \sqrt{2}\chi_4\chi_5$	15
r_{12}^4	Diagonalization	$\phi_{0,0,0} = Y_{0,0}(\mathbf{r})\sqrt{2\pi}(r^4+1)$ $\phi_{1,0,0} = Y_{0,0}(\mathbf{r})\sqrt{2\pi}(r^4-1)\iota$ $\phi_{2,0,0} = Y_{0,0}(\mathbf{r})\sqrt{\frac{40}{3}\pi}r^2$ $\phi_{0,1,m} = Y_{1,m}(\mathbf{r})\sqrt{\frac{8}{3}\pi}(r-r^3)$ [3 functions] $\phi_{1,1,m} = Y_{1,m}(\mathbf{r})\sqrt{\frac{8}{3}\pi}(r+r^3)\iota$ [3 functions] $\phi_{0,2,m} = Y_{2,m}(\mathbf{r})\sqrt{\frac{32}{15}\pi}r^2$ [5 functions]	14

For diagonalization method:

$$\mathcal{K} = \sum_{l=0}^n (2l+1)(n-l+1)$$

For substitution method:

$$\mathcal{K} = \binom{5}{1}\binom{n-1}{0} + \binom{5}{2}\binom{n-1}{1} + \binom{5}{3}\binom{n-1}{2} + \binom{5}{4}\binom{n-1}{3} + \binom{5}{5}\binom{n-1}{4}$$

2.3 Examples of $T(r_{12})$ resolutions

To begin with, we consider a special case where we can use the substitution method. If T is an even and smooth function of r_{12} , for example $\text{erf}(\omega r_{12})/r_{12}$, T can be expanded in a Taylor series [84].

$$T(r_{12}) = \sum_{n=0}^{\infty} \frac{T^{(2n)} r_{12}^{2n}}{(2n)!} \quad (2.50)$$

To resolve this class of T , we need to resolve all r_{12}^{2n} in the equation above.

Table 2.1 shows that the five-term resolution of $r_{12}^2 = r_1^2 + r_2^2 - 2\mathbf{r}_1 \cdot \mathbf{r}_2$ consists of two parts. The $l = 0$ part is obtained by writing T_0 into a two-by-two symmetric matrix and diagonalizing it. The $l = 1$ part resolves naturally and does not require further manipulation. The higher degree terms can be obtained either by diagonalization or by substituting the resolution of r_{12}^2 into $(r_{12}^2)^n$ then expanding the terms out.

Apart from these special cases, resolutions are generally obtained by angular-radial decoupling and resolution of the radial functions T_l . The two steps are demonstrated separately. We consider four long-range Coulomb operators,

Yukawa [91]:

$$T(r_{12}) = \frac{1 - e^{-\omega r_{12}}}{r_{12}} \quad (2.51)$$

$$\hat{T}(x) = \frac{4\pi}{x^2} \left(\frac{\omega^2}{\omega^2 + x^2} \right) \quad (2.52)$$

Ewald [92, 93]:

$$T(r_{12}) = \frac{\text{erf}(\omega r_{12})}{r_{12}} \quad (2.53)$$

$$\hat{T}(x) = \frac{4\pi}{x^2} \exp \left[- \left(\frac{x}{2\omega} \right)^2 \right] \quad (2.54)$$

Heaviside [94]:

$$T(r_{12}) = \frac{1 - H(\omega r_{12})}{r_{12}} \quad (2.55)$$

$$= \begin{cases} 1/r_{12} & \omega r_{12} > 1 \\ 0 & \text{otherwise} \end{cases} \quad (2.56)$$

$$\hat{T}(x) = \frac{4\pi}{x^2} \cos \left(\frac{x}{\omega} \right) \quad (2.57)$$

Optimum [95]:

$$T(r_{12}) = \frac{1 - U(0, \sqrt{2}r)/U(0, 0)}{r_{12}} \quad (2.58)$$

$$\hat{T}(x) = \frac{4\pi}{x^2} \left\{ 1 - \Gamma\left(\frac{3}{4}\right) \sqrt{\pi} \left(\frac{x}{2}\right)^{3/2} \left[I_{1/4}\left(\frac{x^2}{2}\right) - \mathbf{L}_{1/4}\left(\frac{x^2}{2}\right) \right] \right\} \quad (2.59)$$

U , I and \mathbf{L} are parabolic cylinder functions, modified Bessel functions and modified Struve function respectively.

For simplicity, we use $\omega = 1$ for the first three operators.

2.3.1 Decoupling of the angular and the radial parts

We demonstrate this step by considering r_{12}^{-3} , r_{12}^{-1} , r_{12} and the four long-range operators. They are expanded in Legendre polynomials and the first five T_l are plotted in Figure 2.2 and 2.3

Logarithmic plots of T_l in Figure 2.2 show that T_l decays more or less exponentially as l increases. All three plots are continuous but the first derivatives of r_{12}^{-3} and r_{12}^{-1} are discontinuous at $r_1 = r_2$ ($x = \pi/4$). The effect of singularity of T at r_{12} is responsible for this and it is more pronounced when the exponent in $(r_{12})^n$ goes down to -3 . This suggests that resolutions truncated in the l direction may perform poorly in the proximity of strong singularities of T but work fine for the rest of the domain.

In Figure 2.3, T_l of the four functions are plotted. The T_l of the first two functions, Yukawa and Ewald, look like that of Coulomb operator but there is no discontinuity of their first derivative at $r_1 = r_2$. The later two functions result in more complicated T_l in the lower plots of the figure. This is because their T_l are sometimes negative and the plots show $|T_l|$. The sharp downward peaks correspond to the points that T_l change their sign. We conclude that their convergence in the l direction of the long-range Coulomb operators is more or less the same as Coulomb operators but without the problem around $r_1 = r_2$.

2.3.2 Resolution of the radial function T_l

We now investigate resolutions in the n direction by employing the two orthonormalization methods to obtain the V_{nl} . A long-range Yukawa function where $\omega = 1$

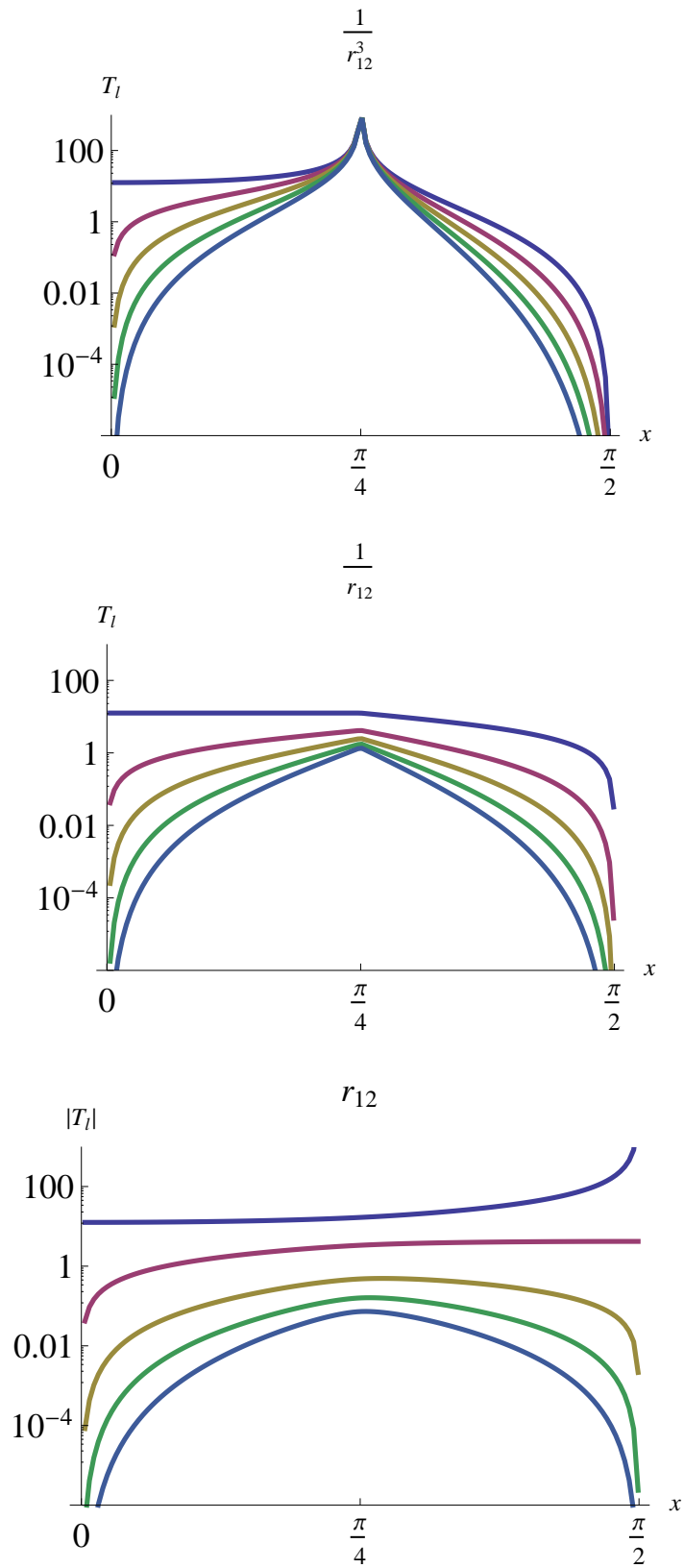


Figure 2.2: Plots of first five T_l for r_{12}^{-3} , r_{12}^{-1} and r_{12} for $r_1 = 1$ and $r_2 = \tan x$

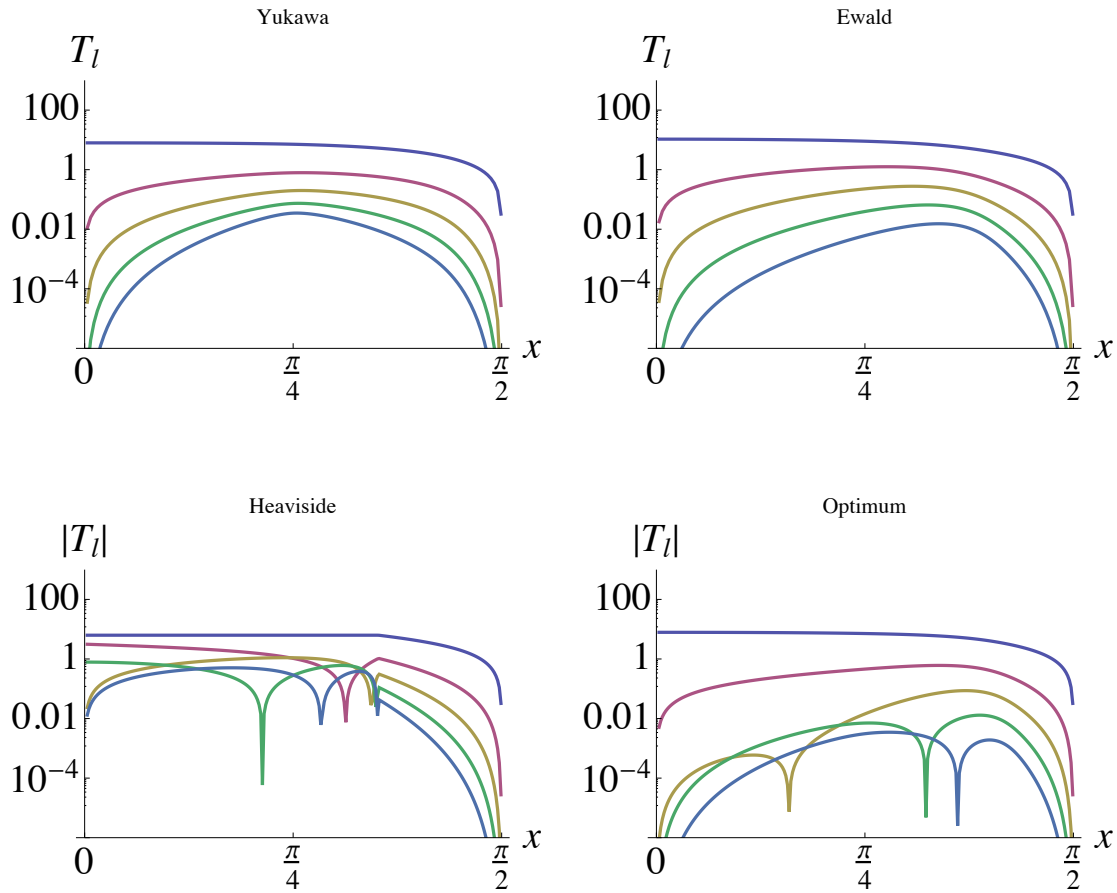


Figure 2.3: Logarithmic plots of first five T_l for long-rang Coulomb operators, Yukawa (upper left), Ewald (upper right), Heaviside (lower left) and optimum (lower right) for $r_1 = 1$ and $r_2 = \tan x$

is chosen as a representative example.

$$T(r_{12}) = \frac{1 - \exp(-r_{12})}{r_{12}} \quad (2.60)$$

$$\begin{aligned} T_0(r_1, r_2) &= 2\pi \frac{-e^{-|r_1-r_2|} - |r_1 - r_2| + e^{-r_1-r_2} + r_1 + r_2}{r_1 r_2} \\ &= \begin{cases} \frac{2\pi e^{-r_1} (2e^{r_1} r_2 + e^{-r_2} - e^{r_2})}{r_1 r_2} & r_1 \geq r_2 \\ \frac{2\pi e^{-r_2} (2r_1 e^{r_2} + e^{-r_1} - e^{r_1})}{r_1 r_2} & r_1 < r_2 \end{cases} \end{aligned} \quad (2.61)$$

$$\begin{aligned} T_1(r_1, r_2) &= \frac{2\pi}{3r_1^2 r_2^2} \left\{ r_1^3 + r_2^3 - (r_1^2 + r_1 r_2 + r_2^2) |r_1 - r_2| \right. \\ &\quad \left. - 3 \left((r_1 + 1)(r_2 + 1) e^{-r_1-r_2} - e^{-|r_1-r_2|} (|r_1 - r_2| - r_1 r_2 + 1) \right) \right\} \\ &= \begin{cases} \frac{4\pi (r_2^3 - 3e^{-r_1} (r_1+1)(r_2 \cosh(r_2) - \sinh(r_2)))}{3r_1^2 r_2^2} & r_1 \geq r_2 \\ \frac{4\pi (r_1^3 - 3e^{-r_2} (r_2+1)(r_1 \cosh(r_1) - \sinh(r_1)))}{3r_1^2 r_2^2} & r_1 < r_2 \end{cases} \end{aligned} \quad (2.62)$$

We use the two techniques to obtain the V_{nl} and plot sums of their products in Figure 2.4. This figure is analogous to Figure 3 and Figure 4 in [3] but T_l here do not have a discontinuous first derivative at $r_1 = r_2$.

For Fourier orthonormalization method, we choose $w(x) = e^{-x}$ and $p_n(x) = L_n(x)$ (Laguerre polynomials) and obtained the V_{nl} in an integral form.

$$V_{nl} = \int_0^\infty L_n(x) j_l(rx) \sqrt{8 \frac{e^{-x}}{1+x^2}} dx \quad (2.63)$$

Thus, we use numerical integration to generate data in Figure 2.4.

For real orthonormalization, we choose the weighted polynomial form.

$$h_{nl}(r) = \sum_{\mu=0}^n c_{n\mu}^l r^\mu e^{-r} \quad (2.64)$$

The $n = 0$ terms,

$$h_{0,0}(r) = 2\sqrt{\frac{2}{35\pi}} e^{-r} \quad (2.65)$$

$$h_{0,1}(r) = 2\sqrt{\frac{2}{5\pi}} e^{-r} \quad (2.66)$$

are determined by normalization.

$$\int_0^\infty \int_0^\infty h_{0,l}(r_1) T_l(r_1, r_2) h_{0,l}(r_2) r_1^2 r_2^2 dr_1 dr_2 = 1 \quad (2.67)$$

The rest of h_{nl} ($n = 1, 2, 3, \dots$) are generated by the Gram-Schmidt procedure. From these h_{nl} functions, we obtain analytical but complicated V_{nl} via (2.48).

$$V_{0,0} = \frac{2\sqrt{\frac{2}{35}}e^{-r}\sqrt{\pi}}{r}(-8 + 8e^r - r(5 + r)) \quad (2.68)$$

$$V_{1,0} = \frac{4e^{-r}\sqrt{\pi}}{3\sqrt{105}r}(-24 + 24e^r - r(30 + r(18 + 5r))) \quad (2.69)$$

$$V_{2,0} = \frac{2\sqrt{\frac{2}{231}}e^{-r}\sqrt{\pi}}{3r}(-48 + 48e^r - r(39 + r(15 + r(10 + 7r)))) \quad (2.70)$$

$$V_{3,0} = \frac{4e^{-r}\sqrt{\pi}}{15\sqrt{3003}r}(-600 + 600e^r - r(690 + r(390 + 7r(5 + 2r(-5 + 3r)))))) \quad (2.71)$$

$$V_{4,0} = \frac{2}{15r}\sqrt{\frac{2}{3003}}e^{-r}\sqrt{\pi}(-840 + 840e^r - r(735 + r(315 + 2r(140 + r(105 + r(-63 + 11r)))))) \quad (2.72)$$

$$V_{5,0} = \frac{4}{315r}\sqrt{\frac{2}{12155}}e^{-r}\sqrt{\pi}(-17640 + 17640e^r + r(-19530 + r(-10710 + r(945 + r(3780 - 11r(504 + r(-140 + 13r)))))) \quad (2.73)$$

$$V_{6,0} = \frac{2}{45r}\sqrt{\frac{2}{440895}}e^{-r}\sqrt{\pi}(-30240 + 30240e^r - r(27405 + r(12285 + r(13230 + r(10395 + r(-15246 + 13r(510 + r(-84 + 5r)))))) \quad (2.74)$$

$$V_{7,0} = \frac{4}{2835r}\sqrt{\frac{2}{2261}}e^{-r}\sqrt{\pi}(-68040 + 68040e^r + r(-73710 + r(-39690 + r(10395 + r(20790 + r(-54054 + r(29988 + r(-7335 + 810r - 34r^2)))))) \quad (2.75)$$

$$V_{8,0} = \frac{2}{4725r}\sqrt{\frac{2}{1716099}}e^{-r}\sqrt{\pi}(-6237000 + 6237000e^r - r(5769225 + r(2650725 + 2r(1663200 + r(1351350 + r(-3513510 + r(2487870 + r(-793980 + 17r(7590 + r(-605 + 19r)))))) \quad (2.76)$$

$$V_{9,0} = \frac{4}{155925\sqrt{15295}r}e^{-r}\sqrt{\pi}(-13721400 + 13721400e^r + r(-14656950 + r(-7796250 + r(3378375 - 2r(-2702700 + r(10810800 + r(-9050580 + r(3594195 + r(-766260 + 19r(4730 + r(-286 + 7r)))))) \quad (2.77)$$

$$V_{0,1} = 2\sqrt{\frac{2}{15}}e^{-r}\sqrt{\pi}\frac{(8e^r - (2 + r)(4 + r(2 + r)))}{r^2} \quad (2.78)$$

$$V_{1,1} = 4e^{-r}\sqrt{\pi}\frac{(-72 + 72e^r - r(72 + r(36 + r(14 + 5r))))}{3\sqrt{105}r^2} \quad (2.79)$$

$$V_{2,1} = 2\sqrt{\frac{2}{35}}e^{-r}\sqrt{\pi}\frac{(-240 + 240e^r - r(240 + r(120 + r(35 + r(5 + 7r))))}{9r^2} \quad (2.80)$$

$$V_{3,1} = 4e^{-r}\sqrt{\pi}\frac{(-600 + 600e^r - r(600 + r(300 + r(110 + r(35 + 2r(-7 + 3r))))))}{45\sqrt{11}r^2} \quad (2.81)$$

$$V_{4,1} = \frac{2}{9r^2} \sqrt{\frac{2}{15015}} e^{-r} \sqrt{\pi} (-7560 + 7560e^r - r(7560 + r(3780 + r(1155 + 2r(105 + r(189 + r(-70 + 11r))))))) \quad (2.82)$$

$$V_{5,1} = \frac{4}{315r^2} \sqrt{\frac{2}{195}} e^{-r} \sqrt{\pi} (-17640 + 17640e^r - r(17640 + r(8820 + r(3150 + r(945 + r(-756 + r(644 + r(-148 + 13r))))))) \quad (2.83)$$

$$V_{6,1} = \frac{2}{135r^2} \sqrt{\frac{2}{595}} e^{-r} \sqrt{\pi} (-30240 + 30240e^r - r(30240 + r(15120 + r(4725 + r(945 + r(2079 + r(-1596 + r(582 + r(-87 + 5r))))))) \quad (2.84)$$

$$V_{7,1} = \frac{4}{2835r^2} \sqrt{\frac{2}{4845}} e^{-r} \sqrt{\pi} (-1020600 + 1020600e^r - r(1020600 + r(510300 + r(179550 + r(51975 + r(-62370 + r(80010 + r(-35820 + r(7965 - 830r + 34r^2))))))) \quad (2.85)$$

$$V_{8,1} = \frac{2}{14175r^2} \sqrt{\frac{2}{1463}} e^{-r} \sqrt{\pi} (-6237000 + 6237000e^r - r(6237000 + r(3118500 + r(987525 + 2r(103950 + r(270270 + r(-318780 + r(183150 + r(-52470 + r(8030 + r(-616 + 19r)))))))))) \quad (2.86)$$

$$V_{9,1} = \frac{4}{31185\sqrt{2415}r^2} e^{-r} \sqrt{\pi} (-13721400 + 13721400e^r - r(13721400 + r(6860700 + r(2390850 + r(675675 + 2r(-540540 + r(928620 + r(-615780 + r(219285 + r(-43780 + r(4928 + r(-290 + 7r)))))))))) \quad (2.87)$$

For $l = 0$ (on the left of Figure 2.4), the resolutions converge quickly in the n direction. The two-, five- and ten-term sums are very close to T_0 and are visually indistinguishable from T_0 in the case of Fourier orthonormalization.

For $l = 1$ (on the right of Figure 2.4), we instead observe a significant deviation from T_1 for the two-term sums. However, the deviation diminishes rapidly as number of terms in the sums increases. Again, the ten-term sums are visually indistinguishable from T_0 for the case of Fourier orthonormalization.

In all four plots, the ten-term sums are reasonably good estimates of T_l and Fourier orthonormalization performs better than real orthonormalization. It might be worrying that the error grows when l is increased. However, as T_l decays rapidly with l , the absolute error from higher l is not going to be significant.

Discussion

The T_l -orthonormality condition in the last three methods ensures that no fewer-term resolution can be obtained by linear combination of terms in the existing resolution.

We observe that the diagonalization method yields a 14-term resolution for r_{12}^4 ,

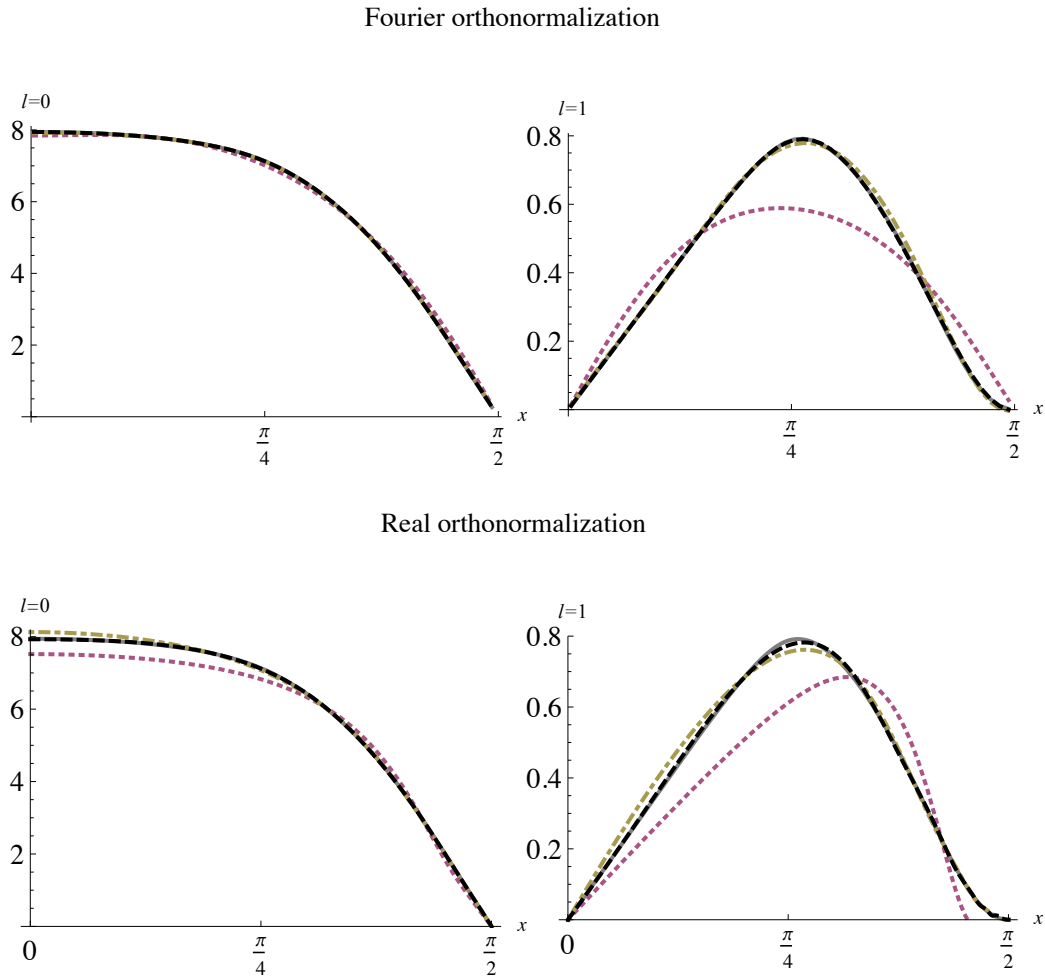


Figure 2.4: Plots of $\sum_{n=0}^{\mathcal{N}} V_{nl}(r_1)V_{nl}(r_2)$, $\mathcal{N} = 1$ (dot), $\mathcal{N} = 4$ (dot-dash), $\mathcal{N} = 9$ (dash) and T_l of $(1 - \exp[-r_{12}])/r_{12}$ (gray line, visually indistinguishable from $\mathcal{N} = 9$ except for the lower right plot) for $r_1 = 1$ and $r_2 = \tan x$

one term smaller than the resolution obtained from the substitution method. The difference can be much larger for more complicated resolutions. For example, the diagonalization method yields a 506-term resolution for r_{12}^{20} but the substitution $(\sum_{k=0}^5 \phi_k(\mathbf{r}_1)\phi_k(\mathbf{r}_2))^{10}$ results in a 1,001-term resolution.

The resolutions described here are theoretically interesting, but may run into numerical difficulties when used in practice. The chief problem is to calculate auxiliary integrals in a stable and efficient manner. We discussed this issue in Chapter 6. Other examples of resolutions of Ewald operator $\text{erf}(\omega r_{12})/r_{12}$ can be found in §5.6.

2.4 Related techniques

The resolutions of the Coulomb operator is conceptually novel to quantum chemistry. However, when implemented it results in a factorization of two-electron integrals and possibly linear-scaling computational methods. There exists other techniques in quantum chemistry that can achieve this integral factorization and linear scaling too. Nonetheless, RO has a number of fundamental advantages.

- RO directly generates three center integrals $(\mu\nu|\phi)$. There is no matrix inversion or extra manipulation required.
- RO integrals generation is ready for a parallel computing implementation. There are several ways to partition the work without compromising the performance of RO.
- If one desires a higher accuracy, RO methods may require just additional calculation from extra ϕ_{nlm} rather than running the whole calculation again. This is generally true if we truncate resolutions that formally have infinite terms. However, it is not the case for resolutions involving coefficients from quadratures. (See Chapter 5.)
- RO opens possibilities of new way of solving the Schrödinger equations. (See Chapter 3 and §8.2.)
- RO naturally benefits from the short-range nature of exchange energy. (See Chapter 5.)

2.4.1 Density fitting or resolution of the identity

The density fitting (DF) or the resolution of the identity (RI) approximation was introduced in 1973 by two different groups [96, 97]. The idea was later revisited in 1993 by Feyereisen and coworkers [98, 99].

In this approach, the AO integrals are written as an inner projection in term of auxiliary (or fitting) basis set labeled by P and Q .

$$(\mu\nu|\bar{T}|\lambda\sigma) \approx \sum_{PQ} (\mu\nu|\bar{T}|P)M_{PQ}^{-1}(Q|\bar{T}|\lambda\sigma) \quad (2.88)$$

All integrals are just standard electron repulsion integrals. The only additional procedure required in density fitting program is matrix inversion. M_{PQ}^{-1} denotes the inverse of Coulomb matrix.

$$M_{PQ} = (P|\bar{T}|Q) = \int P(\mathbf{r}_1)T(r_{12})Q(\mathbf{r}_2)d\mathbf{r}_1d\mathbf{r}_2 \quad (2.89)$$

The above decomposition of two-electron four center integrals into two- and three- index integrals is based on an approximate “resolution of the identity”.

$$\sum_{PQ} |P\rangle M_{PQ}^{-1} \langle Q| \approx \mathbf{I} \quad (2.90)$$

Similar to the resolution of the Coulomb operator and Cholesky decomposition, density fitting leads to a factorization of two-electron integrals. However, the method works best if the auxiliary basis is preoptimized. Thus each auxiliary basis is biased towards conditions used for its optimization and there is no continuous way of improving the results if needed.

Aquilante and coworkers recently showed that Cholesky decomposition can be used to generate unbiased auxiliary basis on the fly [100, 101].

Unlike Cholesky decomposition, density fitting methods *e.g.* RI-MP2, RI-CIS(D), RI-DFT are currently available in many mainstream quantum chemistry packages including GAMESS [102], GAUSSIAN [103], NWCHEM [104], ORCA [105], PSI [106], Q-CHEM [107] and TURBOMOLE [108]. The comparison between the two techniques can be found in [109, 110].

2.4.2 Cholesky decomposition

Mathematically speaking, Cholesky decomposition (CD) is a decomposition of a Hermitian, positive-definite matrix into the product of a lower triangular matrix and its conjugate transpose.

$$\mathbf{A} = \mathbf{L}\mathbf{L}^\dagger \quad (2.91)$$

The decomposition was named after its inventor, André-Louis Cholesky, a french military officer and a mathematician [111].

Cholesky decomposition was first introduced to quantum chemistry by Beebe and Linderberg in 1977 [112] to help with two-electron integral storage. The Cholesky decomposition of the AO integrals may be written as

$$\begin{aligned}
 (\mu\nu|\bar{T}|\lambda\sigma) &= \sum_{k=1}^{B(B+1)/2} L_{\mu\nu}^k L_{\lambda\sigma}^k \\
 &\approx \sum_{k=1}^{\mathcal{K}} L_{\mu\nu}^k L_{\lambda\sigma}^k
 \end{aligned}
 \tag{2.92}$$

where B is the number of atomic orbitals. In contrast to RO, the factorization is formally finite.

When CD is used in quantum chemistry, it slightly differs from its original formulations by mathematicians. First, the decomposition is applied to a symmetric but not positive-definite two-electron integral matrix. Second, the expansion is truncated to \mathcal{K} terms where $\mathcal{K} \ll B(B+1)/2$ so that the factorization can give practical benefit.

CD has been studied by a number of research groups and shown to be a promising technique to reduce computational cost of QM methods [113, 100, 114, 115, 101]. The accuracy of CD can be easily controlled by a single integral screening parameter. The matrix elements that are smaller than the ratio of this parameter to maximum diagonal elements are zeroed out. After this prescreening step, further improvement of the accuracy is not possible [113].

QM methods based on CD are currently available in a few quantum chemistry packages *e.g.* MOLCAS [116] and DALTON [117].

2.4.3 Tensor product approximation

In a series of papers, [118, 119, 120, 121, 122, 123] Hackbusch and co-workers have designed schemes for constructing tensor factorizations of many-electron objects (including the Coulomb operator) and such techniques have recently yielded impressive results in Hartree-Fock [124] and correlated [123] calculations on a variety of small molecules.

The tensor product approximation leads to a factorization of two-electron integral similar to Equations (2.89) and (2.90).

2.4.4 Linear scaling approaches

Linear scaling computational method [125] is a method whose computational cost increases linearly with molecular size, M .

Formally, there are $\mathcal{O}(M^4)$ two-electron integrals in a molecule, but the asymptotic scaling of the number of these integrals reduces to $\mathcal{O}(M^2)$ for large molecules [126]. To accomplish $\mathcal{O}(M)$ scaling, one has to avoid the naive $\mathcal{O}(M^2)$ pairwise summation over electron-electron interactions. Several clever techniques are available to achieve this goal and we summarize them below.

Coulomb energy

The fast multipole methods (FMM) [127] do not treat individual pairwise interactions between point charges but collect them into charge distributions and use a boxing scheme to circumvent the quadratic step of Coulomb matrix calculation. The extended FMM algorithm for continuous charge distribution is called continuous fast multipole methods (CFMM) [128].

The KWIK algorithm [129] partitions Coulomb energy into short- and long-range parts. The short-range one is treated analytically while the other is computed by Fourier summation. This later developed into CASE [93] and CAP(m) [130] methods

It was shown in [2] that the RO technique provides linear-scaling Coulomb energy calculation for point charges. The same algorithm is also used for Gaussian charge distribution in Chapter 3 and Chapter 4.

Exchange energy

The ONX [131] and the LinK [132] methods are linear scaling algorithms for exchange energy. They exploit locality nature of non-metallic system to achieve $\mathcal{O}(M)$ scaling.

Correlation energy

It is also possible to devise a linear-scaling correlated method. In 2002, the linear scaling MP2 method was accomplished by combining local approximation with density fitting [133].

Chapter 3

Reduced-rank Schrödinger equations

$$\bar{\mathcal{H}} = \sum_i^N \bar{h}(\mathbf{r}_i) + \sum_{i<j}^N r_{ij}^{-1}$$
$$\bar{\mathcal{H}}^{\mathcal{K}} = \sum_i^N \bar{h}(\mathbf{r}_i) + \sum_{k=1}^{\mathcal{K}} \sum_{i<j}^N \phi_k(\mathbf{r}_i) \phi_k(\mathbf{r}_j)$$

In this chapter, we consider a modified Schrödinger equation wherein the electron-electron repulsion terms r_{ij}^{-1} are approximated by truncated one-particle resolutions. Numerical results for the He atom and H₂ molecule at the Hartree-Fock, second-order Møller-Plesset, and configuration interaction levels show that the solutions of the resulting reduced-rank Schrödinger equations converge rapidly and that even low-rank approximations can yield energies with chemical accuracy.

3.1 Introduction

The chief difficulty in applying quantum mechanics to problems in chemical physics is that the Coulomb operators $r_{ij}^{-1} \equiv |\mathbf{r}_i - \mathbf{r}_j|^{-1}$ which pervade the rel-

evant Hamiltonians, couple the motions of the particles. It is this coupling that lies at the heart of the Coulomb problem [134], the exchange problem [135] and, in particular, the notorious electron correlation problem [136].

Although ongoing research efforts have produced a range of methods to address this fundamental difficulty, including separating the Coulomb operator into its short- and long-range components [92, 137, 129, 95, 138], treatment of the short-range component by specialized techniques [130, 139, 94] and the long-range component by multipole expansion [127, 140, 141], complete neglect of the long-range component [130, 93, 61], and treatment of the operator in Fourier space [129, 142, 143], none of these has yet yielded a comprehensive solution to the correlation problem.

In [2], Varganov *et al.* introduced a resolution

$$r_{ij}^{-1} = \sum_{nlm}^{\infty} \phi_{nlm}(\mathbf{r}_i) \phi_{nlm}(\mathbf{r}_j) \equiv \sum_k^{\infty} \phi_k(\mathbf{r}_i) \phi_k(\mathbf{r}_j) \quad (3.1)$$

of the two-particle Coulomb operator into one-particle potentials

$$\phi_{nlm}(\mathbf{r}) = Y_{lm}(\mathbf{r}) V_{nl}(r) \quad (3.2)$$

where the radial potentials are given by

$$V_{nl}(r) = 2\sqrt{2} \int_0^{\infty} h_n(x) j_l(xr) dx \quad (3.3)$$

and where Y_{lm} is a spherical harmonic, j_l is a spherical Bessel function and the $h_n(x)$ are a set of functions that are complete and orthonormal on $[0, \infty)$.

This “resolution of the Coulomb operator” (RO) is analogous to the familiar “resolution of the identity” (RI) [97, 144, 99, 109] and allows us to expand Coulomb matrix elements into auxiliary integrals, *i.e.*

$$\langle a | r_{12}^{-1} | b \rangle = \sum_{nlm}^{\infty} \langle a | \phi_{nlm} \rangle \langle \phi_{nlm} | b \rangle \equiv \sum_k^{\infty} \langle a | \phi_k \rangle \langle \phi_k | b \rangle \quad (3.4)$$

If the resolution is truncated after $\mathcal{K} < \infty$ terms, the resulting rank- \mathcal{K} approximation

$$r_{ij}^{-1} \approx \sum_{n=0}^{\mathcal{N}} \sum_{l=0}^{\mathcal{L}} \sum_{m=-l}^l \phi_{nlm}(\mathbf{r}_i) \phi_{nlm}(\mathbf{r}_j) \equiv \sum_{k=1}^{\mathcal{K}} \phi_k(\mathbf{r}_i) \phi_k(\mathbf{r}_j) \quad (3.5)$$

which we will call the $(\mathcal{N}, \mathcal{L})$ resolution, yields integral approximations

$$\langle a | r_{12}^{-1} | b \rangle \approx \sum_{n=0}^{\mathcal{N}} \sum_{l=0}^{\mathcal{L}} \sum_{m=-l}^l \langle a | \phi_{nlm} \rangle \langle \phi_{nlm} | b \rangle \equiv \sum_k^{\mathcal{K}} \langle a | \phi_k \rangle \langle \phi_k | b \rangle \quad (3.6)$$

that are reminiscent of the Cholesky decompositions [112, 100, 109, 101] and Kronecker approximations [118, 119] currently being developed.

Of the myriad ways to resolve the Coulomb operator, only two have been previously explored. In [2], Varganov *et al.* chose the generating functions h_n to be even-order Hermite functions weighted by a Gaussian but observed that calculation of the resulting $V_{nl}(r)$ is unwieldy when \mathcal{N} or \mathcal{L} are large. In [3], Gill and Gilbert chose

$$h_n(x) = \sqrt{2} L_n(2x) \exp(-x) \quad (3.7)$$

where L_n is a Laguerre polynomial [8] and this yields a resolution with potentials such as

$$\phi_{0,0,0}(\mathbf{r}) = \frac{2}{\sqrt{\pi}} \left[\frac{\tan^{-1} r}{r} \right] \quad (3.8)$$

$$\phi_{1,0,0}(\mathbf{r}) = \frac{2}{\sqrt{\pi}} \left[\frac{\tan^{-1} r}{r} - \frac{2}{1+r^2} \right] \quad (3.9)$$

$$\phi_{n,0,0}(\mathbf{r}) = \frac{2}{\sqrt{\pi}} \frac{(-1)^n}{r} \Im \{ B_z(n+1, -n) \} \quad (3.10)$$

where \Im is the imaginary part, B_z is the incomplete Beta function and $z = (1+r\iota)/2$. These are better behaved numerically and were also adopted in recent work by Hoggan [85, 86, 87].

In [3], Gill and Gilbert studied the rate of convergence of the Coulomb self-interaction energy of the hydrogenic ions (H, He⁺, Li²⁺, Be³⁺ and B⁴⁺) with respect to \mathcal{K} and found that the behaviour deteriorates as the nuclear charge increases. This arises because the physical size of the potentials $\phi_k(\mathbf{r})$ becomes increasingly poorly matched to the electron densities $\rho(\mathbf{r})$, which shrink towards the nuclei as the nuclear charge increases. The problem can be solved simply by compressing the density (or orbitals) by a well-chosen scale factor \mathcal{Z} , applying the Coulomb resolution, and then re-scaling the resulting energy by the same factor.

In this chapter, we explore the consequences of replacing the electron-electron terms in the molecular Schrödinger equation by their rank- \mathcal{K} approximations (3.5). We discuss results for He and H₂ at the Hartree-Fock (HF), second-order Møller-Plesset (MP2) and configuration interaction (CI) levels.

3.2 Reduced-rank Schrödinger equations

The non-relativistic electronic Schrödinger equation for an N -electron system is

$$\left[\sum_i^N \bar{h}(\mathbf{r}_i) + \sum_{i<j}^N r_{ij}^{-1} \right] \Psi = E\Psi \quad (3.11)$$

where \bar{h} is the one-electron operator describing an electron's kinetic energy and its interaction with an external field, such as the nuclei. Replacing the problematic electron repulsion terms by the rank- \mathcal{K} approximation (3.5) yields the reduced-rank Schrödinger equation (RRSE)

$$\left[\sum_i^N \bar{h}(\mathbf{r}_i) + \frac{1}{2} \sum_k^{\mathcal{K}} \left| \sum_i^N \phi_k(\mathbf{r}_i) \right|^2 - \frac{1}{2} \sum_k^{\mathcal{K}} \sum_i^N |\phi_k(\mathbf{r}_i)|^2 \right] \Psi = E\Psi \quad (3.12)$$

and, of course, as $\mathcal{K} \rightarrow \infty$, we recover the original Schrödinger equation (3.11).

At first glance, the RRSE may appear more complicated than the original Schrödinger equation, but this is not so. The third term in (3.12) consists of one-electron contributions and therefore presents no difficulty. The second term is more challenging but still offers a considerable simplification over the original equation.

In [3], Gill and Gilbert showed that the Laguerre resolution yields surprisingly rapid convergence of Coulomb and exchange energies and it is therefore interesting to see how well the solutions of (3.12) mimic those of (3.11) as \mathcal{K} increases.

At points where two electrons coincide, *i.e.* $\mathbf{r}_i = \mathbf{r}_j$, the Hamiltonian in (3.11) is singular and this leads to cusps in the exact wavefunction [145]. In contrast, for finite \mathcal{K} , the Hamiltonian in (3.12) is non-singular at such points and the exact solutions of the RRSE therefore lack such cusps. We therefore expect that the approximate solutions of RRSE will converge more rapidly with respect to the size of the one-electron basis than those of the original Schrödinger equation [146, 147].

In this investigation, we will confine our attention to the special case of two-electron systems, for which the RRSE reduces to

$$\left[\bar{h}(\mathbf{r}_1) + \bar{h}(\mathbf{r}_2) + \sum_k^{\mathcal{K}} \phi_k(\mathbf{r}_1)\phi_k(\mathbf{r}_2) \right] \Psi = E\Psi \quad (3.13)$$

We anticipate that the general conclusions that emerge from this study will also apply to larger systems and preliminary studies on Be and LiH confirm this.

3.3 Reduced-rank quantum chemistry models

3.3.1 Hartree-Fock theory

In conventional Hartree-Fock (HF) theory for a two-electron singlet, the Fock operator is

$$\bar{F} = \bar{h} + \bar{J} \quad (3.14)$$

where \bar{J} is the full Coulomb operator. If, however, we develop a reduced-rank Hartree-Fock (RRHF) theory based on the RRSE (3.13), the associated Fock operator becomes

$$\bar{F}^{\mathcal{K}} = \bar{h} + \bar{J}^{\mathcal{K}} \quad (3.15)$$

and, in a finite basis of size B , the resulting Fock matrix elements [11] are given by

$$F_{\mu\nu}^{\mathcal{K}} = \langle \mu | \bar{h} | \nu \rangle + \sum_k^{\mathcal{K}} \langle \mu\nu | \phi_k \rangle \langle \phi_k | \rho \rangle \quad (3.16)$$

where

$$\langle \phi_k | \rho \rangle = \sum_{\mu\nu} P_{\mu\nu} \langle \mu\nu | \phi_k \rangle \quad (3.17)$$

and $P_{\mu\nu}$ is a density matrix element. This shows that an RRHF calculation is analogous to a conventional HF one, except that $\mathcal{O}(B^4)$ two-electron integrals $(\mu\nu|\lambda\sigma)$ are replaced by $\mathcal{O}(B^2\mathcal{K})$ auxiliary integrals $\langle \mu\nu | \phi_k \rangle$. This is reminiscent of the RI and Cholesky schemes but, of course, there is no RRHF metric matrix to invert.

To obtain an initial guess for the self-consistent field (SCF) algorithm, we diagonalize the core Hamiltonian matrix and, to transform the Fock matrix into an orthonormal basis, we use symmetric orthonormalization. We terminate the SCF iterations when the RMS change in the density matrix falls below 10^{-4} [11]. Our algorithm for calculating the auxiliary integrals is discussed in §3.4 below.

We define $E_{\text{HF}}^{\mathcal{N},\mathcal{L}}$ as the ground-state restricted HF energy from the $(\mathcal{N}, \mathcal{L})$ resolution, and it is convenient to quantify its error by

$$\Delta_{\text{HF}}^{\mathcal{N},\mathcal{L}} = -\log_{10} \left(E_{\text{HF}} - E_{\text{HF}}^{\mathcal{N},\mathcal{L}} \right) \quad (3.18)$$

There are several ways to introduce the resolution into post-HF calculations. Henceforth, we use the $(\mathcal{N}, \mathcal{L})$ resolution to generate the orbitals and orbital energies and then employ the same resolution when computing any required molecular orbital (MO) integrals. In this way, we are employing the same reduced-rank Hamiltonian throughout.

3.3.2 Perturbation theory

The second-order Møller-Plesset (MP2) correlation energy [11] is given by

$$E_{\text{MP2}} = \frac{1}{4} \sum_{abrs} \frac{|\langle ab||rs\rangle|^2}{\varepsilon_a + \varepsilon_b - \varepsilon_r - \varepsilon_s} \quad (3.19)$$

where a, b are occupied and r, s are virtual spin orbitals. In a closed-shell two-electron system, this reduces to a sum over virtual spatial orbitals

$$E_{\text{MP2}} = \sum_{rs} \frac{2(1r|1s)(11|rs) - (1r|1s)^2}{2\varepsilon_1 - \varepsilon_r - \varepsilon_s} \quad (3.20)$$

and thus the reduced-rank second-order Møller-Plesset (RRMP2) energy and its error are

$$E_{\text{MP2}}^{\mathcal{N}, \mathcal{L}} = \sum_{rs} \frac{2 \left[\sum_k^{\mathcal{K}} \langle 1r|\phi_k\rangle \langle \phi_k|1s\rangle \right] \left[\sum_k^{\mathcal{K}} \langle 11|\phi_k\rangle \langle \phi_k|rs\rangle \right] - \left[\sum_k^{\mathcal{K}} \langle 1r|\phi_k\rangle \langle \phi_k|1s\rangle \right]^2}{2\varepsilon_1 - \varepsilon_r - \varepsilon_s} \quad (3.21)$$

$$\Delta_{\text{MP2}}^{\mathcal{N}, \mathcal{L}} = -\log_{10} \left(E_{\text{MP2}}^{\mathcal{N}, \mathcal{L}} - E_{\text{MP2}} \right) \quad (3.22)$$

3.3.3 Configuration interaction

The full configuration interaction (FCI) correlation energy E_{FCI} is the lowest eigenvalue of the blocked full CI matrix [11]

$$\mathbf{H} = \begin{pmatrix} \langle \Psi_0|\bar{H} - E_{\text{HF}}|\Psi_0\rangle & 0 & \langle D|\bar{H}|\Psi_0\rangle \\ 0 & \langle S|\bar{H} - E_{\text{HF}}|S\rangle & \langle D|\bar{H}|S\rangle \\ \langle \Psi_0|\bar{H}|D\rangle & \langle S|\bar{H}|D\rangle & \langle D|\bar{H} - E_{\text{HF}}|D\rangle \end{pmatrix} \quad (3.23)$$

where the Hamiltonian \bar{H} is defined in (3.11) and Ψ_0 , S and D are the ground-state, singly-substituted, and (spin-adapted) doubly-substituted determinants, respectively. The largest block is $\langle D|\bar{H}|D\rangle$ and, when r, s, t and u are all distinct, the CI matrix element is

$$\langle \Psi_{11}^{rs}|\bar{H}|\Psi_{11}^{tu}\rangle = (rt|su) + (ru|ts) \quad (3.24)$$

Using the $(\mathcal{N}, \mathcal{L})$ resolution, this becomes

$$\langle \Psi_{11}^{rs}|\bar{H}|\Psi_{11}^{tu}\rangle^{\mathcal{N}, \mathcal{L}} = \sum_k^{\mathcal{K}} [(rt|\phi_k)(\phi_k|su) + (ru|\phi_k)(\phi_k|ts)] \quad (3.25)$$

and, with each matrix element approximated likewise, the lowest eigenvalue becomes $E_{\text{FCI}}^{\mathcal{N}, \mathcal{L}}$. It is convenient to quantify its error by the signed quantity

$$\Delta_{\text{FCI}}^{\mathcal{N}, \mathcal{L}} = -\text{sgn}(E_{\text{FCI}}^{\mathcal{N}, \mathcal{L}} - E_{\text{FCI}}) \log_{10} \left| E_{\text{FCI}}^{\mathcal{N}, \mathcal{L}} - E_{\text{FCI}} \right| \quad (3.26)$$

3.4 Auxiliary integrals

The calculation of auxiliary integrals $\langle \mu\nu | \phi_{nlm} \rangle$ is central to the application of RO theory to any quantum chemical method. The RO can be used with any type of basis function, and Hoggan has demonstrated [85, 87] that it works well with Slater-type functions, but we will employ Cartesian Gaussians in the present work.

Boys differentiation [29] can be used to derive formulae for integrals of higher angular momentum and we can therefore focus on the fundamental auxiliary integrals of the form

$$\langle ss | \phi_{nlm} \rangle = \int e^{-\zeta_A |\mathbf{r}-\mathbf{A}|^2} e^{-\zeta_B |\mathbf{r}-\mathbf{B}|^2} \phi_{nlm}(\mathbf{r}) d\mathbf{r} \quad (3.27)$$

Using the Gaussian product rule [11], this becomes

$$\langle ss | \phi_{nlm} \rangle = G_{AB} \int e^{-\gamma^2 |\mathbf{r}-\mathbf{R}|^2} \phi_{nlm}(\mathbf{r}) d\mathbf{r} \quad (3.28)$$

where $\gamma^2 = \zeta_A + \zeta_B$ and

$$\mathbf{R} = (\zeta_A \mathbf{A} + \zeta_B \mathbf{B}) / \gamma^2 \quad (3.29)$$

$$G_{AB} = \exp(-\zeta_A \zeta_B |\mathbf{A} - \mathbf{B}|^2 / \gamma^2) \quad (3.30)$$

Invoking Parseval's theorem and choosing the Laguerre generator (3.7) then yields

$$\begin{aligned} \langle ss | \phi_{nlm} \rangle &= (2\pi/\gamma^2)^{3/2} G_{AB} Y_{lm}(\mathbf{R}) \int_0^\infty h_n(x) j_l(Rx) e^{-x^2/4\gamma^2} dx \\ &= 4(\pi/\gamma^2)^{3/2} G_{AB} Y_{lm}(\mathbf{R}) A_{nl}(R, \gamma) \end{aligned} \quad (3.31)$$

The spherical harmonics $Y_{lm}(\mathbf{R})$ can be computed efficiently using Libbrecht's method [148] but the accurate and efficient evaluation of the radial integrals

$$A_{nl}(R, \gamma) = \int_0^\infty L_n(2x) j_l(Rx) \exp\left[-x - \frac{x^2}{4\gamma^2}\right] dx \quad (3.32)$$

for $n = 0, 1, \dots, \mathcal{N}$ and $l = 0, 1, \dots, \mathcal{L}$ is non-trivial. We show in §3.7 that they can be computed recursively from Hermite functions and one special function. A special treatment for integrals of higher angular momentum in the $R = 0$ case is also discussed in §3.7.1.

Table 3.1: Basis sets and energies of He and H₂ ($R_{\text{H-H}} = 1.40$)

	He	H ₂
Present basis	[10s3p2d]	[6s3p]
Size (B)	31	30
α_s	0.058 195 9	0.037 866 7
β_s	2.755 780 9	3.367 625 8
α_p	0.177 133 8	0.062 978 7
β_p	3.208 762 4	3.217 837 4
α_d	0.345 853 7	
β_d	3.519 611 2	
E_{HF}	-2.861 647 460	-1.133 287 175
E_{MP2}	-0.035 127 427	-0.030 496 094
E_{FCI}	-0.040 734 987	-0.038 527 089
Infinite basis		
E_{HF}	-2.861 679 996 ^a	-1.133 629 572 ^d
E_{MP2}	-0.037 40 ^b	-0.034 27 ^e
E_{FCI}	-0.042 044 381 ^c	-0.040 845 20 ^f

^aRef. [150]; ^bRef. [151] Slightly different values are also reported in Refs [152, 153];

^cRefs [150, 154]; ^dRef. [155]; ^e $R_{\text{H-H}} = 1.40108$ Ref. [153]; ^fRefs [155, 156]

3.5 Numerical results

3.5.1 Basis sets

For the purposes of this preliminary study, we have used even-tempered (ET) Gaussian basis sets [149] with exponents $\zeta_{kl} = \alpha_l \beta_l^k$, where $k = 1, 2, \dots$. The parameters α_l and β_l , along with the HF, MP2 and FCI energies that they yield for the He atom and H₂ molecule, are listed in Table 3.1. The energies are close to their respective complete basis set limits.

3.5.2 He atom and H₂ molecule

Table 3.2 shows that $E_{\text{HF}}^{\mathcal{N}, \mathcal{L}}$, $E_{\text{MP2}}^{\mathcal{N}, \mathcal{L}}$ and $E_{\text{FCI}}^{\mathcal{N}, \mathcal{L}}$ converge more or less exponentially with \mathcal{N} but that the scaling factor \mathcal{Z} strongly influences the convergence rate. At $\mathcal{Z} = 1$, microhartree accuracy is achieved at $\mathcal{N} = 10$ for all three methods and we have adopted $\mathcal{Z} = 1$ henceforth.

Table 3.2: Log energy errors for He atom for various \mathcal{N} and \mathcal{Z} with $\mathcal{L} = \infty$

$1/\mathcal{Z}$	$\Delta_{\text{HF}}^{\mathcal{N},\mathcal{L}}$						
	1/2	1	2	3	4	5	10
\mathcal{N}							
0	0.2	0.7	1.9	1.5	1.0	0.8	0.4
2	1.3	2.8	2.5	2.2	2.2	2.2	1.1
4	2.2	4.0	4.0	2.8	2.4	2.3	1.9
6	2.9	4.8	4.7	3.7	2.9	2.5	2.3
8	3.5	5.4	5.0	4.7	3.6	3.0	2.3
10	4.0	6.0	5.7	4.8	4.4	3.5	2.3
12	4.5	6.5	6.7	5.0	4.8	4.2	2.5

$1/\mathcal{Z}$	$\Delta_{\text{MP2}}^{\mathcal{N},\mathcal{L}}$							$\Delta_{\text{FCI}}^{\mathcal{N},\mathcal{L}}$						
	1/2	1	2	3	4	5	10	1/2	1	2	3	4	5	10
\mathcal{N}														
0	1.5	1.5	1.5	1.6	1.7	1.8	1.7	1.4	1.4	1.5	1.6	1.7	1.7	1.6
2	1.6	2.5	2.8	2.4	2.1	2.0	1.8	1.6	2.7	2.9	2.4	2.1	1.9	1.8
4	2.2	3.7	3.4	3.0	2.7	2.5	1.9	2.3	4.0	3.5	3.0	2.8	2.5	1.9
6	2.8	4.6	4.1	3.4	3.0	2.9	2.1	2.9	4.8	4.3	3.4	3.1	2.9	2.1
8	3.4	5.3	4.7	3.9	3.4	3.1	2.4	3.6	5.5	5.0	4.0	3.4	3.2	2.4
10	4.0	5.8	5.2	4.3	3.7	3.3	2.6	4.2	6.0	5.4	4.5	3.8	3.4	2.7
12	4.5	6.2	5.6	4.7	4.0	3.6	2.8	4.6	6.4	5.8	5.0	4.2	3.7	2.9

Table 3.3: Log energy errors for He atom for various \mathcal{N} and \mathcal{L} with $\mathcal{Z} = 1$

\mathcal{L}	$\Delta_{\text{HF}}^{\mathcal{N},\mathcal{L}}$					$\Delta_{\text{MP2}}^{\mathcal{N},\mathcal{L}}$					$\Delta_{\text{FCI}}^{\mathcal{N},\mathcal{L}}$				
	0	1	2	3	4	0	1	2	3	4	0	1	2	3	4
\mathcal{N}															
0	0.7	1.5	1.5	1.5	.	.	1.4	1.4	+1.4	+1.4	1.4
2	2.8	1.6	2.3	2.5	.	.	1.6	2.5	+2.7	+2.7	2.7
4	4.0	1.7	2.5	3.7	.	.	1.6	2.9	-3.8	+4.1	4.0
6	4.8	1.7	2.5	4.6	.	.	1.6	2.9	-3.6	-5.3	4.8
8	5.4	1.7	2.5	5.3	.	.	1.6	2.9	-3.6	-4.8	5.5
10	6.0	1.7	2.5	5.8	.	.	1.6	2.9	-3.6	-4.7	6.0
12	6.5	1.7	2.5	6.2	.	.	1.6	2.9	-3.6	-4.7	6.4

Table 3.4: Log energy errors for H₂ for various \mathcal{N} and \mathcal{L} with $\mathcal{Z} = 1$

\mathcal{L}	$\Delta_{\text{HF}}^{\mathcal{N},\mathcal{L}}$						
	0	2	4	6	8	10	12
\mathcal{N}							
0	1.4	1.5	1.5	1.5	1.5	1.5	1.5
2	2.4	3.5	3.6	3.6	3.6	3.6	3.6
4	2.4	3.9	4.4	4.4	4.4	4.4	4.4
6	2.4	4.1	5.0	5.2	5.2	5.2	5.2
8	2.4	4.1	5.3	6.1	6.5	6.6	6.7
10	2.4	4.1	5.3	6.2	6.7	6.9	7.0
12	2.4	4.1	5.3	6.2	6.8	7.3	7.5

\mathcal{L}	$\Delta_{\text{MP2}}^{\mathcal{N},\mathcal{L}}$							$\Delta_{\text{FCI}}^{\mathcal{N},\mathcal{L}}$						
	0	2	4	6	8	10	12	0	2	4	6	8	10	12
\mathcal{N}														
0	1.5	1.6	1.6	1.6	1.6	1.6	1.6	1.4	1.5	1.5	1.5	1.5	1.5	1.5
2	1.6	2.5	2.7	2.7	2.7	2.7	2.7	1.5	2.7	2.8	2.8	2.8	2.8	2.8
4	1.6	2.8	3.7	3.8	3.8	3.8	3.8	1.5	3.1	4.1	4.2	4.2	4.2	4.2
6	1.6	2.9	4.1	4.5	4.5	4.5	4.5	1.5	3.1	4.6	4.9	4.9	4.9	4.9
8	1.6	2.9	4.2	5.0	5.2	5.2	5.2	1.5	3.1	4.8	5.6	5.8	5.8	5.8
10	1.6	2.9	4.2	5.3	5.7	5.8	5.9	1.5	3.1	4.8	5.9	6.4	6.7	6.9
12	1.6	2.9	4.3	5.4	6.0	6.2	6.4	1.5	3.1	4.8	5.9	6.5	6.9	7.2

Table 3.5: Minimum \mathcal{N} and \mathcal{L} required to achieve $\Delta = 3, 6$ accuracy ($\mathcal{Z} = 1$)

B^2	$\Delta_{\text{HF}}^{\mathcal{N},\mathcal{L}} = 3$			$\Delta_{\text{MP2}}^{\mathcal{N},\mathcal{L}} = 3$			$\Delta_{\text{FCI}}^{\mathcal{N},\mathcal{L}} = 3$		
	\mathcal{N}	\mathcal{L}	\mathcal{K}	\mathcal{N}	\mathcal{L}	\mathcal{K}	\mathcal{N}	\mathcal{L}	\mathcal{K}
He 961	4	0	5	4	2	45	4	4	125
H ₂ 900	2	2	27	4	4	125	4	2	45

B^2	$\Delta_{\text{HF}}^{\mathcal{N},\mathcal{L}} = 6$			$\Delta_{\text{MP2}}^{\mathcal{N},\mathcal{L}} = 6$			$\Delta_{\text{FCI}}^{\mathcal{N},\mathcal{L}} = 6$		
	\mathcal{N}	\mathcal{L}	\mathcal{K}	\mathcal{N}	\mathcal{L}	\mathcal{K}	\mathcal{N}	\mathcal{L}	\mathcal{K}
He 961	10	0	11	12	2	117	10	4	275
H ₂ 900	8	6	441	12	8	1053	10	8	891

Table 3.3 explores the convergence of $E_{\text{HF}}^{\mathcal{N},\mathcal{L}}$, $E_{\text{MP2}}^{\mathcal{N},\mathcal{L}}$ and $E_{\text{FCI}}^{\mathcal{N},\mathcal{L}}$ with respect to \mathcal{N} and \mathcal{L} , using dots to indicate that higher \mathcal{L} provide no further improvement. Because the occupied orbital is spherical and the basis contains only s , p and d functions, the ϕ_{nlm} with $l > 0$, $l > 2$ and $l > 4$ contribute nothing to the HF, MP2 and CI energies, respectively.

The MP2 correlation energies converge smoothly towards their limiting values as \mathcal{N} and \mathcal{L} increase but the FCI results are more interesting. At $\mathcal{L} = 0$, only radial correlation energy is recovered from the basis set and, for example, $E_{\text{FCI}}^{12,0} = -0.017344$ is comparable to the value -0.017349 of Goldman [157]. At $\mathcal{L} = 2$ and $\mathcal{L} = 3$, some of the $E_{\text{FCI}}^{\mathcal{N},\mathcal{L}}$ energies are lower than the limiting value because the contributions from the d functions are treated incompletely. For example, at $\mathcal{L} = 2$, $(sd|sd)$ integrals are treated but $(dd|dd)$ are not. We conclude from this that, in practical calculations, one should ensure that $\mathcal{L} \geq 2L$, where L is the maximum angular momentum in the orbital basis set. This is consistent with comparable recommendations for RI [158] and Cholesky calculations [159].

The results in Table 3.4 for the H_2 molecule were obtained with the nuclei at $(0, 0, \pm 0.70)$. Convergence is similar to that for the He atom and, although $\mathcal{N} = \mathcal{L} = \infty$ is required to achieve formal convergence, the (12,10) resolution consistently yields microhartree accuracy.

3.5.3 Cost and accuracy

The obvious advantage of the RO, like the RI and Cholesky schemes, is that the $\mathcal{O}(B^4)$ four-centre $(\mu\nu|\lambda\sigma)$ integrals are replaced by the $\mathcal{O}(B^2\mathcal{K})$ three-centre $\langle\mu\nu|\phi_{nlm}\rangle$ integrals. If $\mathcal{K} < \mathcal{O}(B^2)$ in large systems, this is clearly beneficial and Table 3.5 summarizes the data in Tables 3.3 and 3.4 by listing minimum \mathcal{N} and \mathcal{L} required to obtain milli- and microhartree accuracy for He and H_2 . Even in these tiny systems, \mathcal{K} is competitive with B^2 .

The convergence with \mathcal{N} and \mathcal{L} is impressive. The demand on \mathcal{L} stems from the fact that the orbital basis functions have angular momentum and are not concentric with the ϕ_{nlm} . However, in the cases studied here, it was easy to saturate the \mathcal{L} dimension.

In [3], Gill and Gilbert showed that the reduced-rank Coulomb and exchange energies in a fixed system are sums of squares and thus converge monotonically with respect to \mathcal{K} . Here, the convergence with \mathcal{N} is more or less monotonic for the same reason. In larger systems, monotonicity may be lost because of differential Coulomb and exchange effects.

3.6 Concluding remarks

We have introduced a systematic hierarchy of approximations to the Schrödinger equation (SE) in which the two-electron Coulomb operator is replaced by truncated one-electron expansions.

The resulting rank-reduced Schrödinger equation (RRSE) is a mathematically simpler object than the SE but reduced-rank HF, MP2 and FCI calculations on the He atom and H₂ molecule reveal that the solutions of the RRSE converge rapidly towards the corresponding solutions of the SE.

In principle, we expect that any computational methods that involve r_{ij}^{-1} operator in Coulomb and exchange energy part will benefit from RO technique. In particular, DFT methods which are widely used currently may receive more benefits from our technique than the methods studied in this chapter as there is only easier Coulomb part to be approximated by RO. Though RO technique is fundamentally different from RI and Cholesky schemes, further studies including timing experiments and the comparison of convergence rate with respect to the rank of RRSE (\mathcal{K}) and size of auxiliary basis in other schemes should also be done in the future work.

In conclusion, these preliminary investigations suggest that the RRSE may offer a potent new route to accurate calculations.

Construction of radial integrals

Substituting the explicit formula [8] for the Laguerre polynomials

$$L_n(2x) = \sum_{k=0}^n (-1)^k \binom{n}{k} \frac{(2x)^k}{k!} \quad (3.33)$$

into (3.32) allows us to write the set of radial integrals as the binomial transform [160, 161]

$$A_{nl} = \sum_{k=0}^n (-1)^k \binom{n}{k} M_{kl} \quad (3.34)$$

of the set of monomial integrals

$$M_{kl}(R, \gamma) = \int_0^\infty \frac{(2x)^k}{k!} j_l(Rx) \exp\left[-x - \frac{x^2}{4\gamma^2}\right] dx \quad (3.35)$$

Our algorithm first forms M_{kl} boundary values, then binomially transforms these into A_{nl} boundary values, and finally uses a recurrence relation (RR) to build the remaining A_{nl} .

Substituting Gegenbauer's integral representation [8] of $j_l(Rx)$ into (3.35) and integrating over x yields

$$M_{kl}(R, \gamma) = \frac{(4\gamma)^k}{i^{l+1}R} \int_{Z^*}^Z H_{-(k+1)}(u) P_l\left(\frac{\gamma-u}{\gamma R i}\right) du \quad (3.36)$$

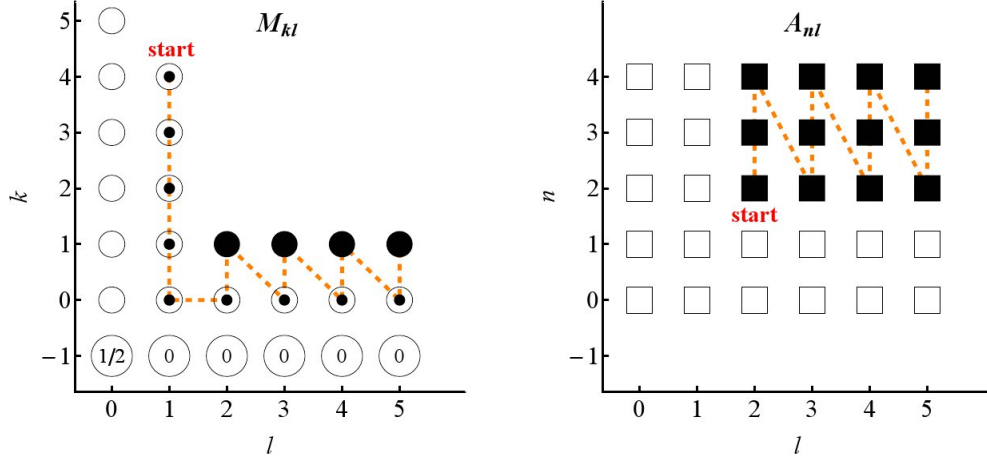


Figure 3.1: A recursive pathway to generate the M_{kl} and A_{nl} integrals.

where $Z = \gamma(1 + R\iota)$, H_{-k} is a Hermite function and P_l is a Legendre polynomial. From (3.36), it is easy to derive the outermost boundary values (the unfilled circles in Figure 3.1)

$$M_{-1,l} = \delta_{l,0}/2 \quad (3.37)$$

$$M_{k,0} = -\frac{(4\gamma)^k}{kR} \Im \{H_{-k}(Z)\} \quad (3.38)$$

The $M_{k,0}$ with $k > 0$ can be generated stably and efficiently by backward recursion, and the $k = 0$ case

$$M_{0,0} = \frac{2}{R} \Im \left\{ \int_0^Z H_{-1}(u) du \right\} \quad (3.39)$$

can be computed, for small $|Z|$, using the Taylor series

$$M_{0,0} = -\frac{\sqrt{\pi}}{R} \Im \left\{ \sum_{j=1}^{\infty} \frac{(-Z)^j}{j \Gamma(\frac{j+1}{2})} \right\} \quad (3.40)$$

and, for large $|Z|$, using the asymptotic expansion

$$M_{0,0} \sim \frac{1}{R} \Im \left\{ \ln Z - \sum_{j=1}^{\infty} \frac{\Gamma(j + \frac{1}{2})}{2j\sqrt{\pi}} (-Z^{-2})^j \right\} \quad (3.41)$$

Using the standard Hermite and Legendre RRs, one can derive from (3.36) the 5-term RR

$$\frac{k+1}{4\gamma^2} M_{k+1,l} = \frac{R}{2l+1} [lM_{k,l-1} - (l+1)M_{k,l+1}] + 2M_{k-1,l} - M_{k,l} \quad (3.42)$$

and this is used to form the $M_{k,1}$ (the vertical dotted circles in Figure 3.1). The standard Bessel RR immediately yields from (3.35) the 3-term RR

$$M_{k,l} = \frac{R}{2} \frac{k+1}{2l+1} (M_{k+1,l+1} + M_{k+1,l-1}) \quad (3.43)$$

and this, alternating with (3.42), is used to form the $M_{1,l}$ (the filled circles) and the $M_{0,l}$ (the horizontal dotted circles). We now have two rows and two columns of M_{kl} values and these are binomially transformed via (3.34) into the corresponding rows and columns of A_{nl} values (the unfilled squares). Finally, multiplying the standard Laguerre RR by the Bessel RR, one finds from (3.32) the 7-term RR

$$\begin{aligned} \frac{2(2l+1)}{R} A_{n,l} &= (2n+1)(A_{n,l+1} + A_{n,l-1}) \\ &\quad - n(A_{n-1,l+1} + A_{n-1,l-1}) - (n+1)(A_{n+1,l+1} + A_{n+1,l-1}) \end{aligned} \quad (3.44)$$

which is used to generate all the remaining A_{nl} (the filled squares in Figure 3.1).

Higher integrals in the $R=0$ case

In cases where $R = 0$, the Gaussian product is concentric with $\phi_k(\mathbf{r})$ and the resulting unnormalized auxiliary integrals are

$$\langle \mu\nu | \phi_{nlm} \rangle = \int x^a y^b z^c \exp(-\gamma^2 r^2) \phi_{nlm}(\mathbf{r}) d\mathbf{r} \quad (3.45)$$

As in (3.31), Parseval's Theorem allows this to be recast as

$$\langle \mu\nu | \phi_{nlm} \rangle = 4(\pi/\gamma^2)^{3/2} y_{lm}(a, b, c) \mathfrak{F}_{nl}^{a+b+c}(\gamma) \quad (3.46)$$

where

$$y_{lm}(a, b, c) = \int_0^\pi \int_0^{2\pi} \sin^{1+a+b} \theta \cos^c \theta \cos^a \varphi \sin^b \varphi Y_{lm}(\theta, \varphi) d\varphi d\theta \quad (3.47)$$

is the angular part and $\mathfrak{F}_{nl}^{l'}(\gamma)$, the binomial transform of $F_{kl}^{l'}(\gamma)$, is the radial part of the integration.

L	$l = 0$	$l = 1$	$l = 2$	$l = 3$	$l = 4$
0 (ss)	f_k^0				
1 (sp)		f_k^1			
2 (pp, sd)	$\frac{3}{2\gamma^2} f_k^0 - f_k^2$		f_k^2		
3 (pd)		$\frac{5}{2\gamma^2} f_k^1 - f_k^3$		f_k^3	
4 (dd)	$\frac{15}{(2\gamma^2)^2} f_k^0 - \frac{10}{2\gamma^2} f_k^2 + f_k^4$		$\frac{7}{2\gamma^2} f_k^2 - f_k^4$		f_k^4

As shown above, the $F_{kl}^{l'}(\gamma)$ are linear combinations of

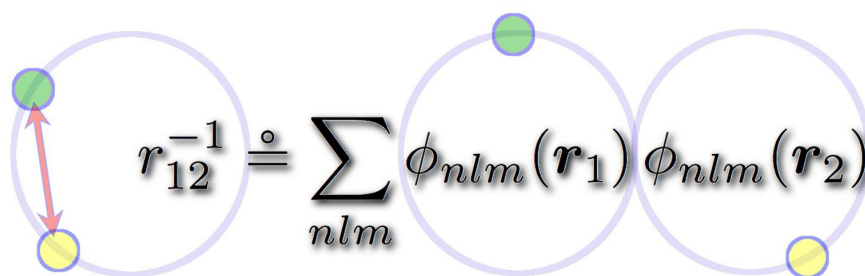
$$f_k^i(\gamma) \equiv \frac{(4\gamma)^{k+1}}{8\pi} \left(-\frac{1}{2\gamma}\right)^i \frac{\partial^i H_{-(k+1)}(\gamma)}{\partial \gamma^i} = \frac{(4\gamma)^{k+1}}{8\pi} \left(\frac{1}{\gamma}\right)^i (k+1)_i H_{-(k+i+1)}(\gamma) \quad (3.48)$$

where $l \leq i \leq l' = a + b + c$ and $(k+1)_i = (k+1)(k+2)\dots(k+i)$.

Because of the high symmetry of the system, most of the integrals (3.45) vanish. The exceptions are those in which the Gaussian product and the RO potential span the same irreducible representations of the spherical group. As a result, as mentioned in §3.5.2, \mathcal{L} is saturated at $2L$, leaving only \mathcal{N} to be improved.

Chapter 4

The Bessel quasi-resolution of the Coulomb operator


$$r_{12}^{-1} \stackrel{\circ}{=} \sum_{nlm} \phi_{nlm}(\mathbf{r}_1) \phi_{nlm}(\mathbf{r}_2)$$

$$\phi_{nlm}(\mathbf{r}) = 2\sqrt{2 - \delta_{n,0}} j_l(nr) Y_{lm}(\mathbf{r})$$

In this chapter, we show that the Coulomb operator can be resolved as $r_{12}^{-1} = \sum_{nlm} \phi_{nlm}(\mathbf{r}_1) \phi_{nlm}(\mathbf{r}_2)$ where $\phi_{nlm}(\mathbf{r})$ is proportional to the product of a spherical Bessel function and a spherical harmonic, provided that $r_1 + r_2 < 2\pi$.

The resolution reduces Coulomb matrix elements to Cholesky-like sums of products of auxiliary integrals. We find that these sums converge rapidly for four prototypical electron densities. To demonstrate its viability in large-scale quantum chemical calculations, we also use a truncated resolution to calculate the Coulomb energy of the nano-diamond crystallite $\text{C}_{84}\text{H}_{64}$.

4.1 Introduction

The apparently innocuous Coulomb operator

$$r_{12}^{-1} \equiv |\mathbf{r}_1 - \mathbf{r}_2|^{-1} \tag{4.1}$$

lies at the heart of many of challenging problems in contemporary quantum chemistry and many ingenious schemes have been devised [130, 129, 93, 162, 163, 127, 128, 143, 112, 113, 100, 109, 99, 164, 119, 165, 166] to treat it efficiently and accurately. In most cases, the full complexity of the operator is avoided by partially decoupling it [130, 129, 93], employing multipole expansions [162, 163, 127, 128], Fourier transforms [143], Cholesky decomposition [112, 113, 100, 109], density fitting [99, 164, 119], or other such methods [165, 166].

Our contributions [2, 3, 4] employ Coulomb resolutions

$$r_{12}^{-1} = \sum_{n=0}^{\infty} \sum_{l=0}^{\infty} \sum_{m=-l}^l \phi_{nlm}(\mathbf{r}_1) \phi_{nlm}(\mathbf{r}_2) \quad (4.2)$$

where the one-particle functions

$$\phi_{nlm}(\mathbf{r}) = V_{nl}(r) Y_{lm}(\mathbf{r}) \quad (4.3)$$

involve a radial function $V_{nl}(r)$ and a real spherical harmonic Y_{lm} . Such resolutions reduce Coulomb matrix elements to sums of auxiliary integrals

$$\langle a | r_{12}^{-1} | b \rangle = \sum_{nlm} \langle a | \phi_{nlm} \rangle \langle \phi_{nlm} | b \rangle \quad (4.4)$$

and thus formally resemble Cholesky schemes [112, 113, 100, 109]. However, our approach forms the ‘‘Cholesky triangle’’ directly, without computing the matrix elements.

To construct a Coulomb resolution, one combines the Legendre expansion and the Addition Theorem [9] to obtain the well-known [9] angular resolution

$$r_{12}^{-1} = \sum_{lm} \frac{4\pi}{2l+1} \frac{r_{<}^l}{r_{>}^{l+1}} Y_{lm}(\mathbf{r}_1) Y_{lm}(\mathbf{r}_2) \quad (4.5)$$

where $r_{<}$ and $r_{>}$ are the smaller and larger of r_1 and r_2 .

To achieve a radial resolution

$$\frac{4\pi}{2l+1} \frac{r_{<}^l}{r_{>}^{l+1}} = \sum_n V_{nl}(r_1) V_{nl}(r_2) \quad (4.6)$$

one possibility [2, 3, 4] is to choose

$$V_{nl}(r) = 2\sqrt{2} \int_0^{\infty} h_n(x) j_l(xr) dx \quad (4.7)$$

where the j_l are spherical Bessel functions and the h_n are *any* functions that form a complete and orthonormal set on $[0, \infty)$. Varganov *et al.* chose Hermite functions

$$h_n(x) = \frac{(2/\pi)^{1/4}}{2^n \sqrt{(2n)!}} H_{2n}(x/\sqrt{2}) \exp(-x^2/4) \quad (4.8)$$

in [2], but Gill and Gilbert adopted Laguerre functions

$$h_n(x) = \sqrt{2} L_n(2x) \exp(-x) \quad (4.9)$$

in later studies [3, 4]. This approach to the radial resolution is theoretically attractive but, unfortunately, the radial functions V_{nl} that emerge from such “natural” choices for the h_n are often computationally expensive [2, 3, 4] and this has led us to explore alternative schemes.

4.2 Bessel quasi-resolution

In the present Chapter, we offer a route based on the Bessel identity (4.11). Originally, we derived the identity from fitting quadrature abscissas and weights* but it can be proven mathematically. (See Chapter 5 and Chapter 7.)

$$\int_0^\infty j_l(nx)j_l(ny)dn \doteq \frac{\delta_{l,0}}{2} + \sum_{n=1}^\infty j_l(nx)j_l(ny) \quad (4.11)$$

where $l = 0, 1, 2, \dots$ and $|x| + |y| < 2\pi$. We use the symbol \doteq to remind us of this domain restriction.

If we begin with the integral representation [167] of the left-hand side of (4.6)

$$\frac{4\pi}{2l+1} \frac{r_{<}^l}{r_{>}^{l+1}} = 8 \int_0^\infty j_l(xr_1)j_l(xr_2)dx \quad (4.12)$$

and apply (4.11), we obtain the radial quasi-resolution

$$\frac{4\pi}{2l+1} \frac{r_{<}^l}{r_{>}^{l+1}} \doteq 8 \left[\frac{\delta_{l,0}}{2} + \sum_{n=1}^\infty j_l(nr_1)j_l(nr_2) \right] \quad (4.13)$$

*See (2.47) and the discussion that follows. We also obtained an equivalent identity.

$$\int_0^\infty j_l(nx)j_l(ny)dn \doteq \sum_{n=0}^\infty j_l\left(\left(n + \frac{1}{2}\right)x\right)j_l\left(\left(n + \frac{1}{2}\right)y\right) \quad (4.10)$$

and thence the spherical Bessel quasi-resolution

$$r_{12}^{-1} \doteq \sum_{nlm} \phi_{nlm}(\mathbf{r}_1) \phi_{nlm}(\mathbf{r}_2) \quad (4.14)$$

where the one-particle functions are

$$\phi_{nlm}(\mathbf{r}) = 2\sqrt{2 - \delta_{n,0}} j_l(nr) Y_{lm}(\mathbf{r}) \quad (4.15)$$

This is the key result of this chapter. As the prefix ‘quasi’ and the symbol \doteq emphasize, it is valid only for $r_1 + r_2 < 2\pi$.

The quasi-resolution, unlike our previous resolutions [2, 3, 4], requires only the calculation of spherical Bessel functions [168] and spherical harmonics [169, 170] which is efficient and stable even for large n , l and m .

Replacing r_{12}^{-1} by the quasi-resolution directly yields the Cholesky-like decomposition

$$\langle a|r_{12}^{-1}|b \rangle \doteq \sum_{nlm} \langle a|\phi_{nlm} \rangle \langle \phi_{nlm}|b \rangle \quad (4.16)$$

but without the need to compute the $\langle a|r_{12}^{-1}|b \rangle$ integrals. The auxiliary integrals

$$\langle a|\phi_{nlm} \rangle = 2\sqrt{2 - \delta_{n,0}} \int a(\mathbf{r}) j_l(nr) Y_{lm}(\mathbf{r}) d\mathbf{r} \quad (4.17)$$

are easily found if the Fourier transform of $a(\mathbf{r})$ is known. For example, if $a(\mathbf{r})$ is the Gaussian

$$a(\mathbf{r}) = (\zeta_A/\pi)^{3/2} \exp(-\zeta_A|\mathbf{r} - \mathbf{R}|^2) \quad (4.18)$$

we have

$$\langle a|\phi_{nlm} \rangle = \exp\left(-\frac{n^2}{4\zeta_A}\right) \phi_{nlm}(\mathbf{R}) \quad (4.19)$$

If $a(\mathbf{r})$ is sufficiently smooth then, by Darboux’s Principle [171], the $\langle a|\phi_{nlm} \rangle$ will decay quickly for large n, l, m , leading to rapid convergence of the sum in (4.16). We see from (4.19), for example, that small ζ_A yield fast decay with n , and small R yield fast decay with l .

One elementary use of the quasi-resolution is to find the Coulomb self-interaction energy

$$E = \frac{1}{2} \langle \rho|r_{12}^{-1}|\rho \rangle \quad (4.20)$$

of a given charge density $\rho(\mathbf{r})$. If the density $\rho(\mathbf{r}) \equiv \rho(r)$ is a normalized, origin-centered radial function, one finds

$$\tilde{E} = \frac{1}{2} \sum_{nlm} \langle \rho|\phi_{nlm} \rangle \langle \phi_{nlm}|\rho \rangle = \frac{1}{2\pi} + \frac{1}{\pi} \sum_n \Delta \tilde{E}^{(n)} \quad (4.21)$$

Table 4.1: Coulomb energies E , components $\Delta\tilde{E}^{(n)}$ and domain-violation errors^a E^{DVE} of four radial charge densities^b $\rho(r)$

	Uniform density ^c	Exponential density
$R^3 \times \rho(r)$	$3/(4\pi)H(R-r)$	$\exp(-r/R)/(8\pi)$
Non-analyticity	Discontinuity at $r = R$	Cusp at $r = 0$
$R \times E$	$3/5$	$5/32$
$\Delta\tilde{E}^{(n)}$	$9j_1^2(nR)/(nR)^2$	$(1 + n^2 R^2)^{-4}$
Convergence	$O[(nR)^{-4}]$	$O[(nR)^{-8}]$
$R \times E_{\text{DVE}}$	$6(1-\theta)^3 H(1-\theta)/\theta^4$	$\frac{1}{6}(\theta+1)^3 \exp(-2\theta)$

	Rational density	Gaussian density
$R^3 \times \rho(r)$	$(1 + (r/R)^2)^{-2}/\pi^2$	$\exp(-r^2/R^2)/\pi^{3/2}$
Non-analyticity	Poles at $r = \pm iR$	No singularities
$R \times E$	$1/(2\pi)$	$1/\sqrt{2\pi}$
$\Delta\tilde{E}^{(n)}$	$\exp(-2nR)$	$\exp(-n^2 R^2/2)$
Convergence	$O[\exp(-2nR)]$	$O[\exp(-n^2 R^2/2)]$
$R \times E_{\text{DVE}}$	$1/(6\theta)$	$\sqrt{2/\pi} \exp(-2\theta^2)$

^a $\theta = \pi/R$

^b R is a parameter that characterizes the radial extent of the density.

^c H is the Heaviside step function

and results for four such densities are given in Table 4.1. These densities consist of a uniform ball (which is discontinuous on its boundary), an exponential (which has a cusp at a point), a rational function (which has poles in the complex plane), and a Gaussian (which is entire).

Consistent with Darboux's Principle [171], the results in the penultimate row of Table 4.1 confirm that the convergence of the resolution (4.21) is algebraic if $\rho(r)$ has a singularity in real space, exponential if it has a singularity in the complex plane, and super-exponential if $\rho(r)$ is entire.

The key weakness of the quasi-resolution is the domain restriction $r_1 + r_2 < 2\pi$. If the quasi-resolution is applied to a density that extends beyond $r = \pi$, it introduces a Domain-Violation Error (DVE)

$$E_{\text{DVE}} = \tilde{E} - E \quad (4.22)$$

and the final row of Table 4.1 illustrates this. The message is clear: in practical applications, one should scale the system so that the DVE is acceptably small.

4.3 Numerical results

We begin our numerical assessment by truncating the radial resolution (4.13) after \mathcal{N} terms. The truncated sums are useful approximations to the left-hand side and Figure 4.1 illustrates this for $l = 0, 1, 2$ with $r_1 = 1$ and $\mathcal{N} = 10$. It confirms that the approximations are satisfactory when $r_1 + r_2 < 2\pi$ but erratic outside that domain. We note however that, even there, the errors are bounded.

Truncating the quasi-resolution (4.14) at $n = \mathcal{N}$ and $l = \mathcal{L}$ yields well-defined approximations to both the operator and its matrix elements. For example, the approximation

$$\tilde{E}^{\mathcal{N}, \mathcal{L}} = \frac{1}{2} \sum_{n=0}^{\mathcal{N}} \sum_{l=0}^{\mathcal{L}} \sum_{m=-l}^l \langle \rho | \phi_{nlm} \rangle \langle \phi_{nlm} | \rho \rangle \quad (4.23)$$

has the Truncation Error

$$E_{\text{TE}} = \tilde{E}^{\mathcal{N}, \mathcal{L}} - \tilde{E} \quad (4.24)$$

Is such a truncation useful in practice? To explore this question, we have used (4.23) to calculate the Coulomb self-interaction energy of the electrons in the octahedral nano-diamond $\text{C}_{84}\text{H}_{64}$ crystallite [172]. This molecule has a diamond-like structure with T_d symmetry and, for the sake of simplicity, we have used C–C

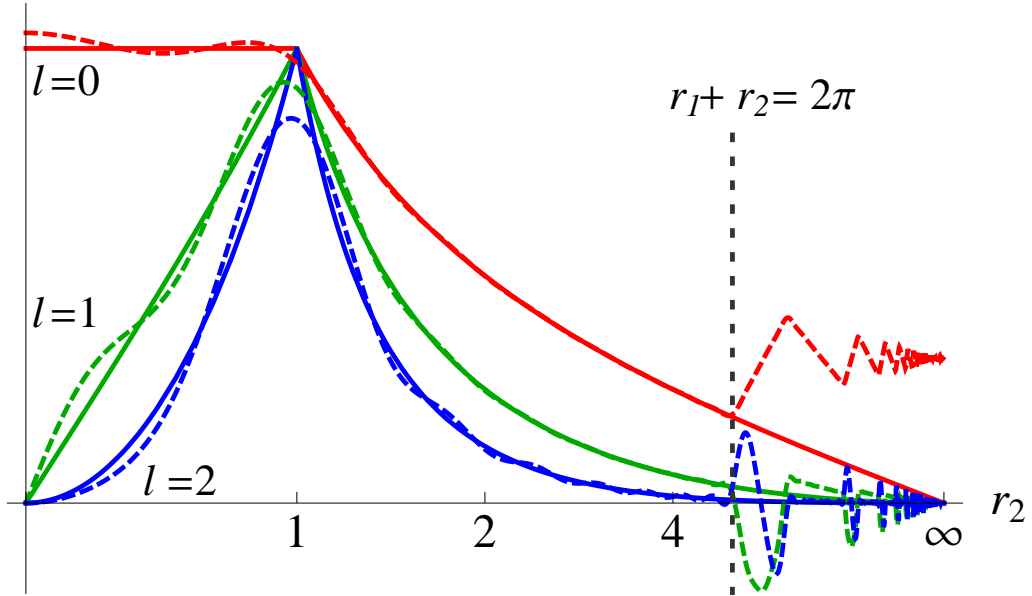


Figure 4.1: The left-hand side (solid) and right-hand side (dashed) of (4.13) for $l = 0, 1, 2$ when $r_1 = 1$ and the sum is truncated after $n = 10$. Plots are scaled so that the left-hand sides coincide at $r_2 = 1$.

and C–H lengths of 154 and 109 pm, respectively. The electron density

$$\rho(\mathbf{r}) = \sum_{A=1}^{148} \rho_A(\mathbf{r}) \quad (4.25)$$

is the sum of the Stewart atomic densities [173, 174, 175]

$$\rho_A(\mathbf{r}) = \sum_{i=1}^{D_A} c_i (\zeta_i/\pi)^{3/2} \exp(-\zeta_i |\mathbf{r} - \mathbf{R}_A|^2) \quad (4.26)$$

generated from the UHF/6-311G densities of isolated 3P carbon and 2S hydrogen atoms. The Stewart parameters are given in Table 4.2 and yield $E = 20511.5578014$ a.u.

We have written a C program to compute (4.23) and we use the relative error

$$\epsilon \equiv \left| \frac{\tilde{E}^{\mathcal{N}, \mathcal{L}} - E}{E} \right| = \left| \frac{E_{\text{DVE}} + E_{\text{TE}}}{E} \right| \quad (4.27)$$

to measure the accuracy of the approximation (4.23) for different $(\mathcal{N}, \mathcal{L})$.

The molecule's center of mass is placed at the origin but most of its nuclei still lie outside the allowed domain (*i.e.* $|\mathbf{R}_A| > \pi$). We therefore compress the entire

Table 4.2: Stewart parameters for atoms

Hydrogen		Carbon	
c_i	ζ_i	c_i	ζ_i
0.29449	0.21	1.71581	0.29
0.63550	0.88	2.54666	0.82
0.05859	3.73	-0.18334	2.31
0.01253	15.90	0.26810	6.50
-0.00111	67.73	1.09048	18.31
		0.45570	51.55
		0.09106	145.16
		0.01337	408.75
		0.00195	1150.99
		0.00016	3241.06
		0.00005	9126.48

system by a scale factor \mathcal{Z} , perform the Coulomb calculation, and then unscale the resulting energy. The relationship between scaled and unscaled systems is described by the following equations.

$$\mathbf{R}'_A = \mathcal{Z}^{-1} \mathbf{R}_A \quad (4.28)$$

$$\zeta'_i = \mathcal{Z}^2 \zeta_i \quad (4.29)$$

$$\rho'(\mathbf{r}') = \mathcal{Z}^3 \rho(\mathbf{r}) \quad (4.30)$$

$$E' = \mathcal{Z}E \quad (4.31)$$

A scaled system described by \mathbf{R}'_A , ζ'_i and $\rho'(\mathbf{r}')$ is mathematically equivalent to the unscaled one. Thus, in theory, this scheme is exact and works for any kind of energies or molecular properties. However, when we use scaling in conjunction with truncated resolution, the compression increases the exponents ζ'_i . As a result, the auxiliary integrals (4.19) decay more slowly, reducing the rate of convergence of (4.23) and increasing the truncation error (4.24).

Figure 4.2 reveals that there is a DVE-dominated region ($\mathcal{Z} \lesssim 4$) and a TE-dominated region ($\mathcal{Z} \gtrsim 5$). The results show that the truncation error grows slowly as \mathcal{Z} is increased but that the domain-violation error grows rapidly as \mathcal{Z} is decreased.

It is therefore important to scale the system to fit in the domain but moderate

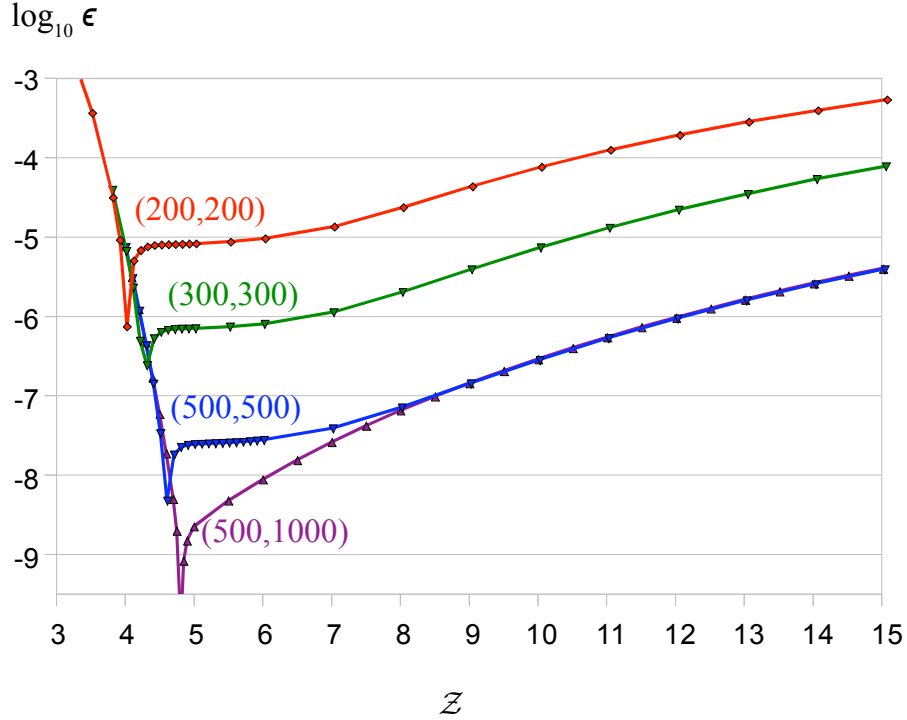


Figure 4.2: Relative error, (4.27), of $\tilde{E}^{\mathcal{N},\mathcal{L}}$ for $3 \leq \mathcal{Z} \leq 15$.

over-compression does not magnify the error by very much. For $\mathcal{N} = 500$, $\mathcal{L} = 1000$, the lowest errors arise near $\mathcal{Z} = 4.8$ but any \mathcal{Z} from 4.5 to 12 leads to $\epsilon < 10^{-6}$.

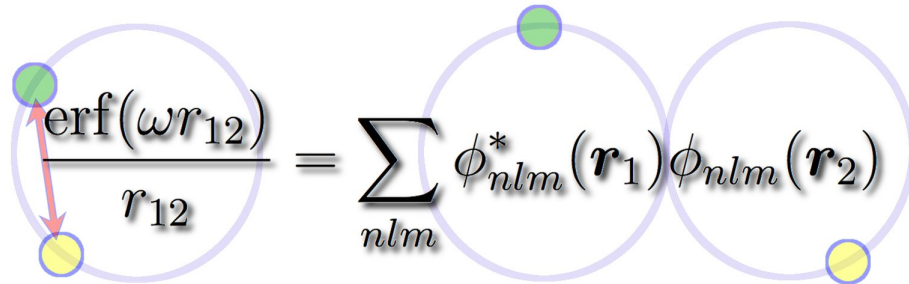
4.4 Concluding remarks

In summary, we have derived a quasi-resolution of the Coulomb operator that allows it to be expressed in terms of products of one-particle functions. Unlike earlier resolutions, the quasi-resolution is based on simple mathematical functions and is well suited for computational purposes. Our numerical study indicates that the quasi-resolution is useful for computing the Coulomb energy, which is an important bottleneck in DFT calculations.

However, the potential scope of the quasi-resolution is much wider than this and there are significant possibilities for applications to other operators and to exchange and correlation energies. (See later chapters.)

Chapter 5

Bessel Resolutions of the long-range Coulomb operators


$$\frac{\text{erf}(\omega r_{12})}{r_{12}} = \sum_{nlm} \phi_{nlm}^*(\mathbf{r}_1) \phi_{nlm}(\mathbf{r}_2)$$

$$\phi_{nlm}(\mathbf{r}) = 4\sqrt{b_n\omega} j_l(2\beta_n\omega r) Y_l^m(\mathbf{r})$$

We show that the long-range Ewald operator can be resolved as $\text{erf}(\omega r_{12})/r_{12} = \sum_k \phi_k^*(\mathbf{r}_1)\phi_k(\mathbf{r}_2)$ where ϕ_k is proportional to the product of a spherical Bessel function and a spherical harmonic. We demonstrate the use of this new resolution by calculating the long-range Coulomb energy of the nano-diamond crystallite $\text{C}_{84}\text{H}_{64}$ and the long-range exchange energy of the graphene $\text{C}_{96}\text{H}_{24}$. The resolution appears particularly effective for long-range exchange calculations.

5.1 Introduction

We have recently published a series of papers [2, 3, 4, 5, 7] concerned with resolving the Coulomb operator

$$r_{12}^{-1} \equiv |\mathbf{r}_1 - \mathbf{r}_2|^{-1} = \sum_{k=1}^{\infty} |\phi_k\rangle \langle \phi_k| \quad (5.1)$$

into one-particle functions, where $|\phi_k\rangle$ and $\langle \phi_k|$ are functions of \mathbf{r}_1 and \mathbf{r}_2 , respectively. Such resolutions factorize a Coulomb integral into a sum of products of auxiliary integrals

$$\langle a|r_{12}^{-1}|b\rangle = \sum_{k=1}^{\infty} \langle a|\phi_k\rangle \langle \phi_k|b\rangle \quad (5.2)$$

and thereby offer the computational benefits of Cholesky decomposition [112, 113, 100, 109] and density fitting [99, 164, 119], but without the need to solve Cholesky or fitting equations.

In Chapter 4 and Chapter 7, we have shown that the one-particle functions can take the form

$$\phi_k(\mathbf{r}) \equiv \phi_{nlm}(\mathbf{r}) = 2\sqrt{2 - \delta_{n,0}} j_l(nr) Y_l^m(\mathbf{r}) \quad (5.3)$$

where j_l is a spherical Bessel function and Y_l^m is a complex spherical harmonic. Although this resolution is valid only for $r_1 + r_2 < 2\pi$, we have shown that this weakness can be overcome by a suitable pre-scaling of the system under study.

There is considerable contemporary interest [137, 129, 173, 95, 84, 138, 143, 176, 177, 178, 179, 62, 180, 181, 182, 183, 184, 63, 185, 186, 64, 65, 187] in partitioning the Coulomb operator as

$$r_{12}^{-1} \equiv S(r_{12}) + L(r_{12}) \quad (5.4)$$

where S is a singular short-range operator and L is a smooth long-range operator, and then treating the short-range and long-range subproblems separately. Ewald introduced this to chemistry to compute Madelung constants [92] but it can be traced, in the mathematics literature, to Riemann [188].

The partition strategy is now employed in many quantum chemical methods. It is particularly prominent in hybrid methodologies, wherein wavefunction-based and density-based approaches are carefully combined to exploit their respective strengths. This has led, for example, to the popular HSE [176, 177, 178, 179], CAM-B3LYP [62], LC- ω PBE [184], LCgau-BOP [186] and ω B97XD [65] methods.

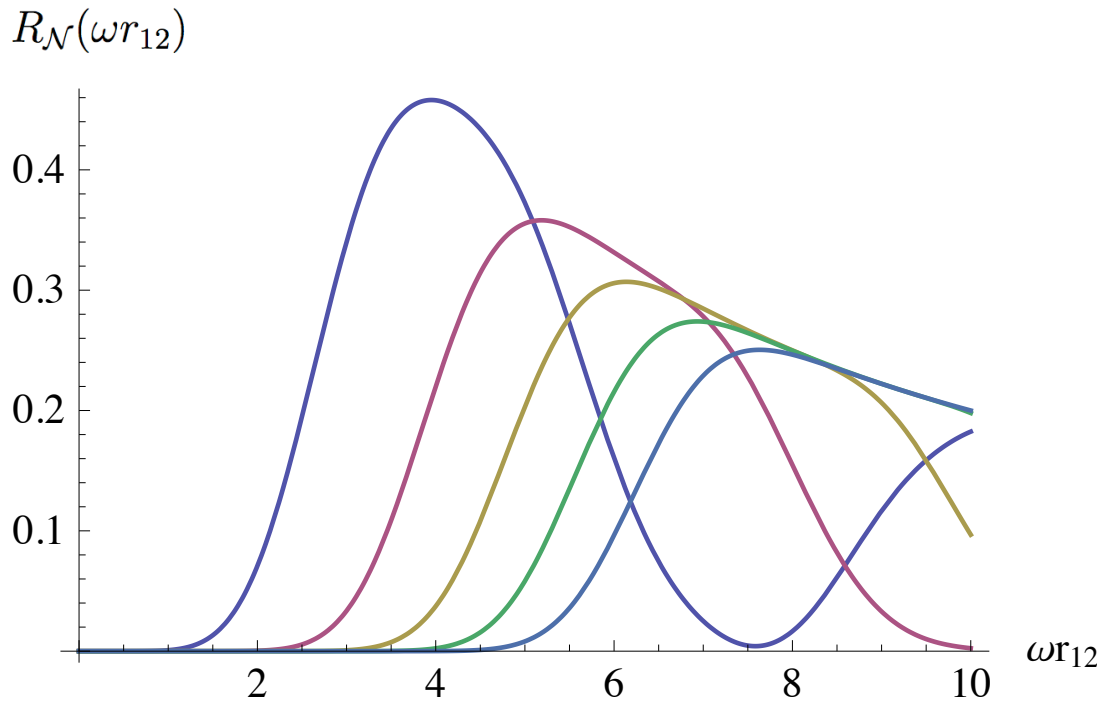


Figure 5.1: Quadrature error $R_{\mathcal{N}}(\omega r_{12})$ in (5.7) for $\mathcal{N} = 1$ (leftmost), 3, 5, 7 and 9 (rightmost)

The short-range operator S can be treated efficiently by the use of boxing schemes [163, 162, 127, 128, 139, 177] that exploit spatial locality. However, the long-range operator L is more computationally difficult and it is natural to ask whether a resolution analogous to (5.1) can be constructed for it.

It turns out that there are many ways to resolve such operators and we will consider several. Our approaches are general but, in this chapter, we focus on the long-range Ewald operator

$$L(r_{12}) = \frac{\operatorname{erf}(\omega r_{12})}{r_{12}} \quad (5.5)$$

The partition parameter ω can take any positive value (the limit $\omega \rightarrow \infty$ recovers the Coulomb operator) but, in practice, often lies between 0.1 and 1. We use atomic units throughout.

5.2 Resolutions of the Ewald operator

We have investigated five approaches for resolving the Ewald operator: orthonormal expansion, Taylor expansion, Gaussian expansion, Bessel expansion and Her-

mite quadrature. The first four are outlined in the §5.6 but we describe the fifth and most promising here.

If we apply $2(\mathcal{N} + 1)$ -point Gauss-Hermite quadrature [9, 189] to the integral representation

$$L(r_{12}) = \frac{2\omega}{\pi} \int_{-\infty}^{\infty} j_0(2\beta\omega r_{12}) \exp(-\beta^2) d\beta \quad (5.6)$$

we obtain the spherical Bessel expansion*

$$L(r_{12}) = \frac{4\omega}{\pi} \left[\sum_{n=0}^{\mathcal{N}} b_n j_0(2\beta_n \omega r_{12}) + R_{\mathcal{N}}(\omega r_{12}) \right] \quad (5.7)$$

where the β_n and b_n are the (positive) Hermite roots and weights.

How accurate are these Bessel expansions? The quadrature error $R_{\mathcal{N}}(\omega r_{12})$ for $\mathcal{N} = 1, 3, 5, 7, 9$ is shown in Figure 5.1. It is initially tiny, indicating that the expansions are accurate for small ωr_{12} , but eventually breaks away from the axis when the expansion becomes unsatisfactory. (We note, however, that the error is bounded for all ωr_{12} .) It is encouraging to observe that the breakaway point moves rapidly to the right as \mathcal{N} is increased, suggesting that even modest values of \mathcal{N} yield Bessel expansions that are useful over large domains of ωr_{12} .

In principle, all \mathcal{N} terms in (5.7) must be included. However, because $|j_0(z)| \leq 1$ and the Hermite weights b_n decay extremely rapidly, it is possible to truncate (5.7) at $n = \mathcal{N}' \ll \mathcal{N}$ with negligible loss of accuracy. The minimum \mathcal{N} and \mathcal{N}' that guarantee that the quadrature error is below ϵ over the domain $0 \leq \omega r_{12} \leq R$ are shown in Table 5.1. This Table reveals that, in a molecule where $\max(r_{12}) \approx 30$ (for example taxol $C_{47}H_{51}NO_{14}$), an accuracy of 10^{-10} requires only $\mathcal{N}' = 50$ terms for $\omega = 1$ or only $\mathcal{N}' = 21$ terms for $\omega = 1/3$.

To resolve the j_0 functions in (5.7), we start with the spherical Bessel addition theorem [9]

$$j_0(\lambda r_{12}) = \sum_{l=0}^{\infty} (2l + 1) j_l(\lambda r_1) j_l(\lambda r_2) P_l(\cos \theta_{12}) \quad (5.8)$$

and apply the Legendre addition theorem [9] to find

$$j_0(\lambda r_{12}) = 4\pi \sum_{l=0}^{\infty} \sum_{m=-l}^l j_l(\lambda r_1) j_l(\lambda r_2) Y_l^{m*}(\mathbf{r}_1) Y_l^m(\mathbf{r}_2) \quad (5.9)$$

*For the history of this discovery, see (2.47) and the discussion that follows.

Table 5.1: \mathcal{N} and \mathcal{N}' such that $R_{\mathcal{N}}(\omega r_{12}) < \epsilon$ for $0 \leq \omega r_{12} \leq R$.

$-\log_{10} \epsilon$	$R = 10$		$R = 20$		$R = 30$		$R = 40$		$R = 50$	
	\mathcal{N}	\mathcal{N}'	\mathcal{N}	\mathcal{N}'	\mathcal{N}	\mathcal{N}'	\mathcal{N}	\mathcal{N}'	\mathcal{N}	\mathcal{N}'
2	30	7	107	12	234	18	409	24	633	29
3	34	9	116	16	247	24	427	31	657	38
4	37	11	121	20	256	28	440	37	673	46
5	39	13	126	23	263	33	449	42	686	52
6	41	15	131	26	269	36	458	47	696	58
7	43	16	134	28	275	40	466	52	706	64
8	45	18	138	31	280	43	472	56	714	69
9	47	19	141	33	285	47	479	60	722	74
10	49	21	144	35	290	50	485	64	730	79
11	50	22	147	37	294	53	490	68	737	83
12	52	23	150	40	298	56	496	72	743	88

Substituting (5.9) into (5.7) then yields our key result — the Ewald resolution

$$L^{\mathcal{N}, \mathcal{L}}(r_{12}) = \sum_{n=0}^{\mathcal{N}} \sum_{l=0}^{\mathcal{L}} \sum_{m=-l}^l |\phi_{nlm}\rangle \langle \phi_{nlm}| \quad (5.10a)$$

$$\phi_{nlm}(\mathbf{r}) = 4\sqrt{b_n\omega} j_l(2\beta_n\omega r) Y_l^m(\mathbf{r}) \quad (5.10b)$$

In contrast to the previous Chapter, we note that the above resolution is insensitive to scaling. This is because we also need to scale $\omega' = \mathcal{Z}\omega$ and the scaling factor \mathcal{Z} cancels out when we use the resolution. (See §2.1.)

5.3 Computational considerations

It is essential to be able to determine *a priori* the minimum values of \mathcal{N} and \mathcal{N}' that will guarantee that (5.7) is accurate to within ϵ over the domain of important ωr_{12} values in one's system. By examining the values of \mathcal{N} in Table 5.1, we have devised the simple quadratic estimate

$$\mathcal{N} \approx R^2/4 + \left(\sqrt{-\log_{10} \epsilon} - 1\right) R + 2 \quad (5.11)$$

and it is then easy to show from the asymptotic behavior of the Hermite roots and weights that

$$\mathcal{N}' \approx \frac{2}{\pi} \sqrt{-(\mathcal{N} + 1) \ln \epsilon} - 1 \quad (5.12)$$

To use the Ewald resolution (5.10) to find long-range energies, we need the auxiliary integrals

$$\langle ab | \phi_{nlm} \rangle = \int a(\mathbf{r}) b(\mathbf{r}) \phi_{nlm}(\mathbf{r}) d\mathbf{r} \quad (5.13)$$

where we will assume that a and b are Gaussian basis functions centered at \mathbf{A} and \mathbf{B} , respectively. Because the Gaussian product rule allows $a(\mathbf{r})b(\mathbf{r})$ to be expanded as a finite linear combination [190] of Gaussians with a centroid \mathbf{P} on the line between \mathbf{A} and \mathbf{B} , the problem reduces to finding two-center integrals of the form

$$\langle G_{n'l'm'} | \phi_{nlm} \rangle = \int r^{n'} \exp(-\zeta r^2) Y_{l'}^{m'*}(\mathbf{r}) \phi_{nlm}(\mathbf{r} + \mathbf{P}) d\mathbf{r} \quad (5.14)$$

These can be solved in closed form and we will discuss an efficient algorithm for Gaussians of arbitrary angular momentum in Chapter 6. However, in a basis that contains only s and p functions, the only necessary formulae are

$$\langle G_{000} | \phi_{nlm} \rangle = c_n C_l^{lm00} j_l Y_l^m \quad (5.15a)$$

$$\langle G_{200} | \phi_{nlm} \rangle = c_n C_l^{lm00} [3/(2\zeta) - x_n^2] j_l Y_l^m \quad (5.15b)$$

$$\langle G_{11m'} | \phi_{nlm} \rangle = c_n x_n \left[C_{l-1}^{lm1m'} j_{l-1} Y_{l-1}^{m-m'} - C_{l+1}^{lm1m'} j_{l+1} Y_{l+1}^{m-m'} \right] \quad (5.15c)$$

$$\langle G_{22m'} | \phi_{nlm} \rangle = c_n x_n^2 \left[C_{l-2}^{lm2m'} j_{l-2} Y_{l-2}^{m-m'} - C_l^{lm2m'} j_l Y_l^{m-m'} + C_{l+2}^{lm2m'} j_{l+2} Y_{l+2}^{m-m'} \right] \quad (5.15d)$$

where $x_n \equiv \beta_n \omega / \zeta$, $j_l \equiv j_l(2\beta_n \omega P)$, $Y_l^m \equiv Y_l^m(\mathbf{P})$

$$c_n = 4\sqrt{b_n \omega} (\pi/\zeta)^{3/2} \exp(-\zeta x_n^2) \quad (5.16)$$

$$C_\ell^{lm'l'm'} = (-1)^{m'} \sqrt{\frac{(2l+1)(2l'+1)}{4\pi(2\ell+1)}} C_{0,0,0}^{l,l',\ell} C_{m,m',m-m'}^{l,l',\ell} \quad (5.17)$$

and the final two factors in (5.17) are Clebsch-Gordan coefficients. We note that $C_l^{lm00} = Y_0^0 = 1/\sqrt{4\pi}$ and, thus, (5.15a) is analogous to (4.19) in the previous chapter.

We have implemented the Ewald resolution in a standalone C program which precomputes the required Hermite roots and weights [189], along with the Clebsch-Gordan coefficients. The j_l and Y_l^m are calculated recursively, as in the previous

Table 5.2: $(\mathcal{N}, \mathcal{L})$ pairs required in long-range Coulomb and exchange calculations

	Long-range Coulomb energy of the nano-diamond $C_{84}H_{64}$			Long-range exchange energy of the graphene $C_{96}H_{24}$		
	$\omega = 0.1$	$\omega = 0.5$	$\omega = 1.0$	$\omega = 0.1$	$\omega = 0.5$	$\omega = 1.0$
$\epsilon = 10^{-3}$	(2 , 0)	(29 , 13)	(113 , 24)	(0 , 4)	(1 , 27)	(4 , 45)
$\epsilon = 10^{-6}$	(4 , 4)	(48 , 23)	(180 , 50)	(1 , 9)	(3 , 44)	(7 , 85)
$\epsilon = 10^{-9}$	(6 , 8)	(64 , 36)	(240 , 68)	(2 , 13)	(5 , 58)	(11 , 99)

chapter. We use the relative error

$$\epsilon = \left| \frac{E^{\mathcal{N}, \mathcal{L}} - E}{E} \right| \quad (5.18)$$

to measure the accuracy of the approximate energies afforded by (5.10).

5.4 Numerical results

The long-range Coulomb energy of a density $\rho(\mathbf{r})$ is

$$E_J = \frac{1}{2} \langle \rho | L(r_{12}) | \rho \rangle \quad (5.19)$$

and applying the Ewald resolution (5.10) to this yields the approximation

$$E_J^{\mathcal{N}, \mathcal{L}} = \frac{1}{2} \sum_{n=0}^{\mathcal{N}} \sum_{l=0}^{\mathcal{L}} \sum_{m=-l}^l \langle \rho | \phi_{nlm} \rangle^2 \quad (5.20)$$

We have applied (5.20) to the electron density in the nano-diamond $C_{84}H_{64}$ which is described in Chapter 4. The $(\mathcal{N}, \mathcal{L})$ pairs that yield various relative errors ϵ for various attenuation parameters ω are shown in the middle columns of Table 5.2.

The long-range exchange energy is

$$E_K = -\frac{1}{2} \sum_{ij} \langle \psi_i \psi_j | L(r_{12}) | \psi_i \psi_j \rangle \quad (5.21)$$

and applying the Ewald resolution (5.10) to this yields the approximation

$$E_K^{\mathcal{N}, \mathcal{L}} = -\frac{1}{2} \sum_{n=0}^{\mathcal{N}} \sum_{l=0}^{\mathcal{L}} \sum_{m=-l}^l \sum_{ij}^{\text{occ}} \langle \psi_i \psi_j | \phi_{nlm} \rangle^2 \quad (5.22)$$

Diamond has a large bandgap and its exchange interactions decay rapidly with distance. We therefore chose to apply (5.22) to the more interesting π -system of the $C_{96}H_{24}$ graphene [191], placing a unit-exponent p_π Gaussian on each C atom, and using its Hückel orbitals [192]. The $(\mathcal{N}, \mathcal{L})$ pairs that yield various relative errors ϵ for various ω are shown in the final columns of Table 5.2.

Because the Ewald operator (5.5) is smooth, the $(\mathcal{N}, \mathcal{L})$ pairs required for the long-range Coulomb energies are much smaller than for the total Coulomb energies [5]. Moreover, we find that long-range exchange energies require surprisingly small \mathcal{N} values, reflecting that, even in the highly delocalized graphene system, the exchange interaction decays fairly quickly with distance [193, 191, 194].

5.5 Concluding remarks

There are a number of ways to resolve the long-range Coulomb (Ewald) operator into products of one-particle functions. Our favorite resolution (5.10) employs a spherical Bessel expansion of the Ewald operator and thereby generalizes our earlier quasi-resolution of the Coulomb operator. Numerical results indicate that this Ewald resolution converges rapidly and may be useful in a range of quantum chemical contexts. It looks particularly promising for the efficient calculation of long-range exchange energies. We will discuss the efficient evaluation of the auxiliary integrals (5.14) and present timing comparisons in Chapter 6.

We note finally that the Bessel expansion method is easy to extend to the erf-gau operator [130, 195, 64]

$$L^{(1)}(r_{12}) = \frac{\text{erf}(\omega r_{12})}{r_{12}} - \frac{2\omega}{\sqrt{\pi}} \exp\left(-\frac{\omega^2 r_{12}^2}{3}\right) \quad (5.23)$$

Applying Gauss-Hermite quadrature as for the Ewald operator yields

$$\begin{aligned} \frac{2\omega}{\sqrt{\pi}} \exp\left(-\frac{\omega^2 r_{12}^2}{3}\right) &= \frac{4\omega}{\pi} \int_{-\infty}^{\infty} \beta^2 j_0\left(\frac{2}{\sqrt{3}}\beta\omega r_{12}\right) \exp(-\beta^2) d\beta \\ &\approx \frac{8\omega}{\pi} \sum_{n=0}^{\mathcal{N}} b_n \beta_n^2 j_0\left(\frac{2}{\sqrt{3}}\beta_n\omega r_{12}\right) \end{aligned} \quad (5.24)$$

where the β_n and b_n have the same meanings as in (5.7).

5.6 Other resolutions of the Ewald operator

Orthonormal expansion

One way to resolve $L(r_{12})$ is to find functions f_k that are complete and Ewald-orthonormal, *i.e.*

$$\langle f_k | L(r_{12}) | f_{k'} \rangle = \delta_{k,k'} \quad (5.25)$$

If these f_k are known, one can show [2] that

$$\phi_k(\mathbf{r}_1) = \int L(r_{12}) f_k(\mathbf{r}_2) d\mathbf{r}_2 \quad (5.26)$$

If f_k is chosen to be a product of Y_l^m and a radial function, one eventually obtains

$$\begin{aligned} \phi_k(\mathbf{r}) &= \sqrt{2/\pi} Y_l^m(\mathbf{r}) \int_0^\infty p_n(x) j_l(rx) \widehat{L}^{1/2}(x) x dx \\ &= 2\sqrt{2} Y_l^m(\mathbf{r}) \int_0^\infty p_n(x) j_l(rx) \exp\left(-\frac{x^2}{8\omega^2}\right) dx \end{aligned} \quad (5.27)$$

where \widehat{L} is the Fourier transform of L and the p_n are any functions that form a complete and orthonormal set on $[0, \infty)$. Unfortunately, this approach is thwarted by the difficulty of selecting p_n that yield tractable integrals.

Taylor expansion

The Taylor expansion of the Ewald operator

$$L(r_{12}) = \frac{2\omega}{\sqrt{\pi}} \sum_{n=0}^{\infty} \frac{(-\omega^2 r_{12}^2)^n}{n!(2n+1)} \quad (5.28)$$

converges for all r_{12} . Because $(r_{12}^2)^n$ expands naturally [84] into a finite sum for any n , it is easy to construct a resolution from (5.28). However, when truncated after $n = \mathcal{N}$ the series (5.28) behaves as $(-r_{12}^2)^\mathcal{N}$ and is therefore worthless at large r_{12} .

Gaussian expansion

If we apply $2(\mathcal{N} + 1)$ -point Gauss-Legendre quadrature [9] to the Ewald integral representation

$$L(r_{12}) = \frac{\omega}{\sqrt{\pi}} \int_{-1}^1 \exp(-\omega^2 \gamma^2 r_{12}^2) d\gamma \quad (5.29)$$

we obtain the Gaussian expansion [130]

$$L(r_{12}) \approx \frac{2\omega}{\sqrt{\pi}} \sum_{n=0}^{\mathcal{N}} g_n \exp(-\omega^2 \gamma_n^2 r_{12}^2) \quad (5.30)$$

where the γ_n and g_n are the (positive) Legendre roots and weights. The function $\exp(-\lambda r_{12}^2)$ can be partially resolved, using the exponential and Legendre addition theorems [9] to find

$$\begin{aligned} \frac{\exp(-\lambda r_{12}^2)}{\exp(-\lambda r_1^2 - \lambda r_2^2)} &= \sum_{l=0}^{\infty} (2l+1) i_l(\lambda r_1 r_2) P_l(\cos \theta_{12}) \\ &= 4\pi \sum_{l=0}^{\infty} \sum_{m=-l}^l i_l(\lambda r_1 r_2) Y_l^{m*}(\mathbf{r}_1) Y_l^m(\mathbf{r}_2) \end{aligned} \quad (5.31)$$

where i_l is a modified spherical Bessel function. However, this does not mirror the form of (5.1) because we cannot resolve $i_l(\lambda r_1 r_2)$.

Bessel expansion

The Fourier-Bessel expansion [9, 196]

$$\begin{aligned} L(r_{12}) &= \frac{2}{\pi} \sum_{n=0}^{\infty} j_0(nr_{12}) \int_0^{\pi} L(x) j_0(nx) n^2 x^2 dx \\ &= \frac{2}{\pi} \sum_{n=1}^{\infty} \left[(-1)^{n+1} \operatorname{erf}(\omega\pi) + \exp\left(-\frac{n^2}{4\omega^2}\right) \Re \left\{ \operatorname{erf}\left(\omega\pi + \frac{n}{2\omega}i\right) \right\} \right] j_0(nr_{12}) \\ &= L(\pi) + \frac{2}{\pi} \sum_{n=1}^{\infty} \exp\left(-\frac{n^2}{4\omega^2}\right) \Re \left\{ \operatorname{erf}\left(\omega\pi + \frac{n}{2\omega}i\right) \right\} j_0(nr_{12}) \end{aligned} \quad (5.32)$$

converges rapidly but, unfortunately, it is valid only on the finite domain $0 \leq r_{12} \leq \pi$. As a consequence, it yields what we have previously termed a “quasi-resolution” in Chapter 4 and, to use it in practice, one would need to scale the system to fit within this domain.

Chapter 6

The evaluation of auxiliary integrals

$$\langle g_{n'l'm'}(\mathbf{r} - \mathbf{P}) | \phi_{nlm} \rangle = \sum_{l''m''} C_{l''m''}^{lml'm'} Y_{l''m''}(\mathbf{P}) H_{l''}^{n'l'nl}(P)$$

We discuss the evaluation of RO auxiliary integrals by explicit formulae in this chapter. In contrast to previous chapters, we show a general technique which is applicable to general $\phi_{nlm}(\mathbf{r})$ of the form $V_{nl}(r)Y_{lm}(\mathbf{r})$. Unlike Boys differentiation, our formulae are based on Fourier transforms and linearization of the products of two spherical harmonics. We apply this new approach to the Bessel resolution of the long-range Ewald operator and demonstrate that our RO calculation is competitive to the conventional long-range exchange energy calculation in a standard quantum chemical program.

6.1 Resolution of two-body operators

We have previously discussed the resolutions of two-body operators $T(r_{12})$ into a sum of products of one-body resolution function $\phi_{nlm}(\mathbf{r})$. The function may take myriad of forms but our favorite resolutions are made of spherical harmonics Y_{lm} and a radial function V_{nl} .

$$T(r_{12}) = \sum_{nlm} Y_{lm}(\mathbf{r}_1) V_{nl}(r_1) Y_{lm}(\mathbf{r}_2) V_{nl}(r_2) \quad (6.1)$$

The resolution reduces a two-particle integral $\langle a | \bar{T} | b \rangle$ to a sum of auxiliary

integrals,

$$\langle a|\bar{T}|b\rangle = \sum_k \left(\int a^*(\mathbf{r})\phi_k(\mathbf{r})d\mathbf{r} \right) \left(\int b(\mathbf{r})\phi_k(\mathbf{r})d\mathbf{r} \right), \quad (6.2)$$

and offer computational benefits similar to Cholesky decomposition [112, 113, 100, 109] and density fitting [99, 164, 119].

Efficient evaluation of the overlap integral between a $\phi_k(\mathbf{r})$ and a basis function is a prerequisite to implementation of resolution technique in quantum chemistry.

In this chapter, we derive the integral evaluation scheme, apply it to the long-range Ewald operator and Gaussian basis functions and devise an RO program to calculate long-range exchange energy.

6.2 Auxiliary integrals

We first define a basis function $g_{n'l'm'}$ and a resolution function ϕ_{nlm} .

$$g_{n'l'm'}(\mathbf{r}) \equiv Y_{l'm'}(\mathbf{r})R_{n'l'}(\zeta, r) \quad (6.3)$$

$$\phi_{nlm}(\mathbf{r}) \equiv Y_{lm}(\mathbf{r})V_{nl}(r) \quad (6.4)$$

We can derive their Fourier transforms $\hat{g}_{n'l'm'}$ and $\hat{\phi}_{nlm}$ which are products of a spherical harmonic and a radial function.

$$\hat{g}_{n'l'm'}(\mathbf{x}) = Y_{l'm'}(\mathbf{x})G_{n'l'}(x) \quad (6.5)$$

$$\hat{\phi}_{nlm}(\mathbf{x}) = Y_{lm}(\mathbf{x})\Phi_{nl}(x) \quad (6.6)$$

The radial functions $G_{n'l'}$, Φ_{nl} are integrals of a spherical Bessel function j_l and the radial part of the function in real space.

$$G_{n'l'}(x) = 4\pi(-i)^{l'} \int_0^\infty j_{l'}(xr)r^2 R_{n'l'}(\zeta, r)dr \quad (6.7)$$

$$\Phi_{nl}(x) = 4\pi(-i)^l \int_0^\infty j_l(xr)r^2 V_{nl}(r)dr \quad (6.8)$$

We can express the auxiliary integral as a sum of products of a spherical harmonic and the function $H_{l''}^{n'l'nl}$. The coefficients $C_{l''m''}^{lm'l'm'}$ arise from linearization

of the product of two spherical harmonics. (see §6.7.)

$$\begin{aligned}
\langle g_{n'l'm'}(\mathbf{r} - \mathbf{P}) | \phi_{nlm} \rangle &= \int g_{n'l'm'}(\mathbf{r} - \mathbf{P}) \phi_{nlm}(\mathbf{r}) d\mathbf{r} \\
&= \frac{1}{(2\pi)^3} \int \int \hat{g}_{n'l'm'}(\mathbf{x}) \exp[i\mathbf{x} \cdot (\mathbf{r} - \mathbf{P})] \phi_{nlm}(\mathbf{r}) d\mathbf{r} d\mathbf{x} \\
&= \frac{1}{(2\pi)^3} \int \hat{g}_{n'l'm'}(\mathbf{x}) \exp[-i\mathbf{x} \cdot \mathbf{P}] \hat{\phi}_{nlm}(\mathbf{x}) d\mathbf{x} \\
&= \frac{1}{(2\pi)^3} \int Y_{l'm'}(\mathbf{x}) Y_{lm}(\mathbf{x}) G_{n'l'}(x) \Phi_{nl}(x) \exp[-i\mathbf{x} \cdot \mathbf{P}] d\mathbf{x} \\
&= \frac{1}{(2\pi)^3} \int \sum_{l''m''} C_{l''m''}^{lml'm'} Y_{l''m''}(\mathbf{x}) G_{n'l'}(x) \Phi_{nl}(x) \exp[-i\mathbf{x} \cdot \mathbf{P}] d\mathbf{x} \\
&= \sum_{l''m''} C_{l''m''}^{lml'm'} Y_{l''m''}(\mathbf{P}) H_{l''}^{n'l'nl}(P)
\end{aligned} \tag{6.9}$$

Thus, the key of this scheme is the evaluation of the function $H_{l''}^{n'l'nl}$ which is an integral of $G_{n'l'}$, Φ_{nl} and $j_{l''}$.

$$H_{l''}^{n'l'nl}(P) = \frac{1}{2\pi^2} \int_0^\infty G_{n'l'}(x) \Phi_{nl}(x) j_{l''}(Px) x^2 dx \tag{6.10}$$

This is, in principle, applicable to any basis function and resolution of the forms (6.3) and (6.4). We, however, give one specific example in the following section.

6.3 Bessel resolution and Gaussian function

We apply the scheme described in the previous section to the resolution of long-range Ewald operator (Chapter 5) and a Gaussian basis function.

$$L(r_{12}) \equiv \frac{\text{erf}(\omega r_{12})}{r_{12}} = \sum_{nlm} \phi_{nlm}(\mathbf{r}_1) \phi_{nlm}(\mathbf{r}_2) \tag{6.11}$$

$$\phi_{nlm} = Y_{lm}(\mathbf{r}) 4\sqrt{b_n\omega} j_l(2\beta_n\omega r) \tag{6.12}$$

$$g_{n'l'm'}(\mathbf{r}) = Y_{l'm'}(\mathbf{r}) r^{n'} \exp(-\zeta r^2) \tag{6.13}$$

We obtain analytical expressions of $G_{n'l'}$, Φ_{nl} and $H_{l''}^{n'l'nl}$.

$$\begin{aligned}
G_{n'l'}(x) &= \left(-\frac{\iota}{2}\right)^{l'} \pi^{\frac{3}{2}} x^{l'} \zeta^{-\frac{1}{2}(3+n'+l')} \Gamma\left(\frac{1}{2}(3+n'+l')\right) \times \\
&\quad {}_1\tilde{F}_1\left(\frac{1}{2}(3+n'+l'); -\frac{x^2}{4\zeta}\right)
\end{aligned} \tag{6.14}$$

$$\Phi_{nl}(x) = 8\pi^2 (-\iota)^l \sqrt{b_n\omega} \frac{\delta(x - 2\beta_n\omega)}{x^2} \tag{6.15}$$

$$H_{l''}^{n'l'nl}(P) = 4(-\iota)^l \sqrt{b_n\omega} G_{n'l'}(2\beta_n\omega) j_{l''}(2\beta_n\omega P) \tag{6.16}$$

The regularized hypergeometric function in $G_{n'l'}(x)$ reduces to a product of a Gaussian and a polynomial in x for all n' and l' that we are interested.

$$G_{0,0}(x) = \frac{e^{-\frac{x^2}{4\zeta}} \pi^{3/2}}{\zeta^{3/2}} \quad (6.17)$$

$$G_{1,1}(x) = -\frac{i e^{-\frac{x^2}{4\zeta}} \pi^{3/2} x}{2\zeta^{5/2}} \quad (6.18)$$

$$G_{2,2}(x) = -\frac{e^{-\frac{x^2}{4\zeta}} \pi^{3/2} x^2}{4\zeta^{7/2}} \quad (6.19)$$

$$G_{2,0}(x) = \frac{e^{-\frac{x^2}{4\zeta}} \pi^{3/2} (6\zeta - x^2)}{4\zeta^{7/2}} \quad (6.20)$$

As a result, the special functions required for the evaluation of the integral (6.9) are only Y_{lm} and j_l whose computation has been discussed in Chapter 4.

6.4 Computational considerations

Since the results in Chapter 5 indicate that the resolution is most promising for long-range exchange energy

$$E_K = -\frac{1}{2} \sum_{ij}^{\text{occ}} \langle \psi_i \psi_j | L(r_{12}) | \psi_i \psi_j \rangle, \quad (6.21)$$

it is our target for further study. Applying resolution to above equation yields the $(\mathcal{N}, \mathcal{L})$ approximation

$$E_K^{\mathcal{N}, \mathcal{L}} = -\frac{1}{2} \sum_{n=0}^{\mathcal{N}} \sum_{l=0}^{\mathcal{L}} \sum_{m=-l}^l \sum_{ij}^{\text{occ}} \langle \psi_i \psi_j | \phi_{nlm} \rangle \quad (6.22)$$

Pseudocode to compute the long-range exchange energy are described below.

1. Form a list of significant Gaussian shell-pairs
2. Calculate initial j_l and Y_{lm}
3. $E_K^{\mathcal{N}, \mathcal{L}} = 0$
4. Loop over l
 - 4.1 Calculate j_l and Y_{lm}

4.2 Loop over n and m

4.2.1 Loop over the shell-pair list

4.2.1.1 Form primitive auxiliaries using HRR,
the Gaussian overlap distribution and (6.9)

4.2.1.2 Multiply the primitives by relevant contraction coefficients
and add them to the contracted AO auxiliaries

4.2.3 Convert AO to MO using DGEMM [197]

4.2.4 Loop over i and j

$$4.2.4.1 E_K^{\mathcal{N},\mathcal{L}} \leftarrow E_K^{\mathcal{N},\mathcal{L}} - \frac{1}{2} \langle \psi_i \psi_j | \phi_{nlm} \rangle$$

For maximum efficiency, we set a cut-off THRESH= 10^{-10} and screen out insignificant quantities at step 1 and step 4.2.1. At step 1, Gaussian products that their prefactors are smaller than THRESH are not included into the list of shell-pairs. At step 4.2.1, if a Gaussian prefactor times $4\sqrt{b_n\omega}$ is smaller than THRESH, the program will skip that shell-pair and go on to the next one.

The most expensive step of this algorithm is 4.2.3 whose formal cost is $\mathcal{O}(B^2\mathcal{K}N)$ where B is the number of basis functions, \mathcal{K} is the number of terms in the truncated Bessel resolution and N is the number of electrons. This looks like a quartic bottleneck but, in practice, it can be done relatively fast because it is handled by DGEMM and because of the screening criteria described above.

For small and moderate size molecules, the actual bottleneck is instead step 4.2.1.1 whose formal cost is $\mathcal{O}(B^2\mathcal{K})$ but involves multi-step calculation.

At step 4.2.1.1, we use the horizontal recurrence relation (HRR) of Head-Gordon and Pople [198] to transfer angular momentum from the second center to the first center of the auxiliary integrals. This process is depicted below.

Cartesian basis functions are shown in the following formulae.

$$x = -\sqrt{\frac{4\pi}{3}} Y_{1,1} r \quad (6.28)$$

$$y = \sqrt{\frac{4\pi}{3}} Y_{1,-1} r \quad (6.29)$$

$$z = -\sqrt{\frac{4\pi}{3}} Y_{1,0} r \quad (6.30)$$

$$x^2 = \left(\sqrt{\frac{4\pi}{15}} Y_{2,2} - \sqrt{\frac{4\pi}{45}} Y_{2,0} + \sqrt{\frac{4\pi}{9}} Y_{0,0} \right) r^2 \quad (6.31)$$

$$y^2 = \left(-\sqrt{\frac{4\pi}{15}} Y_{2,2} - \sqrt{\frac{4\pi}{45}} Y_{2,0} + \sqrt{\frac{4\pi}{9}} Y_{0,0} \right) r^2 \quad (6.32)$$

$$z^2 = \left(\sqrt{\frac{16\pi}{15}} Y_{2,2} + \sqrt{\frac{4\pi}{9}} Y_{0,0} \right) r^2 \quad (6.33)$$

$$xy = \sqrt{\frac{4\pi}{15}} Y_{2,-2} r^2 \quad (6.34)$$

$$xz = -\sqrt{\frac{4\pi}{15}} Y_{2,1} r^2 \quad (6.35)$$

$$yz = -\sqrt{\frac{4\pi}{15}} Y_{2,-1} r^2 \quad (6.36)$$

$$r = \sqrt{x^2 + y^2 + z^2} \quad (6.37)$$

$$Y_{lm} \equiv Y_{lm} \left(\cos^{-1} \frac{z}{r}, \tan^{-1} \frac{y}{x} \right) \quad (6.38)$$

We now have a completed description of the RO integral algorithm. It is implemented in a C program for long-range exchange energy calculation. We report \mathcal{N} , \mathcal{L} and RO calculation time where $-\log_{10} \left| E_{\text{K}}^{\mathcal{N},\mathcal{L}} / E_{\text{K}} - 1 \right| \geq 6$. Fockbuild times (traditional algorithm) from Q-CHEM package [107] are also reported for comparison. The calculation is based on the HF wavefunction/ $\omega = 0.1$ and is run on a 2.66 GHz machine with 2 GB DDR2 memory. Center of mass of molecules are placed at the origin.

6.5 Numerical results

In this section, we report two sets of numerical results. The first is an accuracy test for three groups of molecules and the second is a scaling test of exchange energy calculation algorithm.

6.5.1 Accuracy test

In previous chapters, our systems are either small molecules/big basis sets or large molecules/toy densities. Only four molecules He, H₂, C₈₄H₆₄ and C₉₆H₂₄ were considered so far. It is therefore desirable that the test set is expanded to a variety of molecules and conducted using a chemically sensible basis sets.

For an accuracy test, we choose 6-311G basis and three sets of molecules. Geometries of these molecules are provided in the Appendix A.

1. **Ten selected molecules made of highly electronegative atoms:** These represents a system with elements from the right of the periodic table which are known to be difficult for HFPT [200].
2. **Lithium metal clusters:** These represent a system with elements from the left of periodic table and a system with relatively large exchange energy.
3. **Alanine polypeptides:** These represent a typical biomolecule. They were used to test the scaling of calculation time for RI-TRIM [201]. The long-chain linear molecules and globular molecules are referred to as 1D and 3D respectively.

The results are shown in Table 6.1. RO significantly reduces calculation time for all molecules in the study. The most promising case is Li₄₈ where RO long-range exchange energy calculation is nearly 25 times faster than conventional calculation.

The overall \mathcal{N} and \mathcal{L} requirement is fairly small but we may make some further analysis on them. In the n direction, we see that the lithium metallic clusters require $\mathcal{N} = 4-5$, while insulators require only $\mathcal{N} = 1-2$. Because \mathcal{N} is a parameter that controls the quality of the radial resolution, this confirms the fact that the exchange interaction is very short-ranged [193, 191, 194] even in our metallic lithium clusters. In the l direction, we find that \mathcal{L} grows weakly with the size of the molecule and a long-chain 1D molecule requires larger \mathcal{L} than a compact 3D globular molecule of the same size.

6.5.2 Scaling test

How does the RO long-range exchange algorithm scale with respect to the size of the molecule and with respect to the size of the basis set? We conduct a simple study on alanine polypeptides to answer this question.

Table 6.1: \mathcal{N} , \mathcal{L} and runtime of RO program

	\mathcal{N}	\mathcal{L}	Calculation time/s	
			RO-Exchange	Q-CHEM Fockbuild
S ₂ O	2	3	0.05	0.14
SO ₃	1	3	0.04	0.17
SiF ₄	1	3	0.05	0.23
P ₄	2	3	0.12	0.31
PF ₅	1	4	0.10	0.36
SOCl ₂	2	4	0.18	0.47
POCl ₃	2	4	0.23	0.86
C ₂ F ₆	1	4	0.14	1.44
SF ₆	1	4	0.13	1.81
PCl ₅	2	4	0.38	4.53
Li ₁₄	4	6	2.15	16.43
Li ₂₂	4	7	6.84	83.99
Li ₄₈	5	10	65.69	1619.22
1D-tetrapeptide	1	10	5.06	43.43
1D-octapeptide	1	19	49.63	186.15
1D-hexadecapeptide	1	17	174.85	1019.83
3D-tetrapeptide	1	10	5.95	63.37
3D-octapeptide	1	15	26.94	359.62
3D-hexadecapeptide	1	15	103.99	1831.32

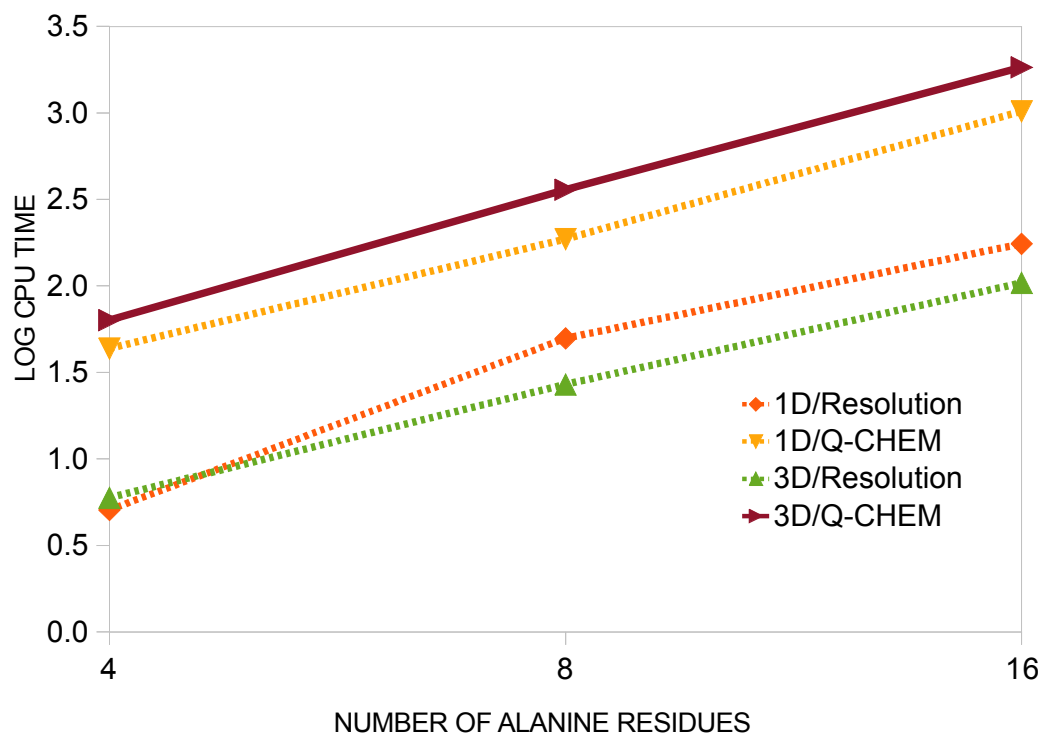


Figure 6.1: Plot of log CPU time vs system size

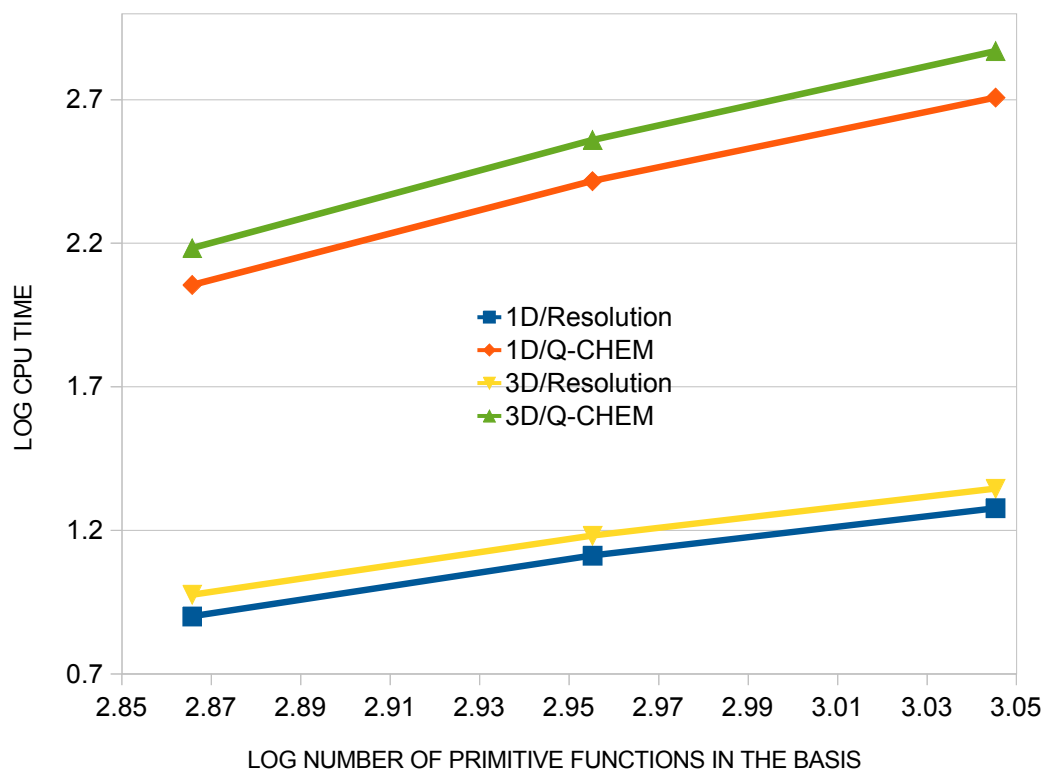


Figure 6.2: Plot of log CPU time vs basis set size

The runtimes of alanine polypeptides from Table 6.1 are plotted in Figure 6.1. Both the conventional and resolution exchange energy calculation scales approximately quadratically with respect to the addition of monomer units. This is because the number of significant shell-pairs at large molecule limit scales linearly with the size of the molecule [126, 125]. With this analysis, the cost of conventional calculation reduces from $\mathcal{O}(B^4)$ to $\mathcal{O}(B^2)$ and the cost of RO calculation reduces from $\mathcal{O}(B^2\mathcal{KN})$ to $\mathcal{O}(B\mathcal{KN})$.

To study the scaling behavior when the quality of basis set is improved, we use only s and p functions of correlation consistent basis. # indicates that the basis has been truncated. The 1D/3D alaninetetrapetides and cc-pVDZ#, cc-pVTZ# and cc-pVQZ# basis set are used in the calculation and the result is shown in Figure 6.2.

This figure indicates that RO calculation scales quadratically with number of primitive functions while conventional calculation scales quartically. This is because the screening strategy does not work and the number of significant shell-pairs does not reduce down to $\mathcal{O}(B)$. We can regard \mathcal{KN} as a constant in this case and the quadratic and quartic scalings are obvious from the formal cost.

6.6 Concluding remarks

In this chapter, we show a general approach to calculate RO auxiliary integrals and use it for long-range exchange energy calculation. It is the first time that we time RO calculation against standard quantum chemistry package. Though the implementation is preliminary and not well-optimized, RO shows a strong computational advantage of up to 25 times faster than conventional calculation. Unlike other technique, RO calculation runtime wins over conventional calculation even for a small molecule containing only a few atoms.

However, the calculation here contains up to p function only and in order to proceed to higher angular momentum basis function efficiently, one might consider deriving a recurrence approach to calculate the auxiliary integrals.

Linearization of the product of two spherical harmonics

In this section, we define $Y_l^m \equiv Y_l^m(\mathbf{r})$, $Y_{lm} \equiv Y_{lm}(\mathbf{r})$ and $C_{0,0,0}^{l,l',\ell}$, $C_{m,m',m+m'}^{l,l',\ell}$ are standard Clebsch-Gordan coefficient notation.

For complex spherical harmonic, the linearization is well-known [202].

$$Y_l^m Y_{l'}^{m'} = \sqrt{\frac{(2l+1)(2l'+1)}{4\pi}} \sum_{\ell=\max(|l-l'|, |m+m'|)}^{l+l'} \frac{C_{0,0,0}^{l,l',\ell} C_{m,m',m+m'}^{l,l',\ell}}{\sqrt{2\ell+1}} Y_\ell^{m+m'} \quad (6.39)$$

For real spherical harmonic, we obtain

$$\begin{aligned} Y_{lm} Y_{l'm'} &= p_{m,m'} \sum_{\ell=\max(|l-l'|, |m+m'|)}^{l+l'} C_\ell^{l,m,l',m'} Y_{\ell, a_{m,m'}(m+m')} + \\ &(-1)^{m'} q_{m,m'} \sum_{\ell=\max(|l-l'|, |m-m'|)}^{l+l'} C_\ell^{l,m,l',-m'} Y_{\ell, b_{m,m'}(m-m')} \end{aligned} \quad (6.40)$$

where

$$a_{m,m'} = \operatorname{sgn}(m) \operatorname{sgn}(m') \operatorname{sgn}(m+m') \quad (6.41)$$

$$b_{m,m'} = \operatorname{sgn}(m) \operatorname{sgn}(m') \operatorname{sgn}(m-m') \quad (6.42)$$

$$C_\ell^{l,m,l',m'} = \sqrt{\frac{(2l+1)(2l'+1)}{4\pi(2\ell+1)}} C_{0,0,0}^{l,l',\ell} C_{m,m',m+m'}^{l,l',\ell} \quad (6.43)$$

$$\begin{aligned} p_{m,m'} &= \frac{r_m r_{m'}}{2} s[a_{m,m'}(m+m')] \\ &\left(\begin{array}{l} -1 \quad m < 0 \text{ and } m' < 0 \\ 0 \quad \operatorname{sgn}(m) \operatorname{sgn}(m') < 0 \text{ and } m+m' = 0 \\ 1 \quad \text{otherwise} \end{array} \right) \\ &\left(\begin{array}{l} (-1)^{m+m'} \quad a_{m,m'} < 0 \text{ and } \operatorname{sgn}(m) \operatorname{sgn}(m') > 0 \\ -(-1)^{m+m'} \quad a_{m,m'} < 0 \text{ and } \operatorname{sgn}(m) \operatorname{sgn}(m') < 0 \\ 1 \quad \text{otherwise} \end{array} \right) \end{aligned} \quad (6.44)$$

$$\begin{aligned} q_{m,m'} &= \frac{r_m r_{m'}}{2} s[b_{m,m'}(m-m')] \\ &\left(\begin{array}{l} -1 \quad m \geq 0 \text{ and } m' < 0 \\ 0 \quad \operatorname{sgn}(m) \operatorname{sgn}(m') < 0 \text{ and } m-m' = 0 \\ 1 \quad \text{otherwise} \end{array} \right) \\ &\left(\begin{array}{l} (-1)^{m-m'} \quad b_{m,m'} < 0 \text{ and } \operatorname{sgn}(m) \operatorname{sgn}(m') > 0 \\ -(-1)^{m-m'} \quad b_{m,m'} < 0 \text{ and } \operatorname{sgn}(m) \operatorname{sgn}(m') < 0 \\ 1 \quad \text{otherwise} \end{array} \right) \end{aligned} \quad (6.45)$$

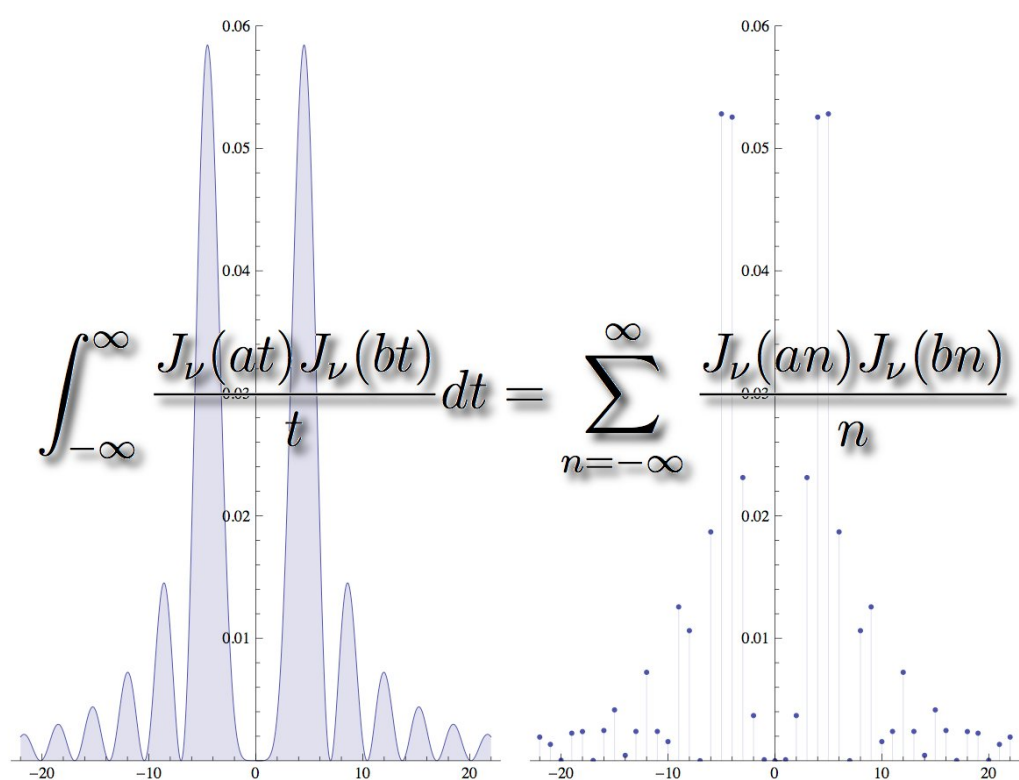
$$r_m = \begin{cases} \sqrt{2} & m > 0 \\ 1 & m = 0 \\ -(-1)^m \sqrt{2} & m < 0 \end{cases} \quad (6.46)$$

$$s(m) = 1/r_m \quad (6.47)$$

$$\operatorname{sgn}(x) = \begin{cases} 1 & x \geq 0 \\ -1 & \text{otherwise} \end{cases} \quad (6.48)$$

Chapter 7

A remarkable identity involving Bessel functions



We consider a new identity involving integrals and sums of Bessel functions. The identity provides a new way to evaluate integrals of products of two Bessel functions. The identity is remarkably simple and powerful since the summand and integrand are of exactly the same form and the sum converges to the integral relatively fast for most cases. A proof and numerical examples of the identity are discussed.

7.1 Introduction

The Newtonian kernel

$$T(\mathbf{r}, \mathbf{r}') = \frac{1}{|\mathbf{r} - \mathbf{r}'|}, \quad \mathbf{r}, \mathbf{r}' \in \mathbb{R}^3, \quad (7.1)$$

is ubiquitous in mathematical physics and is essential to an understanding of both gravitation and electrostatics [203]. It is central in classical mechanics [204] but plays an equally important role in quantum mechanics [205] where it mediates the dominant two-particle interaction in electronic Schrödinger equations of atoms and molecules.

Although the Newtonian kernel has many beautiful mathematical properties, the fact that it is both singular and long-ranged is awkward and expensive from a computational point of view [206] and this has led to a great deal of research into effective methods for its treatment. Of the many schemes that have been developed, Ewald partitioning [92], multipole methods [127] and Fourier transform techniques [207] are particularly popular and have enabled the simulation of large-scale particulate and continuous systems, even on relatively inexpensive computers.

A recent alternative [1, 2, 3, 4] to these conventional techniques is to resolve (7.1), a non-separable kernel, into a sum of products of one-body functions

$$T(\mathbf{r}, \mathbf{r}') = \sum_{l=0}^{\infty} \sum_{m=-l}^l Y_{lm}(\mathbf{r}) Y_{lm}(\mathbf{r}') T_l(r, r') = \sum_{n,l=0}^{\infty} \sum_{m=-l}^l \phi_{nlm}(\mathbf{r}) \phi_{nlm}(\mathbf{r}') \quad (7.2)$$

where $Y_{lm}(\mathbf{r})$ is a real spherical harmonic [9, 14.30.2] of the angular part of three dimensional vector \mathbf{r} ,

$$T_l(r, r') = 4\pi \int_0^{\infty} \frac{J_{l+1/2}(tr) J_{l+1/2}(tr')}{t\sqrt{rr'}} dt, \quad (7.3)$$

$J_l(z)$ is a Bessel function of the first kind, and $r = |\mathbf{r}|$. The resolution (7.2) is computationally useful because it decouples the coordinates \mathbf{r} and \mathbf{r}' and allows the two-body interaction integral

$$E[\rho_a, \rho_b] = \iint \rho_a(\mathbf{r}) T(\mathbf{r}, \mathbf{r}') \rho_b(\mathbf{r}') d\mathbf{r} d\mathbf{r}', \quad (7.4)$$

between densities $\rho_a(\mathbf{r})$ and $\rho_b(\mathbf{r})$ to be recast as

$$E[\rho_a, \rho_b] = \sum_{n=0}^{\infty} \sum_{l=0}^{\infty} \sum_{m=-l}^l A_{nlm} B_{nlm}, \quad (7.5)$$

where A_{nlm} is a one-body integral of the product of $\rho_a(\mathbf{r})$ and $\phi_{nlm}(\mathbf{r})$. If the one-body integrals can be evaluated efficiently and the sum converges rapidly, (7.5) may offer a more efficient route to $E[\rho_a, \rho_b]$ than (7.4).

The key question is how best to obtain the T_l resolution

$$T_l(r, r') = \sum_{n=0}^{\infty} V_{nl}(r) V_{nl}(r'). \quad (7.6)$$

Previous attempts [1, 2, 3, 4] yielded complicated V_{nl} whose practical utility is questionable but, recently, we have discovered the remarkable identity (See Chapter 4.)

$$\int_0^{\infty} \frac{J_{\nu}(at) J_{\nu}(bt)}{t} dt = \sum_{n=0}^{\infty} \kappa_n \frac{J_{\nu}(an) J_{\nu}(bn)}{n} \quad (7.7)$$

where κ_n is defined by

$$\kappa_n = \begin{cases} \frac{1}{2}, & n = 0 \\ 1, & n \geq 1 \end{cases}. \quad (7.8)$$

$a, b \in [0, \pi]$, $\nu = \frac{1}{2}, \frac{3}{2}, \frac{5}{2}, \dots$ and we take the appropriate limit for the $n = 0$ term in the sum (7.7). This yields the functions

$$\phi_{nlm}(\mathbf{r}) = \sqrt{\frac{4\pi\kappa_n}{rn}} J_{l+1/2}(rn) Y_{lm}(\mathbf{r}), \quad (7.9)$$

and these provide a resolution which is valid provided that $r < \pi$. We note that ϕ_{nlm} vanish for $n = 0$ unless $l = 0$.

If we write (7.7) as an integral from $-\infty$ to ∞ ,

$$\int_{-\infty}^{\infty} \frac{J_{\nu}(at) J_{\nu}(bt)}{t} dt = \sum_{n=-\infty}^{\infty} \frac{J_{\nu}(an) J_{\nu}(bn)}{n}, \quad (7.10)$$

the summand and integrand are of exactly the same form. There has been a number of studies in this kind of sum-integral equality by various groups, for example, Krishnan & Bhatia in 1940s [208, 209, 210, 211] and Boas, Pollard & Shisha in 1970s [212, 213, 214].

These discoveries were inspired by a practice to “approximate” an intractable sum that arises in physics by an integral. They realized that the “approximation” was in fact exact for a number of cases.

In this chapter, however, our goal is the opposite. We originally aimed to use the sum to approximate the integral and later found that it was exact. Our identity (7.7) is also considerably different from theirs but we may regard their [214, (1)] when $c = 0$ as a special case of our (7.7) when $\nu = 1/2$.

The aim of this chapter is to prove an extended version of the identity (7.7) and demonstrate its viability in approximating the integral of Bessel functions.

7.2 Preliminaries

The Bessel function of the first kind $J_\nu(z)$ is defined by [196, 3.1 (8)]

$$J_\nu(z) = \sum_{n=0}^{\infty} \frac{(-1)^n}{\Gamma(\nu + n + 1) n!} \left(\frac{z}{2}\right)^{\nu+2n}. \quad (7.11)$$

It follows from (7.11) that

$$J_\nu(z) \left(\frac{z}{2}\right)^{-\nu} \quad (7.12)$$

is an entire function of z and we have

$$\lim_{z \rightarrow 0} J_\nu(z) \left(\frac{z}{2}\right)^{-\nu} = \frac{1}{\Gamma(\nu + 1)}. \quad (7.13)$$

Gauss' hypergeometric function is defined by [215, 2.1.2]

$${}_2F_1 \left(\begin{matrix} a, b \\ c \end{matrix} ; z \right) = \sum_{k=0}^{\infty} \frac{(a)_k (b)_k}{(c)_k} \frac{z^k}{k!}, \quad (7.14)$$

where $(u)_k$ is the Pochhammer symbol (or rising factorial), given by

$$(u)_k = u(u+1) \cdots (u+k-1). \quad (7.15)$$

The series (7.14) converges absolutely for $|z| < 1$ [215, 2.1.1]. If $\operatorname{Re}(c - a - b) > 0$, we have [215, 2.2.2]

$${}_2F_1 \left(\begin{matrix} a, b \\ c \end{matrix} ; 1 \right) = \frac{\Gamma(c) \Gamma(c - a - b)}{\Gamma(c - a) \Gamma(c - b)}. \quad (7.16)$$

Many special functions can be defined in terms of the hypergeometric function. In particular, the Gegenbauer (or ultraspherical) polynomials $C_n^{(\lambda)}(x)$ are defined by [216, 9.8.19]

$$C_n^{(\lambda)}(x) = \frac{(2\lambda)_n}{n!} {}_2F_1 \left(\begin{matrix} -n, n + 2\lambda \\ \lambda + \frac{1}{2} \end{matrix} ; \frac{1-x}{2} \right), \quad (7.17)$$

with $n \in \mathbb{N}_0$ and

$$\mathbb{N}_0 = \{0, 1, \dots\}. \quad (7.18)$$

In this chapter, we will use the following Lemmas.

Lemma 7.2.1. *For $k \in \mathbb{N}_0$, we have*

$$C_{2k}^{(\mu-2k)}(x) = \frac{(k+1-\mu)_k}{k!} (1-x^2)^{\frac{1}{2}-\mu+2k} \times {}_2F_1 \left(\begin{matrix} \frac{1}{2} + k, \frac{1}{2} - \mu + k \\ \frac{1}{2} \end{matrix} ; x^2 \right), \quad |x| < 1. \quad (7.19)$$

Proof. Using the formula [215, 3.1.12]

$$\begin{aligned} {}_2F_1\left(\begin{matrix} 2a, 2b \\ a+b+\frac{1}{2} \end{matrix}; \frac{x+1}{2}\right) &= \frac{\Gamma(a+b+\frac{1}{2})\Gamma(\frac{1}{2})}{\Gamma(a+\frac{1}{2})\Gamma(b+\frac{1}{2})} {}_2F_1\left(\begin{matrix} a, b \\ \frac{1}{2} \end{matrix}; x^2\right) \\ &\quad - x \frac{\Gamma(a+b+\frac{1}{2})\Gamma(-\frac{1}{2})}{\Gamma(a)\Gamma(b)} {}_2F_1\left(\begin{matrix} a+\frac{1}{2}, b+\frac{1}{2} \\ \frac{3}{2} \end{matrix}; x^2\right) \end{aligned} \quad (7.20)$$

in (7.17), we obtain

$$C_{2k}^{(\mu-2k)}(x) = \frac{2^{2\mu-2k-1}\Gamma(\mu-2k+\frac{1}{2})\Gamma(\mu-k)}{\Gamma(\frac{1}{2}-k)\Gamma(2\mu-4k)(2k)!} {}_2F_1\left(\begin{matrix} -k, \mu-k \\ \frac{1}{2} \end{matrix}; x^2\right), \quad (7.21)$$

since $\frac{1}{\Gamma(-k)} = 0$ for $k = 0, 1, \dots$

Applying Euler's transformation [215, 2.2.7]

$${}_2F_1\left(\begin{matrix} a, b \\ c \end{matrix}; x\right) = (1-x)^{c-a-b} {}_2F_1\left(\begin{matrix} c-a, c-b \\ c \end{matrix}; x\right) \quad (7.22)$$

to (7.21), we get

$$\begin{aligned} C_{2k}^{(\mu-2k)}(x) &= \frac{2^{2\mu-2k-1}\Gamma(\mu-2k+\frac{1}{2})\Gamma(\mu-k)}{\Gamma(\frac{1}{2}-k)\Gamma(2\mu-4k)(2k)!} \times \\ &\quad (1-x^2)^{\frac{1}{2}-\mu+2k} {}_2F_1\left(\begin{matrix} \frac{1}{2}+k, \frac{1}{2}-\mu+k \\ \frac{1}{2} \end{matrix}; x^2\right), \end{aligned} \quad (7.23)$$

and (7.19) follows since

$$\frac{2^{2\mu-2k-1}\Gamma(\mu-2k+\frac{1}{2})\Gamma(\mu-k)}{\Gamma(\frac{1}{2}-k)\Gamma(2\mu-4k)(2k)!} = \frac{(k+1-\mu)_k}{k!}. \quad (7.24)$$

□

Lemma 7.2.2. *Let the function $h(x; a)$ be defined by*

$$h(x; a) = \begin{cases} A_k^\mu(a) \left(1 - \frac{x^2}{a^2}\right)^{\mu-2k-\frac{1}{2}} C_{2k}^{(\mu-2k)}\left(\frac{x}{a}\right) & 0 \leq x < a \\ 0 & a \leq x \leq \pi \end{cases}, \quad (7.25)$$

where $0 < a < \pi$,

$$A_k^\mu(a) = \frac{(-1)^k (2k)! \Gamma(\mu-2k) 2^{2\mu-2k-1}}{a^{2k+1} \Gamma(2\mu-2k)}, \quad (7.26)$$

$\operatorname{Re}(\mu) > 2k - \frac{1}{2}$ and $k \in \mathbb{N}_0$.

Then, $h(x; a)$ can be represented by the Fourier cosine series

$$h(x; a) = \sum_{n=0}^{\infty} \kappa_n \frac{J_{\mu}(na)}{\left(\frac{1}{2}an\right)^{\mu}} n^{2k} \cos(nx), \quad (7.27)$$

where κ_n was defined in 7.8.

Proof. For $\operatorname{Re}(\sigma) > -\frac{1}{2}$, $\alpha > 0$ and $k \in \mathbb{N}_0$, we have [196, 3.32]

$$\int_0^1 (1-t^2)^{\sigma-\frac{1}{2}} C_{2k}^{(\sigma)}(t) \cos(\alpha t) dt = \frac{\pi (-1)^k \Gamma(2k+2\sigma)}{(2k)! \Gamma(\sigma) (2\alpha)^{\sigma}} J_{\sigma+2k}(\alpha). \quad (7.28)$$

Replacing $\sigma = \mu - 2k$ and $\alpha = na$ in (7.28), we obtain

$$\frac{J_{\mu}(na) n^{2k}}{\left(\frac{1}{2}an\right)^{\mu}} = 2a \int_0^1 A_k^{\mu}(a) (1-t^2)^{\mu-2k-\frac{1}{2}} C_{2k}^{(\mu-2k)}(t) \cos(nat) dt \quad (7.29)$$

or

$$\frac{J_{\mu}(na)}{\left(\frac{1}{2}an\right)^{\mu}} n^{2k} = \frac{2}{\pi} \int_0^a h(x; a) \cos(nx) dx, \quad (7.30)$$

and the result follows. \square

7.3 Main results

The discontinuous integral

$$I(a, b) = \int_0^{\infty} \frac{J_{\mu}(at) J_{\nu}(bt)}{t^{\lambda}} dt, \quad (7.31)$$

was investigated by Weber [217], Sonine [218] and Schafheitlin [219]. They proved that [196, 13.4 (2)]

$$I(a, b) = \frac{a^{\lambda-\nu-1} b^{\nu} \Gamma\left(\frac{\nu+\mu-\lambda+1}{2}\right)}{2^{\lambda} \Gamma(\nu+1) \Gamma\left(\frac{\lambda+\mu-\nu+1}{2}\right)} {}_2F_1\left(\begin{matrix} \frac{\nu+\mu-\lambda+1}{2}, \frac{\nu-\mu-\lambda+1}{2} \\ \nu+1 \end{matrix}; \left(\frac{b}{a}\right)^2\right), \quad (7.32)$$

for

$$\operatorname{Re}(\mu + \nu + 1) > \operatorname{Re}(\lambda) > -1 \quad (7.33)$$

and $0 < b < a$. The corresponding expression for the case when $0 < a < b$, is obtained from (7.32) by interchanging a, b and also μ, ν . When $a = b$, we have [196, 13.41 (2)]

$$I(a, a) = \frac{a^{\lambda-1} \Gamma\left(\frac{\nu + \mu - \lambda + 1}{2}\right) \Gamma(\lambda)}{2^\lambda \Gamma\left(\frac{\lambda + \mu - \nu + 1}{2}\right) \Gamma\left(\frac{\lambda + \nu - \mu + 1}{2}\right) \Gamma\left(\frac{\nu + \mu + \lambda + 1}{2}\right)}, \quad (7.34)$$

provided that $\operatorname{Re}(\mu + \nu + 1) > \operatorname{Re}(\lambda) > 0$. This result also follows from Gauss' summation formula (7.16) and (7.32).

Theorem 7.3.1. *If $0 < b < a < \pi$, $\operatorname{Re}(\mu) > 2k - \frac{1}{2}$, $\operatorname{Re}(\nu) > -\frac{1}{2}$, $k \in \mathbb{N}_0$, and*

$$S_k(a, b) = \sum_{n=0}^{\infty} \kappa_n \frac{J_\mu(an) J_\nu(bn)}{\left(\frac{1}{2}an\right)^\mu \left(\frac{1}{2}bn\right)^\nu} \left(\frac{an}{2}\right)^{2k}, \quad (7.35)$$

then,

$$S_k(a, b) = \frac{\Gamma\left(k + \frac{1}{2}\right)}{a \Gamma(\nu + 1) \Gamma\left(\mu - k + \frac{1}{2}\right)} {}_2F_1\left(\begin{matrix} \frac{1}{2} + k, \frac{1}{2} - \mu + k \\ \nu + 1 \end{matrix}; \left(\frac{b}{a}\right)^2\right). \quad (7.36)$$

Proof. Multiplying (7.27) by $A_0^\nu(b) \frac{2}{\pi} \left(1 - \frac{x^2}{b^2}\right)^{\nu - \frac{1}{2}}$ and integrating from 0 to b , we get

$$S_k(a, b) = \frac{2}{\pi} A_0^\nu(b) A_k^\mu(a) \int_0^b \left(1 - \frac{x^2}{b^2}\right)^{\nu - \frac{1}{2}} \left(1 - \frac{x^2}{a^2}\right)^{\mu - 2k - \frac{1}{2}} C_{2k}^{(\mu - 2k)}\left(\frac{x}{a}\right) dx, \quad (7.37)$$

where we have used the integral representation (7.30). Setting $x = bt$ and $b = \omega a$ in (7.37), we obtain

$$S_k(a, b) = \frac{2b}{\pi} A_0^\nu(b) A_k^\mu(a) \int_0^1 (1 - t^2)^{\nu - \frac{1}{2}} (1 - \omega^2 t^2)^{\mu - 2k - \frac{1}{2}} C_{2k}^{(\mu - 2k)}(\omega t) dt. \quad (7.38)$$

Thus, we can re-write (7.38) as

$$S_k(a, b) = \frac{2b}{\pi} A_0^\nu(b) A_k^\mu(a) \frac{2^{2\mu - 2k - 1} \Gamma\left(\mu - 2k + \frac{1}{2}\right) \Gamma(\mu - k)}{\Gamma\left(\frac{1}{2} - k\right) \Gamma(2\mu - 4k) (2k)!} \times \int_0^1 (1 - t^2)^{\nu - \frac{1}{2}} {}_2F_1\left(\begin{matrix} \frac{1}{2} + k, \frac{1}{2} - \mu + k \\ \frac{1}{2} \end{matrix}; \omega^2 t^2\right) dt, \quad (7.39)$$

or, using (7.26) and changing variables in the integral,

$$S_k(a, b) = \frac{(-1)^k 2^{2k} \sqrt{\pi}}{a^{2k+1} \Gamma(\mu - k + \frac{1}{2}) \Gamma(\nu + \frac{1}{2}) \Gamma(\frac{1}{2} - k)} \times \int_0^1 s^{-\frac{1}{2}} (1-s)^{\nu-\frac{1}{2}} {}_2F_1\left(\begin{matrix} \frac{1}{2} + k, \frac{1}{2} - \mu + k \\ \frac{1}{2} \end{matrix}; \omega^2 s\right) ds. \quad (7.40)$$

Recalling the formula [215, Th. 2.2.4]

$${}_2F_1\left(\begin{matrix} a, b \\ c \end{matrix}; x\right) = \frac{\Gamma(c)}{\Gamma(d) \Gamma(c-d)} \int_0^1 t^{d-1} (1-t)^{c-d-1} {}_2F_1\left(\begin{matrix} a, b \\ d \end{matrix}; xt\right) dt, \quad (7.41)$$

valid for $\operatorname{Re}(c) > \operatorname{Re}(d) > 0$, $x \in \mathbb{C} \setminus [1, \infty)$, we conclude that

$$S_k(a, b) = \frac{(-1)^k 2^{2k} \sqrt{\pi}}{a^{2k+1} \Gamma(\mu - k + \frac{1}{2}) \Gamma(\nu + \frac{1}{2}) \Gamma(\frac{1}{2} - k)} \times \frac{\sqrt{\pi} \Gamma(\nu + \frac{1}{2})}{\Gamma(\nu + 1)} {}_2F_1\left(\begin{matrix} \frac{1}{2} + k, \frac{1}{2} - \mu + k \\ \nu + 1 \end{matrix}; \omega^2\right). \quad (7.42)$$

But since [215, 1.2.1]

$$\Gamma\left(k + \frac{1}{2}\right) \Gamma\left(\frac{1}{2} - k\right) = (-1)^k \pi, \quad k = 0, 1, \dots, \quad (7.43)$$

the result follows. \square

The special case of Theorem 7.3.1 in which $k = 0$, was derived by Cooke in [220], as part of his work on Schlömilch series.

Corollary 7.3.2. *If $0 < b < a < \pi$, $\operatorname{Re}(\mu) > 2k - \frac{1}{2}$, $\operatorname{Re}(\nu) > -\frac{1}{2}$, $k \in \mathbb{N}_0$, then*

$$\int_0^\infty \frac{J_\mu(at) J_\nu(bt)}{t^{\mu+\nu-2k}} dt = \sum_{n=0}^\infty \kappa_n \frac{J_\mu(an) J_\nu(bn)}{n^{\mu+\nu-2k}}. \quad (7.44)$$

Proof. The result follows immediately from (7.32) and (7.36), after taking $\lambda = \mu + \nu - 2k$. Note that since for all $k \in \mathbb{N}_0$

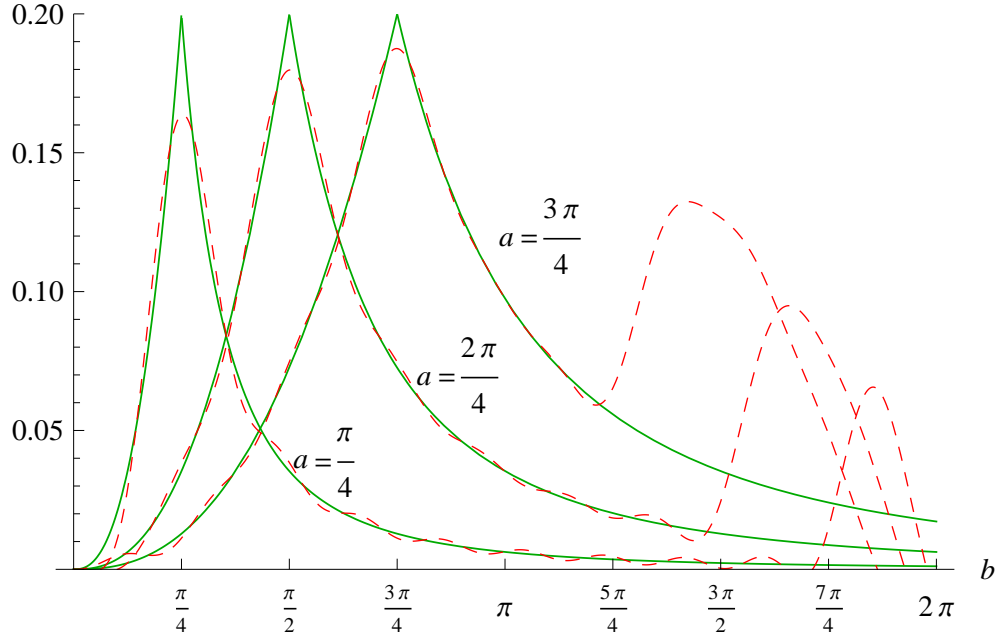
$$\operatorname{Re}(\mu + \nu + 1) = \operatorname{Re}(2k + 1 + \lambda) > \operatorname{Re}(1 + \lambda) > \operatorname{Re}(\lambda) \quad (7.45)$$

and

$$\operatorname{Re}(\lambda) = \operatorname{Re}(\mu + \nu - 2k) > -1, \quad (7.46)$$

the conditions (7.33) are satisfied. \square

Figure 7.1: $\frac{1}{5} \left[\frac{\min(a,b)}{\max(a,b)} \right]^{5/2}$ (solid) and $M_{10}(a,b)$ (dashed), for $a = \frac{\pi}{4}, \frac{2\pi}{4}, \frac{3\pi}{4}$ and $b \in [0, 2\pi]$



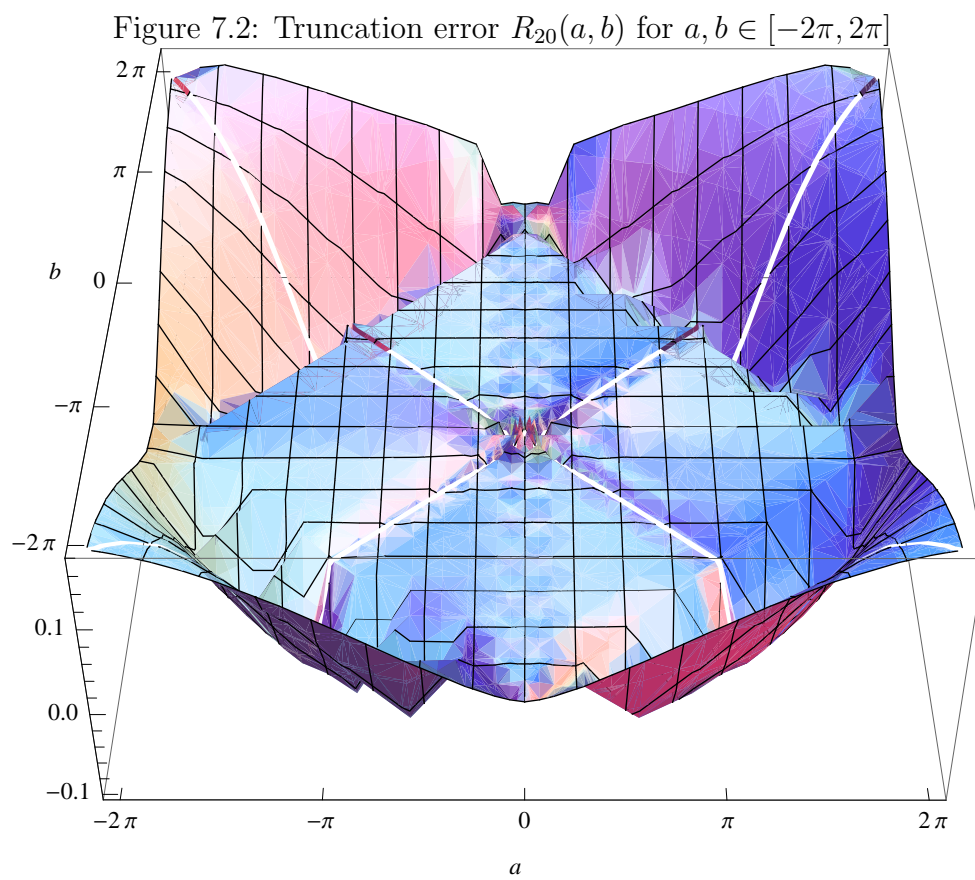
Corollary 7.3.3. *If $0 < a, b < \pi$, and $\nu - \frac{1}{2} \in \mathbb{N}_0$, then*

$$\sum_{n=0}^{\infty} \kappa_n \frac{J_{\nu}(an) J_{\nu}(bn)}{n} = \int_0^{\infty} \frac{J_{\nu}(at) J_{\nu}(bt)}{t} dt = \begin{cases} \frac{1}{2\nu} \left(\frac{a}{b}\right)^{\nu}, & a \leq b \\ \frac{1}{2\nu} \left(\frac{b}{a}\right)^{\nu}, & a \geq b \end{cases}. \quad (7.47)$$

Proof. The result is a consequence of Corollary 7.3.2 and a special case of the integral (7.32) (see [196, 13.42 (1)]). □

Table 7.1: $R_{\mathcal{N}}(a, b)$ for $a = \pi/2$ and various b and \mathcal{N}

\mathcal{N}	b					
	$\pi/4$	$2\pi/4$	$3\pi/4$	$4\pi/4$	$5\pi/4$	$6\pi/4$
1	3.15E-02	1.81E-01	3.15E-02	-2.37E-02	-4.12E-02	-3.09E-2
10	-3.10E-03	2.02E-02	-2.40E-03	1.45E-04	1.74E-03	-1.16E-2
100	-1.79E-06	2.03E-03	-4.81E-07	-1.39E-07	7.46E-07	-1.17E-3
1000	1.81E-09	2.03E-04	4.86E-10	-1.37E-10	-7.46E-10	-1.17E-4
10000	1.81E-12	2.03E-05	4.86E-13	-1.37E-13	-7.46E-13	-1.17E-5



7.4 Numerical results

In previous sections, we have proven the equality of integrals and sums of Bessel functions. However, before the identity is used in practice, we need to consider its convergence behavior.

Firstly, the Weierstrass M-test shows that the series converges uniformly as long as $\mu + \nu - 2k > 1$ and $\mu, \nu > 0$ because the numerator is bounded $|J_\mu(at) J_\nu(bt)| \leq 1$ [196, 13.42 (10)].

To explore the rate of convergence of the sum in Corollary 7.3.3, we choose $\nu = 5/2$. The exact value of the integral is

$$\int_0^\infty \frac{J_{5/2}(at) J_{5/2}(bt)}{t} dt = \frac{1}{5} \sqrt{\frac{|a|}{a}} \sqrt{\frac{|b|}{b}} \left[\frac{\min(|a|, |b|)}{\max(|a|, |b|)} \right]^{5/2} \quad (7.48)$$

and truncation of the infinite series yields the finite sum

$$M_{\mathcal{N}}(a, b) = \sum_{n=1}^{\mathcal{N}} \frac{J_{5/2}(an) J_{5/2}(bn)}{n} \quad (7.49)$$

and a truncation error

$$R_{\mathcal{N}}(a, b) = \frac{1}{5} \left[\frac{\min(|a|, |b|)}{\max(|a|, |b|)} \right]^{5/2} - \sqrt{\frac{|a|}{a}} \sqrt{\frac{|b|}{b}} M_{\mathcal{N}}(a, b). \quad (7.50)$$

The integral in (7.48) and sum in (7.49) are illustrated in Figure 7.1 and their difference (7.50) is shown in Figure 7.2 and Table 7.1.

The excellent agreement region in Figure 7.1, an apparently flat plateau in Figure 7.2, and the decaying error from the 2nd to the 7th column of Table 7.1 strongly suggest that Corollary 7.3.3 is true over the larger domain $|a| + |b| < 2\pi$ for $\nu = 5/2$. Additional numerical experiments not shown here suggest that it is true for all ν . Furthermore, we believe that this larger domain conjecture also applies to Corollary 7.3.2 but we have not yet managed to find a proof for this.

If a and b are in the domain where the integral equals the infinite sum, the difference (7.50) is only due to truncation and can be recast as

$$R_{\mathcal{N}}(a, b) = \sqrt{\frac{|a|}{a}} \sqrt{\frac{|b|}{b}} \sum_{n=\mathcal{N}+1}^{\infty} \frac{J_{5/2}(an) J_{5/2}(bn)}{n} \quad (7.51)$$

Table 7.1 reveals that the rate of convergence of the Bessel sum is strongly dependent on the value of a and b . For $b = 2\pi/4$ and $b = 6\pi/4$, the truncation error appears to decay as $1/\mathcal{N}$ but, for the other values of b , it appears to decay

as $1/\mathcal{N}^3$. Because a, b are multiples of $\pi/4$, these two convergence behaviors can be explained analytically by substituting the first sine or cosine term from the expansion [196, 7.21 (1)] into (7.51). We have examined at other values of a, b in the $|a| + |b| < 2\pi$ domain and found empirically that the decay rate is between $1/\mathcal{N}$ and $1/\mathcal{N}^3$.

7.5 Concluding remarks

We provide a rigorous proof that the identity (7.7) is valid on the square domain $a, b \in (0, \pi)$. A numerical study indicates that the rate of convergence of the sum in the identity is sensitive to the values of a and b and further work to quantify this would be helpful. Generalization of the identity is possible and should be explored in the future work.

Chapter 8

Summary and future directions



Niels Henrik David Bohr (1885–1962)

The Nobel Prize in Physics 1922 was awarded to Niels Bohr “for his services in the investigation of the structure of atoms and of the radiation emanating from them” [12].

“Those who are not shocked when they first come across quantum mechanics cannot possibly have understood it.”

— Bohr [221]

8.1 Summary

In Chapter 1, we look back into the history of quantum mechanics and review attempts to solve the Schrödinger equation since its birth in 1926. Despite the enormous effort of scientists and mathematicians over 85 years and the exponentially growing computing power, *ab initio* QM calculations are still very expensive and limited to moderate-size molecules.

“Why Schrödinger equations are so difficult?”, we raise this question in the second chapter. We find that r_{ij}^{-1} are chiefly responsible for the complexity of the equations. One approach to avoid this problem is to resolve r_{ij}^{-1} into a sum of $\phi_k(\mathbf{r}_i)$ and $\phi_k(\mathbf{r}_j)$. This chapter reviews three existing works on the resolutions and touches on two related techniques, Cholesky decomposition and density fitting. We also derive an extension to the resolution theory and devise four strategies to resolve a symmetric function $T(r_1, r_2, \theta_{12})$.

In the third chapter, we replace r_{ij}^{-1} in the Schrödinger equations by the truncated Laguerre resolution and obtain reduced-rank Schrödinger equations (RRSE). The RRSEs are mathematically simpler objects than the original equations yet their solutions are chemically meaningful. This is confirmed by HF, MP2 and FCI calculations on He and H₂ using even-tempered basis sets.

Though the resolution of Coulomb operator is a theoretically powerful tool for quantum chemistry, it cannot reach its full potential unless auxiliary integrals can be generated efficiently. We endeavored to devise an efficient algorithm for auxiliary integrals arising from Laguerre but to no avail. We later abandoned it and looked for alternatives. The works in §2.2 and §2.3 were derived during the quest for a better resolution of the Coulomb operator.

Chapter 4 describes the most important discovery in this thesis. We tried to construct a quadrature or a sum that approximates T_l which is represented by an integral (2.46). Instead, we found an exact formula that relates the integral to the sum and led to the Bessel resolution of Coulomb operator. The resolution function ϕ_k are just a product of a spherical harmonic and a spherical Bessel function. Auxiliary integrals $\langle a | \phi_k \rangle$ for spherical density a centered at \mathbf{R} are simply a product of $\phi_k(\mathbf{R})$, a resolution function evaluated at \mathbf{R} and $\hat{a}(\lambda)$, a Fourier transform of a evaluated at λ .

The Bessel resolution of Coulomb operator is, however, a “quasi-resolution” which means that it is valid only within a certain domain. We need to scale our system of interest to fit within the validity domain $r_1 + r_2 < 2\pi$ to obtain the best performance. The Coulomb energy calculation on a large nanodiamond molecule C₈₄H₆₄ shows that the domain restriction can be easily circumvented and that the auxiliary integral difficulty has been solved.

Because of the success of the resolution of Coulomb operator, we extend it to the long-range Ewald operator in the fifth chapter. The resolution functions and the auxiliary integrals are basically in the same form as Bessel resolution of the Coulomb operator. Having said that, the Bessel resolution of the Ewald operator is not a quasi-resolution and converges much faster than the Coulomb one.

We tested it for both Coulomb energy of nanodiamond $C_{84}H_{64}$ and exchange energy of graphene $C_{96}H_{24}$ and found that the resolution is exceptionally promising for long-range exchange energy calculation. This is because our resolution is capable of exploiting the short-sightedness of exchange interaction.

In Chapter 6, we discuss the building up of angular momentum on the basis function. Unlike the Boys approach in Chapter 3, we derive explicit formulae by using Fourier transform and Clebsch-Gordan coefficients. The theory is applicable to any resolution of the form $V_{nl}(r)Y_{lm}(\mathbf{r})$.

We use the explicit formulae to calculate long-range exchange energy. Correlation-consistent and 6-311G basis set and three representative groups of molecules are considered. This is a few steps further from the previous work. (In Chapter 3, we use uncontracted basis sets containing p and d functions, but only on He and H_2 . In Chapter 4 and Chapter 5, the two molecules investigated are fairly large containing over a hundred of atoms but only toy densities are used.)

The implementation of resolution in Chapter 6, though being preliminary and not well-optimized, wins over a traditional long-range exchange energy calculation in a standard quantum chemical program.

The seventh chapter revisits the identity involving Bessel integrals and sums. The similarity of the summand and the integrand is a remarkable mathematical discovery. We generalize the identity statement and provide a proof for it.

8.2 Future directions

The resolutions of Coulomb operator is a simple yet powerful idea in quantum chemistry. This dissertation has extended the theory of resolution and created new efficient practical resolutions of the Coulomb operator and the long-range Ewald operator. There are three major directions for future research that will build upon the work in this thesis.

1. **Implementation:** The resolutions discussed in Chapter 4 and Chapter 5 are ready for an implementation in any quantum chemical methods. In principle, the resolutions of Coulomb operator can at least perform the same task as Cholesky decomposition and density fitting that are widely used in quantum chemistry. However, the resolution have several advantages over other techniques as discussed in §2.4. This research direction, parallel computing implementation, in particular, will be explored in the near future.

2. **Theoretical development:** This thesis mainly deals with resolutions of the Coulomb operator and its long-range analogues. However, we provide a general discussion on the resolution theory in Chapter 2. It opens a significant possibility for future study. For example, the resolutions of r_{12} may benefit explicit r_{12} methods.
3. **RRSE:** It is also possible to explore the use of the resolutions of Coulomb operator beyond the two-electron integral factorization picture. We stated in Chapter 3 that RRSEs are mathematically simpler than SEs but still solved them numerically using traditional methods, HF, MP2 and FCI. It is worth looking at the possibility of solving RRSEs analytically or even numerically via other means. This is a more challenging and more rewarding research question that may remain open for a long period of time.

Appendix A

Computational notes on special functions

Three-term recurrence relations

A three-term recurrence relation of the form

$$y_{n+1} + a_n y_n + b_n y_{n-1} = 0 \quad (\text{A.1})$$

where a_n, b_n are given sequence of real or complex numbers, $b_n \neq 0$ and $n = 1, 2, 3, \dots$ generally has two linearly independent solutions. [222] The calculation of one of the solutions by the recurrence relation is usually numerically stable in one direction but not the other. In his 1952 book [223], Miller suggested that the Bessel functions are calculated by using the recurrence relation in the backward direction. It is now known as “Miller’s backward recurrence algorithm” [222] or simply “backward recurrence algorithm” [224]. The idea, however, can be traced back to Lord Rayleigh’s 1910 paper. [225] The behavior of the recurrence relation of this form has been studied by Gautschi [222], Olver [226, 224] and many other groups [227, 228]

Hermite functions, Bessel functions and associated Legendre polynomials (ALPs) discussed below obey three-term recurrence relations.

- Hermite functions H_{-n} , $n = 1, 2, 3, \dots$ are closely related to the complex error functions and the Faddeeva function $w(z) = e^{-z^2} \operatorname{erfc}(-iz)$. We have obtained an algorithm for H_{-n} by modifying the algorithm for the Faddeeva function by Poppe, Wijers and Gautschi. [229, 230]
- The Argonne’s Bessel function code written by Sookne and distributed through R project [168] is used for calculating spherical Bessel functions.

A simple algorithm by Thompson [231] cited by Varganov *et. al.* [2] does not work for our purpose.

- A spherical harmonic is product of an ALP P_l^m , a sine or cosine function and a normalization factor. Since 1960 numerous algorithms for calculating the ALPs or the modified ALPs have been developed. [232, 233, 234, 235, 169, 170, 148, 236, 237, 238, 239, 240, 241] However, Equation (4.23) requires that the ALPs are calculated from high to low degree. Thus, the generation of ALPs using m -only recursion in [169, 242, 170] is modified and used in Chapter 4. There is no such requirement in other chapters and the algorithm for the modified ALPs in *Numerical Recipe 3rd edition* [243] is the preferred method.

The error function of complex argument

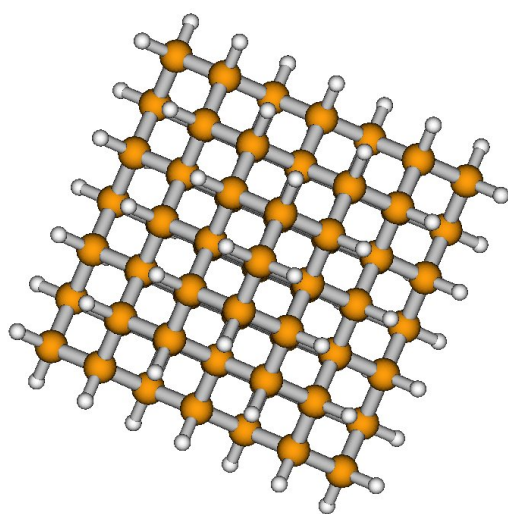
There are several methods for the computation of the error function of complex argument. [244, 245] Strand algorithm [245] is modified and used for (5.32).

Appendix B

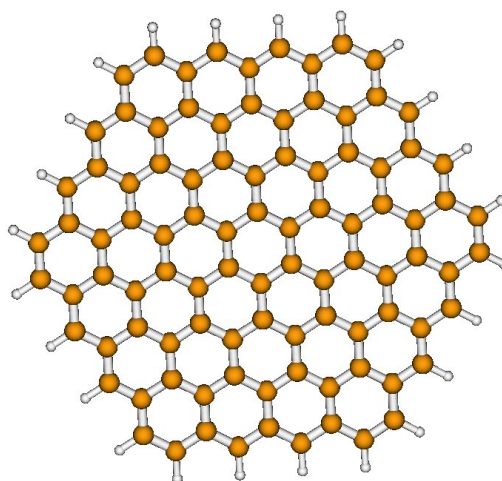
Molecular geometries

Nuclear orientations in this appendix are reported in angstroms.

Molecules in Chapter 4 and Chapter 5



Nanodiamond $C_{84}H_{64}$



Graphene $C_{96}H_{24}$

Nanodiamond $C_{84}H_{64}$

C	0.000000	0.000000	5.334716
C	-0.889119	0.889119	4.445597
C	-1.778239	0.000000	3.556478
C	-0.889119	-0.889119	2.667358
C	0.000000	-1.778239	3.556478
C	0.889119	-0.889119	4.445597
C	-1.778239	-1.778239	1.778239
C	-0.889119	-2.667358	0.889119

C	0.000000	-1.778239	0.000000
C	0.889119	-0.889119	0.889119
C	0.000000	0.000000	1.778239
C	-0.889119	0.889119	0.889119
C	0.000000	1.778239	0.000000
C	0.889119	0.889119	-0.889119
C	1.778239	0.000000	0.000000
C	-0.889119	-0.889119	-0.889119
C	0.000000	0.000000	-1.778239
C	0.889119	-2.667358	-0.889119
C	1.778239	-1.778239	-1.778239
C	2.667358	-0.889119	-0.889119
C	3.556478	-1.778239	0.000000
C	2.667358	-2.667358	0.889119
C	1.778239	-1.778239	1.778239
C	0.889119	0.889119	2.667358
C	1.778239	1.778239	1.778239
C	2.667358	0.889119	0.889119
C	2.667358	-0.889119	2.667358
C	3.556478	0.000000	1.778239
C	-1.778239	0.000000	0.000000
C	1.778239	-3.556478	0.000000
C	0.889119	-2.667358	2.667358
C	0.000000	-3.556478	1.778239
C	1.778239	0.000000	3.556478
C	0.889119	2.667358	0.889119
C	0.889119	-0.889119	-2.667358
C	3.556478	0.000000	-1.778239
C	2.667358	0.889119	-2.667358
C	1.778239	1.778239	-1.778239
C	3.556478	1.778239	0.000000
C	2.667358	2.667358	-0.889119
C	4.445597	-0.889119	0.889119
C	4.445597	0.889119	-0.889119
C	-0.889119	0.889119	-2.667358
C	-1.778239	1.778239	-1.778239
C	-0.889119	2.667358	-0.889119
C	0.889119	2.667358	-2.667358
C	0.000000	3.556478	-1.778239
C	1.778239	3.556478	0.000000
C	0.000000	1.778239	-3.556478
C	1.778239	0.000000	-3.556478
C	-2.667358	-0.889119	0.889119
C	0.000000	-3.556478	-1.778239
C	-0.889119	-2.667358	-2.667358

C	-1.778239	-1.778239	-1.778239
C	-1.778239	-3.556478	0.000000
C	-2.667358	-2.667358	-0.889119
C	-0.889119	-4.445597	-0.889119
C	0.889119	-4.445597	0.889119
C	-3.556478	-1.778239	0.000000
C	-2.667358	0.889119	-0.889119
C	-2.667358	-0.889119	-2.667358
C	-3.556478	0.000000	-1.778239
C	-1.778239	0.000000	-3.556478
C	0.000000	-1.778239	-3.556478
C	-2.667358	0.889119	2.667358
C	-1.778239	1.778239	1.778239
C	0.000000	1.778239	3.556478
C	-0.889119	2.667358	2.667358
C	-3.556478	0.000000	1.778239
C	-3.556478	1.778239	0.000000
C	-2.667358	2.667358	0.889119
C	-4.445597	0.889119	0.889119
C	-4.445597	-0.889119	-0.889119
C	0.000000	3.556478	1.778239
C	-1.778239	3.556478	0.000000
C	0.889119	4.445597	-0.889119
C	-0.889119	4.445597	0.889119
C	0.889119	0.889119	-4.445597
C	-0.889119	-0.889119	-4.445597
C	-5.334716	0.000000	0.000000
C	0.000000	5.334716	0.000000
C	0.000000	0.000000	-5.334716
C	0.000000	-5.334716	0.000000
C	5.334716	0.000000	0.000000
H	-3.296670	-3.296670	-1.518431
H	2.407551	-2.407551	-2.407551
H	-2.407551	2.407551	-2.407551
H	-2.407551	-2.407551	2.407551
H	2.407551	2.407551	2.407551
H	-2.407551	0.629312	-4.185789
H	0.629312	-2.407551	-4.185789
H	-0.629312	2.407551	-4.185789
H	2.407551	-0.629312	-4.185789
H	-4.185789	2.407551	-0.629312
H	-4.185789	-0.629312	2.407551
H	-4.185789	0.629312	-2.407551
H	-4.185789	-2.407551	0.629312
H	-2.407551	-0.629312	4.185789
H	0.629312	2.407551	4.185789
H	-0.629312	-2.407551	4.185789
H	2.407551	0.629312	4.185789

H	0.629312	4.185789	2.407551
H	2.407551	4.185789	0.629312
H	-2.407551	4.185789	-0.629312
H	-0.629312	4.185789	-2.407551
H	-2.407551	-4.185789	0.629312
H	-0.629312	-4.185789	2.407551
H	2.407551	-4.185789	-0.629312
H	0.629312	-4.185789	-2.407551
H	4.185789	-2.407551	-0.629312
H	4.185789	0.629312	2.407551
H	4.185789	-0.629312	-2.407551
H	4.185789	2.407551	0.629312
H	5.074909	1.518431	-1.518431
H	5.074909	-1.518431	1.518431
H	-5.074909	-1.518431	-1.518431
H	-5.074909	1.518431	1.518431
H	1.518431	1.518431	-5.074909
H	-1.518431	-1.518431	-5.074909
H	1.518431	-1.518431	5.074909
H	-1.518431	1.518431	5.074909
H	-1.518431	-5.074909	-1.518431
H	1.518431	-5.074909	1.518431
H	-1.518431	5.074909	1.518431
H	1.518431	5.074909	-1.518431
H	0.629312	0.629312	5.964028
H	-0.629312	-0.629312	5.964028
H	0.629312	-0.629312	-5.964028
H	-0.629312	0.629312	-5.964028
H	0.629312	-5.964028	-0.629312
H	-0.629312	-5.964028	0.629312
H	0.629312	5.964028	0.629312
H	-0.629312	5.964028	-0.629312
H	-5.964028	-0.629312	0.629312
H	-5.964028	0.629312	-0.629312
H	5.964028	-0.629312	-0.629312
H	5.964028	0.629312	0.629312
H	3.296670	1.518431	-3.296670
H	3.296670	3.296670	-1.518431
H	1.518431	3.296670	-3.296670
H	1.518431	-3.296670	3.296670
H	3.296670	-1.518431	3.296670
H	3.296670	-3.296670	1.518431
H	-3.296670	3.296670	1.518431
H	-1.518431	3.296670	3.296670
H	-3.296670	1.518431	3.296670
H	-1.518431	-3.296670	-3.296670
H	-3.296670	-1.518431	-3.296670

Graphene C₉₆H₂₄

Since this graphene is a planar molecule, only x and y coordinates are given.

C	0.000000	0.000000
C	0.000000	1.400000
C	1.212436	2.100000
C	2.424871	1.400000
C	2.424871	0.000000
C	1.212436	-0.700000
C	3.637307	2.100000
C	4.849742	1.400000
C	4.849742	0.000000
C	3.637307	-0.700000
C	6.062178	2.100000
C	7.274613	1.400000
C	7.274613	0.000000
C	6.062178	-0.700000
C	8.487049	-0.700000
C	9.699485	0.000000
C	9.699485	1.400000
C	8.487049	2.100000
C	6.062178	-2.100000
C	4.849742	-2.800000
C	3.637307	-2.100000
C	1.212436	-2.100000
C	2.424871	-2.800000
C	4.849742	-4.200000
C	3.637307	-4.900000
C	2.424871	-4.200000
C	3.637307	-6.300000
C	2.424871	-7.000000
C	1.212436	-6.300000
C	1.212436	-4.900000
C	4.849742	-7.000000
C	4.849742	-8.400000
C	3.637307	-9.100000
C	2.424871	-8.400000
C	1.212436	-9.100000
C	1.212436	-10.500000
C	2.424871	-11.200000
C	3.637307	-10.500000
C	6.062178	-9.100000
C	6.062178	-10.500000
C	4.849742	-11.200000

C	0.000000	-8.400000
C	0.000000	-7.000000
C	-1.212436	-6.300000
C	-1.212436	-4.900000
C	0.000000	-4.200000
C	0.000000	-2.800000
C	2.424871	-12.600000
C	3.637307	-13.300000
C	4.849742	-12.600000
C	7.274613	-11.200000
C	7.274613	-12.600000
C	6.062178	-13.300000
C	8.487049	-10.500000
C	9.699485	-11.200000
C	9.699485	-12.600000
C	8.487049	-13.300000
C	0.000000	-11.200000
C	0.000000	-12.600000
C	1.212436	-13.300000
C	-1.212436	-9.100000
C	-1.212436	-10.500000
C	-2.424871	-7.000000
C	-2.424871	-8.400000
C	-2.424871	-4.200000
C	-3.637307	-4.900000
C	-3.637307	-6.300000
C	-1.212436	-2.100000
C	-2.424871	-2.800000
C	-1.212436	-0.700000
C	8.487049	-9.100000
C	9.699485	-8.400000
C	10.911920	-9.100000
C	10.911920	-10.500000
C	12.124356	-8.400000
C	12.124356	-7.000000
C	10.911920	-6.300000
C	9.699485	-7.000000
C	8.487049	-6.300000
C	8.487049	-4.900000
C	9.699485	-4.200000
C	10.911920	-4.900000
C	9.699485	-2.800000
C	8.487049	-2.100000
C	7.274613	-2.800000
C	7.274613	-4.200000
C	6.062178	-4.900000
C	6.062178	-6.300000

C	7.274613	-7.000000
C	10.911920	-2.100000
C	12.124356	-2.800000
C	12.124356	-4.200000
C	13.336791	-4.900000
C	13.336791	-6.300000
C	7.274613	-8.400000
C	10.911920	-0.700000
H	-4.581274	-6.845000
H	-3.368839	-8.945000
H	-2.156403	-11.045000
H	-0.943968	-13.145000
H	-4.581274	-4.355000
H	-3.368839	-2.255000
H	-2.156403	-0.155000
H	-0.943968	1.945000
H	1.212436	3.190000
H	3.637307	3.190000
H	6.062178	3.190000
H	10.643452	1.945000
H	11.855888	-0.155000
H	13.068323	-2.255000
H	14.280759	-4.355000
H	14.280759	-6.845000
H	13.068323	-8.945000
H	11.855888	-11.045000
H	10.643452	-13.145000
H	8.487049	-14.390000
H	6.062178	-14.390000
H	3.637307	-14.390000
H	1.212436	-14.390000
H	8.487049	3.190000

Molecules in Chapter 6

Ten selected molecules & Alanine polypeptides

The geometries of ten selected molecules are obtained by private communication with Deng, one of the authors of [200]. Alanine polypeptides' geometries are available online in a supplementary information section of [201].

Lithium clusters

These clusters are body-centered cubic with a metallic radii of 1.496 [246].

Li₁₄

Li	-1.727432	-1.727432	-3.454864
Li	-1.727432	-1.727432	0.000000
Li	-1.727432	-1.727432	3.454864
Li	-1.727432	1.727432	-3.454864
Li	-1.727432	1.727432	0.000000
Li	-1.727432	1.727432	3.454864
Li	1.727432	-1.727432	-3.454864
Li	1.727432	-1.727432	0.000000
Li	1.727432	-1.727432	3.454864
Li	1.727432	1.727432	-3.454864
Li	1.727432	1.727432	0.000000
Li	1.727432	1.727432	3.454864
Li	0.000000	0.000000	-1.727432
Li	0.000000	0.000000	1.727432

Li₂₂

Li	-3.454864	-3.454864	-1.727432
Li	-3.454864	-3.454864	1.727432
Li	-3.454864	0.000000	-1.727432
Li	-3.454864	0.000000	1.727432
Li	-3.454864	3.454864	-1.727432
Li	-3.454864	3.454864	1.727432
Li	0.000000	-3.454864	-1.727432
Li	0.000000	-3.454864	1.727432
Li	0.000000	0.000000	-1.727432
Li	0.000000	0.000000	1.727432
Li	0.000000	3.454864	-1.727432
Li	0.000000	3.454864	1.727432
Li	3.454864	-3.454864	-1.727432
Li	3.454864	-3.454864	1.727432
Li	3.454864	0.000000	-1.727432
Li	3.454864	0.000000	1.727432
Li	3.454864	3.454864	-1.727432
Li	3.454864	3.454864	1.727432
Li	-1.727432	-1.727432	0.000000
Li	-1.727432	1.727432	0.000000
Li	1.727432	-1.727432	0.000000
Li	1.727432	1.727432	0.000000

Li₄₈

Li	-3.454864	-3.454864	-5.182296
Li	-3.454864	-3.454864	-1.727432

Li	-3.454864	-3.454864	1.727432
Li	-3.454864	-3.454864	5.182296
Li	-3.454864	0.000000	-5.182296
Li	-3.454864	0.000000	-1.727432
Li	-3.454864	0.000000	1.727432
Li	-3.454864	0.000000	5.182296
Li	-3.454864	3.454864	-5.182296
Li	-3.454864	3.454864	-1.727432
Li	-3.454864	3.454864	1.727432
Li	-3.454864	3.454864	5.182296
Li	0.000000	-3.454864	-5.182296
Li	0.000000	-3.454864	-1.727432
Li	0.000000	-3.454864	1.727432
Li	0.000000	-3.454864	5.182296
Li	0.000000	0.000000	-5.182296
Li	0.000000	0.000000	-1.727432
Li	0.000000	0.000000	1.727432
Li	0.000000	0.000000	5.182296
Li	0.000000	3.454864	-5.182296
Li	0.000000	3.454864	-1.727432
Li	0.000000	3.454864	1.727432
Li	0.000000	3.454864	5.182296
Li	3.454864	-3.454864	-5.182296
Li	3.454864	-3.454864	-1.727432
Li	3.454864	-3.454864	1.727432
Li	3.454864	-3.454864	5.182296
Li	3.454864	0.000000	-5.182296
Li	3.454864	0.000000	-1.727432
Li	3.454864	0.000000	1.727432
Li	3.454864	0.000000	5.182296
Li	3.454864	3.454864	-5.182296
Li	3.454864	3.454864	-1.727432
Li	3.454864	3.454864	1.727432
Li	3.454864	3.454864	5.182296
Li	-1.727432	-1.727432	-3.454864
Li	-1.727432	-1.727432	0.000000
Li	-1.727432	-1.727432	3.454864
Li	-1.727432	1.727432	-3.454864
Li	-1.727432	1.727432	0.000000
Li	-1.727432	1.727432	3.454864
Li	1.727432	-1.727432	-3.454864
Li	1.727432	-1.727432	0.000000
Li	1.727432	-1.727432	3.454864
Li	1.727432	1.727432	-3.454864
Li	1.727432	1.727432	0.000000
Li	1.727432	1.727432	3.454864

Bibliography

- [1] Gilbert, A. T. B. *Coulomb orthonormal polynomials*. B.Sc. (Hons) thesis, Massey University, (1996).
- [2] Varganov, S. A., Gilbert, A. T. B., Deplazes, E., and Gill, P. M. W. *J. Chem. Phys.* **128**, 201104 (2008).
- [3] Gill, P. M. W. and Gilbert, A. T. B. *Chem. Phys.* **356**, 86 (2009).
- [4] Limpanuparb, T. and Gill, P. M. W. *Phys. Chem. Chem. Phys.* **11**, 9176 (2009).
- [5] Limpanuparb, T., Gilbert, A. T. B., and Gill, P. M. W. *J. Chem. Theory Comput.* **7**, 830 (2011).
- [6] Limpanuparb, T. and Gill, P. M. W. *J. Chem. Theory Comput.* **7**, 2353 (2011).
- [7] Dominici, D. E., Gill, P. M. W., and Limpanuparb, T. arXiv:1103.0058v1, (2011).
- [8] Abramowitz, M. and Stegun, I. E., editors. *Handbook of mathematical functions*. Dover, (1972).
- [9] Olver, F. W. J., Lozier, D. W., Boisvert, R. F., and Clark, C. W., editors. *NIST handbook of mathematical functions*. Cambridge University Press, (2010).
- [10] <http://mathworld.wolfram.com>.
- [11] Szabo, A. and Ostlund, N. S. *Modern quantum chemistry*. McGraw-Hill, (1989).
- [12] <http://www.nobelprize.org>.
- [13] Schrödinger, E. *Ann. der Physik* **384**, 361 (1926).
- [14] Schrödinger, E. *Phys. Rev.* **28**, 1049 (1926).
- [15] Dirac, P. A. M. *Proc. R. Soc. A* **123**, 714 (1929).
- [16] Boltzmann, L. *Nature* **51**, 413 (1895).
- [17] Planck, M. *Ann. der Physik* **309**, 553 (1901).
- [18] Einstein, A. *Ann. der Physik* **322**, 132 (1905).
- [19] de Broglie, L. *Recherches sur la théorie des quanta (Researches on the quantum theory)*. Ph.D. thesis, University of Paris, (1924).
- [20] Heisenberg, W. *The Physical Principles of the Quantum Chemistry*. Dover, (1949).
- [21] Born, M. and Jordan, P. *Z. Physik* **34**, 858 (1925).

- [22] Dirac, P. A. M. *Proc. R. Soc. A* **117**, 610 (1928).
- [23] Born, M. and Oppenheimer, J. R. *Ann. der Physik* **389**, 457 (1927).
- [24] Hartree, D. R. *Math. Proc. Cambridge* **24**, 89 (1928).
- [25] Pauli, W. *Z. Physik* **31**, 765 (1925).
- [26] Fock, V. *Z. Physik* **61**, 126 (1930).
- [27] Lennard-Jones, J. E. *Trans. Faraday Soc.* **25**, 668 (1929).
- [28] Slater, J. C. *Phys. Rev.* **36**, 57 (1930).
- [29] Boys, S. F. *Proc. R. Soc. A* **200**, 542 (1950).
- [30] André, J.-M., Gouverneur, L., and Leroy, E. G. *Int. J. Quantum Chem.* **1**, 451 (1967).
- [31] Hall, G. G. *Proc. R. Soc. A* **205**, 541 (1951).
- [32] Roothaan, C. C. J. *Rev. Mod. Phys.* **23**, 69 (1951).
- [33] Hehre, W. J., Radom, L., Schleyer, P. v. R., and Pople, J. A. *Ab Initio Molecular Orbital Theory*. John Wiley & Sons, (1986).
- [34] Schrödinger, E. *Ann. der Physik* **385**, 437 (1926).
- [35] Lord Rayleigh (J. W. Strutt). *Theory of Sound. I*. Macmillan, 2nd edition, (1894).
- [36] Møller, C. and Plesset, M. S. *Phys. Rev.* **46**, 618 (1934).
- [37] Leininger, M. L., Allen, W. D., Schaefer, H. F., and Sherrill, C. D. *J. Chem. Phys.* **112**, 9213 (2000).
- [38] Handy, N. C., Pople, J. A., and Shavitt, I. *J. Phys. Chem.* **100**, 6007 (1996).
- [39] Čížek, J. *J. Chem. Phys.* **45**, 7256 (1966).
- [40] Paldus, J., Čížek, J., and Shavitt, I. *Phys. Rev. A* **5**, 50 (1972).
- [41] Raghavachari, K., Trucks, G. W., Pople, J. A., and Head-Gordon, M. *Chem. Phys. Lett.* **157**, 479 (1989).
- [42] Ohlinger, W. S., Klunzinger, P. E., Deppmeier, B. J., and Hehre, W. J. *J. Phys. Chem. A* **113**, 2165 (2009).
- [43] Pople, J. A., Head-Gordon, M., Fox, D. J., Raghavachari, K., and Curtiss, L. A. *J. Chem. Phys.* **90**, 5622 (1989).
- [44] Curtiss, L. A., Raghavachari, K., Trucks, G. W., and Pople, J. A. *J. Chem. Phys.* **94**, 7221 (1991).
- [45] Jensen, F. *Introduction to Computational Chemistry*. John Wiley & Sons, 2nd edition, (2007).
- [46] Petersson, G. A., Bennett, A., Tensfeldt, T. G., Al-Laham, M. A., Shirley, W. A., and Mantzaris, J. *J. Chem. Phys.* **89**, 2193 (1988).
- [47] Curtiss, L. A., Redfern, P. C., and Raghavachari, K. *J. Chem. Phys.* **126**, 084108 (2007).

- [48] Martin, J. M. L. and de Oliveira, G. *J. Chem. Phys.* **111**, 1843 (1999).
- [49] DeYonker, N. J., Grimes, T., Yockel, S., Dinescu, A., Mintz, B., Cundari, T. R., and Wilson, A. K. *J. Chem. Phys.* **125**, 104111 (2006).
- [50] Tajti, A., Szalay, P. G., Császár, A. G., Kállay, M., Gauss, J., Valeev, E. F., Flowers, B. A., Vázquez, J., and Stanton, J. F. *J. Chem. Phys.* **121**, 11599 (2004).
- [51] Schmidt, M. W. and Gordon, M. S. *Annu. Rev. Phys. Chem.* **49**, 233 (1998).
- [52] Thomas, L. H. *Math. Proc. Cambridge* **23**, 542 (1927).
- [53] Fermi, E. *Rend. Accad. Naz. Lincei* **6**, 602 (1927).
- [54] Hohenberg, P. and Kohn, W. *Phys. Rev.* **136**, B864 (1964).
- [55] Kohn, W. and Sham, L. J. *Phys. Rev.* **140**, A1113 (1965).
- [56] Becke, A. D. *J. Chem. Phys.* **98**, 5648 (1993).
- [57] Stephens, P. J., Devlin, F. J., Chabalowski, C. F., and Frisch, M. J. *J. Phys. Chem.* **98**, 11623 (1994).
- [58] Kim, K. and Jordan, K. *J. Phys. Chem.* **98**, 10089 (1994).
- [59] Brittain, D. R. B., Lin, C. Y., Gilbert, A. T. B., Izgorodina, E. I., Gill, P. M. W., and Coote, M. L. *Phys. Chem. Chem. Phys.* **11**, 1138 (2009).
- [60] Gill, P. M. W. *Aust. J. Chem.* **54**, 661 (2001).
- [61] Heyd, J., Scuseria, G. E., and Ernzerhof, M. *J. Chem. Phys.* **118**, 8207 (2003).
- [62] Yanai, T., Tew, D. P., and Handy, N. C. *Chem. Phys. Lett.* **393**, 51 (2004).
- [63] Vydrov, O. A. and Scuseria, G. E. *J. Chem. Phys.* **125**, 234109 (2006).
- [64] Song, J. W., Tokura, S., Sato, T., Watson, M. A., and Hirao, K. *J. Chem. Phys.* **127**, 154109 (2007).
- [65] Chai, J. D. and Head-Gordon, M. *Phys. Chem. Chem. Phys.* **10**, 6615 (2008).
- [66] von Lilienfeld, O. A., Tavernelli, I., and Rothlisberger, U. *Phys. Rev. Lett.* **93**, 153004 (2004).
- [67] Zimmerli, U., Parrinello, M., and Koumoutsakos, P. *J. Chem. Phys.* **120**, 2693 (2004).
- [68] Grimme, S. *J. Comput. Chem.* **25**, 1463 (2004).
- [69] Hylleraas, E. A. *Z. Physik* **44**, 871 (1927).
- [70] Werner, H.-J. and Gill, P. M. W. *Phys. Chem. Chem. Phys.* **10**, 3318 (2008).
- [71] Gill, P. M. W., Crittenden, D. L., O'Neill, D. P., and Besley, N. A. *Phys. Chem. Chem. Phys.* **8**, 15 (2006).
- [72] Nakatsuji, H. *Phys. Rev. Lett.* **93**, 030403 (2004).
- [73] Coleman, A. J. and Yukalo, V. I. *Reduced Density Matrices, Coulson's Challenge: v. 72 (Lecture Notes in Chemistry)*. Springer-Verlag, (2000).

- [74] Acioli, P. H. *J. Mol. Struct. (Theochem)* **394**, 75 (1997).
- [75] Popelier, P., editor. *Solving the Schrödinger Equation: Has Everything Been Tried?* Imperial College Press, (2011).
- [76] Gill, P. M. W. *Adv. Quantum Chem.* **25**, 141 (1994).
- [77] Legendre, A.-M. *Mémoires de Mathématiques et de Physique, présentés à l'Académie royale des sciences (Paris) par sçavants étrangers* **10**, 411 (1785).
- [78] Hilbert, D. *Gött. Nachr.*, 49 (1904).
- [79] Schmidt, E. *Math. Ann.* **63**, 433 (1907).
- [80] Mercer, J. *Phil. Trans. R. Soc. A* **209**, 415 (1909).
- [81] Mercer, J. *Proc. R. Soc. A* **83**, 69 (1909).
- [82] Aizerman, M. A., Braverman, E. M., and Rozonoer, L. I. *Automat. Rem. Contr.* **25**, 821 (1964).
- [83] Szegő, G. *Orthogonal Polynomials*. American Mathematical Society, (1975).
- [84] Gill, P. M. W. *Chem. Phys. Lett.* **270**, 193 (1997).
- [85] Hoggan, P. E. *Self-Organization of Molecular Systems*, chapter How Exponential Type Orbitals Recently Became a Viable Basis Set Choice in Molecular Electronic Structure Work and When to Use Them. Springer (2009).
- [86] Hoggan, P. E. *Int. J. Quantum Chem.* **109**, 2926 (2009).
- [87] Hoggan, P. E. *Int. J. Quantum Chem.* **110**, 98 (2010).
- [88] Stein, E. M. and Weiss, G. *Introduction to Fourier Analysis on Euclidian Spaces*. Princeton University Press, (1971).
- [89] Newton, R. G. *Scattering Theory of Particles and Waves*. McGraw-Hill, (2002).
- [90] Greub, W. *Linear Algebra*. Springer, 4th edition, (1975).
- [91] Yukawa, H. *Proc. Phys. Math. Soc. Jpn.* **17**, 48 (1935).
- [92] Ewald, P. P. *Ann. der Physik* **369**, 253 (1921).
- [93] Adamson, R. D., Dombroski, J. P., and Gill, P. M. W. *Chem. Phys. Lett.* **254**, 329 (1996).
- [94] Varganov, S. A., Gilbert, A. T. B., and Gill, P. M. W. *J. Chem. Phys.* **128**, 241101 (2008).
- [95] Lee, A. M., Taylor, S. W., Dombroski, J. P., and Gill, P. M. W. *Phys. Rev. A* **55**, 3233 (1997).
- [96] Whitten, J. L. *J. Chem. Phys.* **58**, 4496 (1973).
- [97] Baerends, E. J., Ellis, D. E., and Ros, P. *Chem. Phys.* **2**, 41 (1973).
- [98] Feyereisen, M., Fitzgerald, G., and Komornicki, A. *Chem. Phys. Lett.* **208**, 359 (1973).
- [99] Vahtras, O., Almlöf, J., and Feyereisen, M. *Chem. Phys. Lett.* **213**, 514 (1993).

- [100] Aquilante, F., Lindh, R., and Pedersen, T. B. *J. Chem. Phys.* **127**, 114107 (2007).
- [101] Aquilante, F., Gagliardi, L., Pedersen, T. B., and Lindh, R. *J. Chem. Phys.* **130**, 154107 (2009).
- [102] Schmidt, M. W., Baldrige, K. K., Boatz, J. A., Elbert, S. T., Gordon, M. S., Jensen, J. H., Koseki, S., Matsunaga, N., Nguyen, K. A., Su, S. J., Windus, T. L., Dupuis, M., and Montgomery, J. A. *J. Comput. Chem.* **14**, 1347 (1993).
- [103] Frisch, M. J., Trucks, G. W., Schlegel, H. B., Scuseria, G. E., Robb, M. A., Cheeseman, J. R., Scalmani, G., Barone, V., Mennucci, B., Petersson, G. A., Nakatsuji, H., Caricato, M., Li, X., Hratchian, H. P., Izmaylov, A. F., Bloino, J., Zheng, G., Sonnenberg, J. L., Hada, M., Ehara, M., Toyota, K., Fukuda, R., Hasegawa, J., Ishida, M., Nakajima, T., Honda, Y., Kitao, O., Nakai, H., Vreven, T., Montgomery, Jr., J. A., Peralta, J. E., Ogliaro, F., Bearpark, M., Heyd, J. J., Brothers, E., Kudin, K. N., Staroverov, V. N., Kobayashi, R., Normand, J., Raghavachari, K., Rendell, A., Burant, J. C., Iyengar, S. S., Tomasi, J., Cossi, M., Rega, N., Millam, J. M., Klene, M., Knox, J. E., Cross, J. B., Bakken, V., Adamo, C., Jaramillo, J., Gomperts, R., Stratmann, R. E., Yazyev, O., Austin, A. J., Cammi, R., Pomelli, C., Ochterski, J. W., Martin, R. L., Morokuma, K., Zakrzewski, V. G., Voth, G. A., Salvador, P., Dannenberg, J. J., Dapprich, S., Daniels, A. D., Farkas, Ö., Foresman, J. B., Ortiz, J. V., Cioslowski, J., and Fox, D. J. *Gaussian 09 Revision A.1*. Gaussian Inc. Wallingford CT 2009.
- [104] Valiev, M., Bylaska, E. J., Govind, N., Kowalski, K., Straatsma, T. P., van Dam, H. J. J., Wang, D., Nieplocha, J., Apra, E., Windus, T. L., and de Jong, W. A. *Comput. Phys. Commun.* **181**, 1477 (2010).
- [105] <http://www.thch.uni-bonn.de/tc/orca/>.
- [106] Turney, J. M., Simmonett, A. C., Parrish, R. M., Hohenstein, E. G., Evangelista, F., Fermann, J. T., Mintz, B. J., Burns, L. A., Wilke, J. J., Abrams, M. L., Russ, N. J., Leininger, M. L., Janssen, C. L., Seidl, E. T., Allen, W. D., Schaefer, H. F., King, R. A., Valeev, E. F., Sherrill, C. D., and Crawford, T. D. *WIREs Comput. Mol. Sci.* **In press**, doi: 10.1002/wcms.93 (2011).
- [107] Shao, Y., Fusti-Molnar, L., Jung, Y., Kussmann, J., Ochsenfeld, C., Brown, S. T., Gilbert, A. T. B., Slipchenko, L. V., Levchenko, S. V., O'Neill, D. P., DiStasio, Jr, R. A., Lochan, R. C., Wang, T., Beran, G. J. O., Besley, N. A., Herbert, J. M., Lin, C. Y., Voorhis, T. V., Chien, S. H., Sodt, A., Steele, R. P., Rassolov, V. A., Maslen, P. E., Korambath, P. P., Adamson, R. D., Austin, B., Baker, J., Byrd, E. F. C., Dachsel, H., Doerksen, R. J., Dreuw, A., Dunietz, B. D., Dutoi, A. D., Furlani, T. R., Gwaltney, S. R., Heyden, A., Hirata, S., Hsu, C. P., Kedziora, G., Khalliulin, R. Z., Klunzinger, P., Lee, A. M., Lee, M. S., Liang, W. Z., Lotan, I., Nair, N., Peters, B., Proynov, E. I., Pieniazek, P. A., Rhee, Y. M., Ritchie, J., Rosta, E., Sherrill, C. D., Simmonett, A. C., Subotnik, J. E., Woodcock III, H. L., Zhang, W., Bell, A. T., Chakraborty, A. K., Chipman, D. M., Keil, F. J., Warshel, A., Hehre, W. J., Schaefer III, H. F., Kong, J., Krylov, A. I., Gill, P. M. W., and Head-Gordon, M. *Phys. Chem. Chem. Phys.* **8**, 3172 (2006).

- [108] *TURBOMOLE V6.1 2009, a development of University of Karlsruhe and Forschungszentrum Karlsruhe GmbH, 1989-2007, TURBOMOLE GmbH, since 2007; available from <http://www.turbomole.com>.*
- [109] Weigend, F., Kattannek, M., and Ahlrichs, R. *J. Chem. Phys.* **130**, 164106 (2009).
- [110] Hohenstein, E. G. and Sherrill, C. D. *J. Chem. Phys.* **132**, 184111 (2010).
- [111] Brenzinski, C. *Numer. Algor.* **43**, 279 (2006).
- [112] Beebe, N. H. F. and Linderberg, J. *Int. J. Quantum Chem.* **12**, 683 (1977).
- [113] Koch, H., Sanchez de Meras, A., and Pedersen, T. B. *J. Chem. Phys.* **118**, 9481 (2003).
- [114] Røeggen, I. and Johansen, T. *J. Chem. Phys.* **128**, 194107 (2008).
- [115] Boman, L., Koch, H., and Sánchez de Merás, A. *J. Chem. Phys.* **129**, 134107 (2008).
- [116] Aquilante, F., Vico, L. D., Ferré, N., Ghigo, G., Malmqvist, P., Neogrady, P., Pedersen, T., Pitonak, M., Reiher, M., Roos, B., Serrano-Andrés, L., Urban, M., Velyazov, V., and Lindh, R. *J. Comput. Chem.* **31**, 224 (2010).
- [117] <http://dirac.chem.sdu.dk/daltonprogram.org/>.
- [118] Hackbusch, W. and Khoromskij, B. N. *Computing* **76**, 177 (2006).
- [119] Chinnamsetty, S. R., Espig, M., Khoromskij, B. N., Hackbusch, W., and Flad, H.-J. *J. Chem. Phys.* **127**, 084110 (2007).
- [120] Hackbusch, W. and Khoromskij, B. N. *J. Complexity* **23**, 697 (2007).
- [121] Khoromskij, B. N., Khoromskaia, V., Chinnamsetty, S. R., and Flad, H.-J. *J. Comput. Phys.* **228**, 5749 (2009).
- [122] Chinnamsetty, S. R., Espig, M., Flad, H.-J., and Hackbusch, W. *Z. Phys. Chem.* **224**, 681 (2010).
- [123] Benedikt, U., Auer, A. A., Espig, M., and Hackbusch, W. *J. Chem. Phys.* **134**, 054118 (2011).
- [124] Bischoff, F. A. and Valeev, E. F. *J. Chem. Phys.* **134**, 104104 (2011).
- [125] Ochsenfeld, C., Kussmann, J., and Lambrecht, D. S. *Rev. Comp. Ch.* **23**, 1 (2007).
- [126] Dyczmons, V. *Theor. Chim. Acta* **28**, 307 (1973).
- [127] Greengard, L. *The rapid evaluation of potential fields in particle systems*. MIT Press, (1987).
- [128] White, C. A., Johnson, B. G., Gill, P. M. W., and Head-Gordon, M. *Chem. Phys. Lett.* **253**, 268 (1996).
- [129] Dombroski, J. P., Taylor, S. W., and Gill, P. M. W. *J. Phys. Chem.* **100**, 6272 (1996).
- [130] Gill, P. M. W. and Adamson, R. D. *Chem. Phys. Lett.* **261**, 105 (1996).
- [131] Schwegler, E., Challacombe, M., and Head-Gordon, M. *J. Chem. Phys.* **106**, 9708 (1997).
- [132] Ochsenfeld, C., White, C. A., and Head-Gordon, M. *J. Chem. Phys.* **109**, 1663 (1998).

- [133] Werner, H.-J., Manby, F. R., and Knowles, P. J. *J. Chem. Phys.* **118**, 8149 (2003).
- [134] Dovesi, R., Pisani, C., Roetti, C., and Saunders, V. R. *Phys. Rev. B* **28**, 5781 (1983).
- [135] Schwegler, E. and Challacombe, M. *J. Chem. Phys.* **105**, 2726 (1996).
- [136] Löwdin, P.-O. *Int. J. Quantum Chem.* **55**, 77 (1995).
- [137] Savin, A. *Recent Developments of Modern Density Functional Theory*. Elsevier, Amsterdam (1996).
- [138] Iikura, H., Tsuneda, T., Yanai, T., and Hirao, K. *J. Chem. Phys.* **115**, 3540 (2001).
- [139] Adamson, R. D., Dombroski, J. P., and Gill, P. M. W. *J. Comput. Chem.* **20**, 921 (1999).
- [140] White, C. A., Johnson, B. G., Gill, P. M. W., and Head-Gordon, M. *Chem. Phys. Lett.* **230**, 8 (1994).
- [141] Strain, M. C., Scuseria, G. E., and Frisch, M. J. *Science* **271**, 51 (1996).
- [142] Lippert, G., Hutter, J., and Parrinello, M. *Mol. Phys.* **92**, 477 (1997).
- [143] Fusti-Molnar, L. and Pulay, P. *J. Chem. Phys.* **117**, 7827 (2002).
- [144] Dunlap, B. I., Connolly, J. W. D., and Sabin, J. R. *J. Chem. Phys.* **71**, 3396 (1979).
- [145] Kato, T. *Comm. Pure. Appl. Math* **10**, 151 (1957).
- [146] Schwartz, C. *Phys. Rev.* **126**, 1015 (1962).
- [147] Kutzelnigg, W. and Morgan III, J. D. *J. Chem. Phys.* **96**, 4484 (1992).
- [148] Libbrecht, K. G. *Sol. Phys.* **99**, 371 (1985).
- [149] Schmidt, M. W. and Ruedenberg, K. *J. Chem. Phys.* **71**, 3951 (1979).
- [150] Szalewicz, K. and Monkhorst, H. J. *J. Chem. Phys.* **75**, 5785 (1981).
- [151] Klopper, W. *J. Chem. Phys.* **102**, 6168 (1995).
- [152] Bakowies, D. *J. Chem. Phys.* **127**, 164109 (2007).
- [153] Lee, J. S. and Park, S. Y. *J. Chem. Phys.* **112**, 10746 (2000).
- [154] Schwartz, C. *Phys. Rev.* **128**, 1146 (1962).
- [155] Jensen, F. *J. Chem. Phys.* **110**, 6601 (1999).
- [156] Kolos, W. and Wolniewicz, L. *J. Chem. Phys.* **43**, 2429 (1965).
- [157] Goldman, S. P. *Phys. Rev. A* **52**, 3718 (1995).
- [158] Eichkorn, K., Treutler, O., Ohm, H., Haser, M., and Ahlrichs, R. *Chem. Phys. Lett.* **240**, 283 (1995).
- [159] Boström, J., Aquilante, F., Pedersen, T. B., and Lindh, R. *J. Chem. Theory Comput.* **5**, 1545 (2009).
- [160] Knuth, D. E. *The Art of computer programming*, volume 3. Addison-Wesley, (1998).
- [161] Poblete, P. V., Munro, J. I., and Papadakis, T. *Theor. Comput. Sci.* **352**, 136 (2006).

- [162] Rokhlin, V. *J. Comput. Phys.* **60**, 187 (1985).
- [163] Appel, A. W. *SIAM J. Sci. Stat. Comput.* **6**, 85 (1985).
- [164] Jung, Y., Sodt, A., Gill, P. M. W., and Head-Gordon, M. *Proc. Natl. Acad. Sci. USA* **102**, 6692 (2005).
- [165] Kinoshita, T., Hino, O., and Bartlett, R. J. *J. Chem. Phys.* **119**, 7756 (2003).
- [166] Hino, O., Kinoshita, T., and Bartlett, R. J. *J. Chem. Phys.* **121**, 1206 (2004).
- [167] Gradshteyn, I. S. and Ryzhik, I. M. *Table of integrals, series and products*. Academic, (2007).
- [168] R Development Core Team. *R: A Language and Environment for Statistical Computing*. R Foundation for Statistical Computing, Vienna, Austria, (2010).
- [169] Smith, J. M., Olver, F. W. J., and Lozier, D. W. *ACM T. Math. Software* **7**, 93 (1981).
- [170] Olver, F. W. J. and Smith, J. M. *J. Comput. Phys.* **51**, 502 (1983).
- [171] Boyd, J. P. *Chebyshev and Fourier spectral methods*. Dover, New York, 2nd edition (2000).
- [172] Filik, J., Harvey, J. N., Allan, N. L., May, P. W., Dahl, J. E. P., Liu, S., and Carlson, R. M. K. *Phys. Rev. B* **74**, 035423 (2006).
- [173] Gill, P. M. W. *J. Phys. Chem.* **100**, 15421 (1996).
- [174] Lee, A. M. and Gill, P. M. W. *Chem. Phys. Lett.* **286**, 226 (1998).
- [175] Gilbert, A. T. B., Gill, P. M. W., and Taylor, S. W. *J. Chem. Phys.* **120**, 7887 (2004).
- [176] Heyd, J., Scuseria, G. E., and Ernzerhof, M. *J. Chem. Phys.* **118**, 8207 (2003).
- [177] Izmaylov, A. F., Scuseria, G. E., and Frisch, M. J. *J. Chem. Phys.* **125**, 104103 (2006).
- [178] Krukau, A. V., Vydrov, O. A., Izmaylov, A. F., and Scuseria, G. E. *J. Chem. Phys.* **125**, 224106 (2006).
- [179] Brothers, E. N., Izmaylov, A. F., Normand, J. O., Barone, V., and Scuseria, G. E. *J. Chem. Phys.* **129**, 011102 (2008).
- [180] Tawada, Y., Tsuneda, T., and Yanagisawa, S. *J. Chem. Phys.* **120**, 8425 (2004).
- [181] Baer, R. and Neuhauser, D. *Phys. Rev. Lett.* **94**, 043002 (2005).
- [182] Gerber, I. C. and Angyan, J. G. *Chem. Phys. Lett.* **415**, 100 (2005).
- [183] Lochan, R. C., Jung, Y., and Head-Gordon, M. *J. Phys. Chem. A* **109**, 7598 (2005).
- [184] Vydrov, O. A., Heyd, J., Krukau, A. V., and Scuseria, G. E. *J. Chem. Phys.* **125**, 074106 (2006).
- [185] Toulouse, J. and Savin, A. *J. Mol. Struct. (Theochem)* **762**, 147 (2006).
- [186] Sato, T., Tsuneda, T., and Hirao, K. *J. Chem. Phys.* **126**, 234114 (2007).
- [187] Chai, J. D. and Head-Gordon, M. *J. Chem. Phys.* **128**, 084106 (2008).
- [188] Crandall, R. E. *Experiment. Math.* **8**, 367 (1999).

- [189] Takemasa, T. *Comput. Phys. Commun.* **48**, 265 (1988).
- [190] McMurchie, L. E. and Davidson, E. R. *J. Comput. Phys.* **26**, 218 (1978).
- [191] Gill, P. M. W., Lee, A. M., Nair, N., and Adamson, R. D. *J. Mol. Struct. (Theochem)* **506**, 303 (2000).
- [192] Heilbronner, E. and Bock, H. *The HMO-Model and its applications: Basis and Manipulation*. Verlag Chemie, (English translation 1976).
- [193] Kohn, W. *Phys. Rev. Lett.* **76**, 3168 (1996).
- [194] Prodan, E. and Kohn, W. *Proc. Natl. Acad. Sci. USA* **102**, 11635 (2005).
- [195] Toulouse, J., Colonna, F., and Savin, A. *Phys. Rev. A* **70**, 062505 (2004).
- [196] Watson, G. N. *A treatise on the theory of Bessel functions*. Cambridge University Press, (1995). Reprint of the second (1944) edition.
- [197] Dongarra, J. J., du Croz, J., Hammarling, S., and Duff, I. *ACM T. Math. Software* **16**, 1 (1990).
- [198] Head-Gordon, M. and Pople, J. A. *J. Chem. Phys.* **89**, 5777 (1988).
- [199] Helgaker, T., Jørgensen, P., and Olsen, J. *Molecular Electronic-Structure Theory*. John Wiley & Sons, (2000).
- [200] Deng, J., Gilbert, A. T. B., and Gill, P. M. W. *J. Chem. Phys.* **133**, 044116 (2010).
- [201] DiStasio, R. A., Jung, Y., and Head-Gordon, M. *J. Chem. Theory Comput.* **1**, 862 (2005).
- [202] Condon, E. U. and Shortley, G. *The Theory of Atomic Spectra*. Cambridge University Press, (1959).
- [203] Kellogg, O. D. *Foundations of potential theory*. Frederick Ungar Publishing Company, (1929).
- [204] Goldstein, H. *Classical Mechanics*. Addison-Wesley, Cambridge, MA, 2nd edition, (1980).
- [205] Landau, L. D. and Lifshitz, E. M. *Quantum mechanics*. Pergamon Press, 2nd edition, (1965).
- [206] Hockney, R. W. and Eastwood, J. W. *Computer simulation using particles*. McGraw-Hill, (1981).
- [207] Payne, M. C., Teter, M. P., Allan, D. C., and Joannopoulos, J. D. *Rev. Mod. Phys.* **64**, 1045 (1992).
- [208] Krishnan, K. H. *Nature* **162**, 215 (1948).
- [209] Krishnan, K. H. *J. Indian Math. Soc.* **12**, 79 (1948).
- [210] Bhatia, A. B. and Krishnan, K. S. *Proc. R. Soc. A* **192**, 181 (1948).
- [211] Simon, R. *Resonance* **7**, 20 (2002).
- [212] Boas, Jr., R. P. and Stutz, C. *Am. J. Phys.* **39**, 745 (1971).
- [213] Pollard, H. and Shisha, O. *Am. Math. Mon.* **79**, 495 (1972).

- [214] Boas, Jr., R. P. and Pollard, H. *Am. Math. Mon.* **80**, 18 (1973).
- [215] Andrews, G. E., Askey, R., and Roy, R. *Special functions*, volume 71 of *Encyclopedia of Mathematics and its Applications*. Cambridge University Press, (1999).
- [216] Koekoek, R., Lesky, P. A., and Swarttouw, R. F. *Hypergeometric orthogonal polynomials and their q -analogues*. Springer Monographs in Mathematics. Springer-Verlag, (2010).
- [217] Weber, H. *Journal für Math.* **75**, 75 (1873).
- [218] Sonine, N. *Math. Ann.* **16**, 1 (1880).
- [219] Schafheitlin, P. *Math. Ann.* **30**, 161 (1887).
- [220] Cooke, R. G. *Proc. London Math. Soc.* **28**, 207 (1928).
- [221] Heisenberg, W. *Physics and Beyond*. Harper and Row, (1971).
- [222] Gautschi, W. *SIAM Rev.* **9**, 24 (1967).
- [223] British Association for the Advancement of Science. *Mathematical Tables, vol. X, Bessel functions*. Cambridge University Press, (1952).
- [224] Olver, F. W. J. and Sookne, D. J. *Math. Comput.* **26**, 941 (1972).
- [225] Lord Rayleigh (J. W. Strutt). *Proc. R. Soc. A* **84**, 25 (1910).
- [226] Olver, F. W. J. *Math. Comput.* **18**, 65 (1964).
- [227] Mattheij, R. M. M. and van der Sluis, A. *Numer. Math.* **26**, 61 (1976).
- [228] Zahar, R. V. M. *Numer. Math.* **27**, 427 (1977).
- [229] Gautschi, W. *SIAM J. Numer. Anal.* **7**, 187 (1970).
- [230] Poppe, G. P. M. and Wijers, C. M. J. *ACM T. Math. Software* **16**, 38 (1990).
- [231] Thompson, W. J. *Atlas for computing mathematical function*. John Wiley & Sons, (1997).
- [232] Galler, G. M. *Commun. ACM* **3**, 353 (1960).
- [233] Herndon, J. R. *Commun. ACM* **4**, 178 (1961).
- [234] Wiggins, R. A. and Saito, M. *B. Seismol. Soc. Am.* **61**, 375 (1971).
- [235] Braithwaite, W. J. *Comput. Phys. Commun.* **5**, 390 (1973).
- [236] Press, W. H., Teukolsky, S. A., Vetterling, W. T., and Flannery, B. P. *Numerical Recipes in C, The Art of Scientific Computing*. Cambridge University Press, 2nd edition, (1992).
- [237] Holmes, S. A. and Featherstone, W. E. *J. Geod.* **76**, 279 (2002).
- [238] Jekeli, C., Lee, J. K., and Kwon, J. H. *J. Geod.* **81**, 603 (2007).
- [239] Wittwer, T., Klees, R., Seitz, K., and Heck, B. *J. Geod.* **82**, 223 (2008).
- [240] Fantino, E. and Casotto, S. *J. Geod.* **83**, 595 (2009).
- [241] Schneider, B. I., Segura, J., Gil, A., Guan, X., and Bartschat, K. *Comput. Phys. Commun.* **181**, 2091 (2010).

- [242] Lozier, D. W. and Smith, J. M. *ACM T. Math. Software* **7**, 141 (1981).
- [243] Press, W. H., Teukolsky, S. A., Vetterling, W. T., and Flannery, B. P. *Numerical Recipes, The Art of Scientific Computing*. Cambridge University Press, 3rd edition, (2007).
- [244] Kestin, J. and Persen, L. N. *Z. Angew. Math. Phys.* **7**, 33 (1956).
- [245] Strand, O. N. *Math. Comput.* **19**, 127 (1965).
- [246] Pauling, L. *J. Am. Chem. Soc.* **69**, 542 (1947).